U N I V E R S I T Y *of* H O U S T O N

Rawinsonde Launches, Tethered-Balloon Ozone Soundings, and Micrometeorological Flux Measurements and Analyses

Grant No. 582-5-64594

Final Report

Submitted to

Texas Commission on Environmental Quality

By:

University of Houston
Department of Geosciences
Institute of Multi-Dimensional Air Quality Studies
Houston, TX

September 2007

Contact information:

Dr. Bernhard Rappenglück (PI)
Department of Geosciences
University of Houston
4800 Calhoun Rd
Houston, TX 77204-5007

Office 225A Old Science
Phone 713-743-1834
Fax 713-748-7906
Email brappenglueck@uh.edu

Dr. Barry Lefer (Co-PI)
Department of Geosciences
University of Houston
4800 Calhoun Road
Houston, TX 77204-5007

Office 223 Old Science
Phone 713-743-3399
Fax 713-748-7906
Email blefer@uh.edu

External collaborator:

Ozonesondes: Dr. Gary Morris (Valparaiso University/IN)

Lead graduate students (University of Houston - Department of Geosciences):

Radiosondes:	Ryan Perna	(MS 2007; advisor: Rappenglück),
Tethersonde/Ozonesondes:	Bridget McEvoy-Day	(MS expected 2008; advisor: Rappenglück),
Tethersonde:	Craig Clements	(PhD 2007; advisor: Zhong)

Student field support (University of Houston - Department of Geosciences):

Renee Boudreaux, James Flynn, Ricky Fuller, Paulina Guerrero, Dr. Meongdo Jang, Daegyun Lee, Dr. Michael Leuchner, Beryl Onakpoya, Monica Patel, Leonardo Pedemonte, Barry Shaulis, Susan Street, and Wenqing Yao

Data and model support (University of Houston - Department of Geosciences):

Soontae Kim, Fantine Ngan, Fang-Yi Cheng

Contents:

1. Introduction 3

2. Experimental Approach 5

2.1 Field measurement design and logistics during TexAQS-II 5

2.2 Radiosondes 6

2.3 Ozonesondes 7

2.4 Tethersonde 10

3. Results 11

3.1 Relationship between the planetary boundary layer depth, its rate of growth, and observed ground-based pollutant concentrations (Sub-Task 6.1) 11

3.2 Land-sea-bay breeze interaction with planetary boundary layer growth, depth, and observed ozone concentrations (Sub-Task 6.2). 21

3.3 PBL observations vs. the MM5-modeled PBL dynamics, and the parameterization of vertical mixing in photochemical grid modelling (Sub-Task 6.3). 29

3.4 Vertical ozone structures variations over a typical diurnal cycle and the relation of the diurnal variation in ozone structure to the evolution of boundary layer dynamics and thermodynamic structure (Sub-Task 6.4). 31

3.4.1 Case Study August 31 – September 01, 2006 31

3.4.2 Case Study September 26, 2006 36

3.5 The relation of the vertical ozone structure to surface ozone observations, including to what degree the ozone concentration in the residual layer contributes to the next morning concentration as a result of convective boundary layer growth (Sub-Task 6.5) 40

3.6 Identify the relative role of regional transport and local concentration in determining the vertical ozone distribution (Sub-Task 6.6). 41

3.7 Describe ozone distribution within the free troposphere, and how it varies with regional transport patterns (Sub-Task 6.7). 43

4. Conclusions 51

5. References 53

Appendix I – Plots of Radiosonde and Ozonesonde Launches on IOPs 55

Appendix II – AQI and Ozone Levels – August and September 2006 67

1. Introduction

Although the Gulf Coast is simple in topography, the boundary layer structure and wind circulation in the Gulf Coast region of southeastern Texas can be highly variable due to the frequent presence of sea-land breeze circulations, strong nocturnal low-level jets, and larger-scale diurnal wind oscillation. These complex wind patterns pose significant challenges for mesoscale numerical weather forecasting and for air quality forecasting in the region.

Using data from six radar wind profilers in southeastern Texas, *Angevine et al.* [2002] demonstrated that the afternoon mixed layer, an important meteorological variable for air pollution, can vary significantly across the region. Based on cluster analysis of surface wind observations from a meteorological network in the Houston and Galveston area, *Darby et al.* [2005] revealed complex surface wind patterns and related the different patterns to the observed surface ozone (O_3) distribution. Using Lidar and aircraft observations, *Banta et al.* [2005] linked the sea-land breeze circulations to ozone episodes in Houston area.

Various mesoscale numerical weather forecast models, such as the Penn-State/NCAR MM5 (National Centre of Atmospheric Research Mesoscale Model) model [*Grell et al.*, 1994] and the Weather Research and Forecast (WRF) model [*Michalakes et al.*, 1998] have been applied to this region. Despite the success of these models in capturing the general patterns and day-to-day variations of local meteorology in response to changes in synoptic conditions, the errors in the simulated local circulations and boundary layer structures are relatively large. For example, *Cheng et al.* [2003] showed that the MM5 model produced a delayed onset of sea breeze and that the simulated nighttime winds were generally stronger than the observed winds. This higher simulated wind velocity produces stronger ventilation and lower pollution concentrations than actually exist. *Ching et al.* (2004) showed that the MM5 model, even with an advanced urban parameterization, produced lower heat and momentum fluxes and mixed layer depths over the Houston area. Because of the sensitivity of air quality to the details of the boundary layer structure and local circulations, small errors in numerical simulations, which may be of minor concern for weather forecasting, may nevertheless lead to erroneous forecasted air quality concentrations.

The efforts to improve weather and air quality forecasting for southeastern Texas and regions of similar coastal and urban characteristics have been hampered by the lack of routine measurements of several key boundary layer phenomena and properties such as the low-level jet, the vertical structure of sea-land breezes, and the mixed layer heights.

To better understand these boundary layer phenomena and properties and to improve model forecasting, we carried out a suite of boundary layer measurements during the TexAQS-II (Texas Air Quality Study – II) field campaign as requested by the Texas Commission on Environmental Quality (TCEQ). These measurements included

I. Rawinsonde soundings of the atmospheric thermodynamic structure and wind over urban areas of Houston.
II. Ozonesonde soundings to retrieve information about the vertical distribution of ozone (collaboration with University of Valparaiso)
III. Tethersonde launchings to obtain finescale information of the behaviour of the nighttime and early morning boundary layer

Despite the rapid advances in upper-air observations using remote sensing instruments such as radar wind profilers, rawinsonde sounding profiles still provide the most accurate depictions of the vertical atmospheric dynamic and thermodynamic structures. In addition to providing upper-level atmospheric conditions affected by synoptic-scale forcing, rawinsonde profiles also provide important information on vertical wind shear associated with local sea-breeze circulations and low-level jets, mixed-layer heights, and the strengths and heights of surface-based nocturnal inversion or synoptic subsidence inversion, all of which are critical for the understanding of ozone transport and

transformation in the Houston area and for the validation of model predictions. These boundary layer properties and their time variations will be linked to ozone concentrations in the region. The profiles will also be used to validate the real-time MM5 simulations for the Houston-Galveston area produced at the Institute for Multidimensional Air Quality Studies (IMAQS) at the University of Houston (UH).

During TexAQS-II multiple soundings were launched from UH – Main Campus on forecast episode days, while twice-per-day launches occurred on non-episode days. The data from multiple soundings in a single day can be used to determine the rate of mixed layer growth in the morning, an important factor for peak ozone values, as well as the maximum mixed layer heights in the afternoon. The afternoon soundings can be used for sea-breeze characterization, whereas the early morning soundings help to determine the structure of the low-level jet and the strength of nocturnal inversions.

In a collaborative effort vertical ozone data was retrieved using ozone sounding systems These measurements are used for specific objectives: 1) complement other routine ground-based ozone monitoring and validate special aircraft observations; 2) validate and improve air quality model simulations of ozone episodes; and 3) help achieve better understanding of ozone transport vs. local production [e.g. *Morris et al.*, 2006].

This Final Report addresses the following tasks as outlined in the Grant Activity Description for Grant Activities No. 582-5-64594-FY05-01-Amendment2:

1) Relationship between the planetary boundary layer depth, its rate of growth, and observed ground-based pollutant concentrations (Sub-Task 6.1).
2) Land-sea-bay breeze interaction with planetary boundary layer growth, depth, and observed ozone concentrations (Sub-Task 6.2).
3) PBL observations vs. the MM5-modeled PBL dynamics, and the parameterization of vertical mixing in photochemical grid modelling (Sub-Task 6.3).
4) Vertical ozone structures variations over a typical diurnal cycle and the relation of the diurnal variation in ozone structure to the evolution of boundary layer dynamics and thermodynamic structure (Sub-Task 6.4).
5) The relation of the vertical ozone structure to surface ozone observations, including to what degree the ozone concentration in the residual layer contributes to the next morning concentration as a result of convective boundary layer growth (Sub-Task 6.5).
6) Identify the relative role of regional transport and local concentration in determining the vertical ozone distribution (Sub-Task 6.6).
7) Describe ozone distribution within the free troposphere, and how it varies with regional transport patterns (Sub-Task 6.7).

2. Experimental Approach

2.1 Field measurement design and logistics during TexAQS-II

The Houston area has a unique meteorological and chemical environment that can create high levels of ozone rapidly. Within the framework of TexAQS-II this particular study funded by TCEQ attempts to categorize the vertical meteorological and ozone profile above the University of Houston (UH) to better understand the conditions that favor high ozone levels in the Houston area. The UH – Main Campus site was chosen due to its central location approximately 5 km to the southeast of downtown Houston and thus it is the most representative site to characterize the structure and dynamics of the urban boundary layer. Since the launching site for radio and ozone sondes as well as for the tethersonde could be established on UH campus, logistical problems to run such a 2-month field study in a continuous way (e.g. location for research trailer, coordination of personnel staff for the field work) could be kept at a minimum. This was especially important with regard to intensive observation periods (IOPs) which were determined at short notice.

For this study, the August-thru-September time frame was chosen since these months usually exhibit the highest frequency of "high ozone" days based on long-term ground-based ozone observations. A "high ozone" day was defined using the criteria specified by the U.S. Environmental Protection Agency (EPA) where the measured 8-hour average ozone mixing ratio in any given station is greater than or equal to 85 ppbv [see also *TCEQ*, 2006]. Radiosondes were launched twice per day at 700 and 1900 CDT (Central Daylight Time), corresponding with the standard launches completed across the country by the National Weather Service (00Z and 12Z). On IOPs that were forecasted to be high ozone days (ozone 8-hour averages greater than 85 ppbv), radiosondes were launched at 500, 1000, 1300, 1600, and 2200 CDT in addition to the standard twice daily launches in order to capture the temporal and vertical development of the planetary boundary layer (PBL) height. IOPs occurred on the following 10 days: 8/17, 8/31, 9/1, 9/2, 9/8, 9/14, 9/15, 9/20, 9/25 an 9/26.

Ozonesondes were kindly provided by Dr. Gary Morris as part of a collaborative work with Valaparaiso University. Ozonesondes were also launched at 700 CDT during the forecasted high-ozone IOPs to illustrate the complex nature of the vertical ozone profile before mixing took place, and to capture the pre-existing residual layer(s). On IOPs and other selected days during the TexAQS-II period, ozonesondes were launched at 1300 CDT in order to capture the vertical distribution of ozone concentrations at a time of the day when the mixed boundary layer height is fully developed.

Tethersonde studies were completed on selected nights and early mornings during IOPs to capture the development of the nocturnal residual layer and the break-up of the morning inversion. Profiles were taken up to 200 meters above ground level (AGL). They included temperature, pressure, relative humidity, and ozone mixing ratio.

The logistics plan for the above launches was a difficult task that required organized schedules and considerable manpower. Most of the available employees were students, therefore the launches became much more challenging in mid-August when fall semester classes began. Despite the difficult logistics of scheduling, radiosonde data coverage was excellent due to the high level of operational expertise (182 successful launches out of 185 launches, i.e. 98.4%). Ozonesonde data coverage was 87.5%, representing 35 successes out of 40 launches. Losses for both types of sondes were primarily due to mechanical and/or technical difficulties with the equipment. The radiosonde launchings were relatively easy to manage, however the ozonesondes were very time-consuming for the employees involved because each sonde required several hours of advance preparation in the lab. In addition to this advance preparation, the launches were more time-consuming. Two students were always required to launch an ozonesonde and after lift-off one student was needed to monitor the launch in real-time to ensure the most complete data collection. It is estimated that each ozonesonde launch required approximately 7-8 hours of labor. The radiosonde launches required approximately 2 hours of labor for each launch. Overall, a comprehensive data set was collected during the TexAQS-II experiment in August and September 2006. An overview of the IOP data is given in Appendix 1.

2.2 Radiosondes

Radiosondes were launched from the University of Houston campus, located at 29.7421 N and 95.3395 W. The launch site was located 11 m above sea level. Launches were conducted daily at 700 and 1900 CDT, with additional launches occurring at 100 (occasionally, not always possible due to logistical reasons), 500, 1000, 1300 1600 and 2200 on IOPs.

Radiosondes were typically launched using 100 g balloons since this size was the most cost-effective method to study the boundary layer. The balloons typically measured approximately 1 meter in diameter. Occasionally larger balloons were used, allowing the sonde to reach higher altitudes. In general, the 100 g balloons burst at approximately 110 hPa or 16 km altitudes with an average ascent rate of 5 m/s. The balloons were attached to parachutes, and the sonde was attached to the base of the parachute. The sondes utilized were Vaisala, Inc. RS-92 sondes. According to the manufacturer [*Vaisala, Inc.*, 2005], these sondes have a size of 220 x 80 x 75 mm, weigh 250 g, and have an operating time of 135 minutes. Additional specifications can be found in the table below:

Table 1. Specifications of the Vaisala RS 92-GPS Radiosonde

Vaisala RS 92-GPS Radiosonde Specifications	
Pressure Sensor	Silicon
- Measuring Range	1080 hPa to 3 hPa
- Resolution	0.1 hPa
- Total uncertainty in sounding	1 hPa at 1080-100hPa, 0.6 hPa at 100-3 hPa
- Accuracy (Reproducibility)	0.5 hPa
- Accuracy (Repeatability of calibration)	0.4 hPa
Temperature Sensor	Capacitive Wire
- Measuring Range	+60 °C to -90 °C
- Resolution	0.1 °C
- Accuracy (Reproducibility)	0.2 °C up to 100 hPa, 0.3 °C for 100-20 hPa, 0.5 °C above 20 hPa level
-Response Time(62.2%, 6 m/s flow)	<0.4 s at 1000 hPa, <1 s at 100 hPa, <2.5 s at 10 hPa
-Accuracy (Repeatability of calibration)	0.2 °C
- Lag	< 2.5 seconds
Humidity Sensor	Thin Film Capacitor, Heated Twin Sensor
- Measuring Range	0% to 100% relative humidity (RH)
- Resolution	1% RH
- Accuracy (Reproducibility)	2% RH
- Accuracy (Repeatability of calibration)	2% RH
- Response Time(6 m/s, 1000hPa)	<0.5 s at 20°C, <20 s at -40°C
GPS-Based Wind detector	
-Number of Channels	12
-Navigation Accuracy	
-Positioning uncertainty, horizontal	10 m
-Velocity measurement uncertainty	0.15 m/s
-Directional measurement uncertainty	2 degrees
Sampling Rate	1 sample per second
Battery	Water activated
Voltage	8 volts

2.3 Ozonesondes

Ozonesonde launches

Table 2 gives a survey about the ozonesonde launchings at UH campus. Ozonesondes were launched on 20 days during August 2006 and 11 days during September 2006. Launches occurred at approximately 1300 CDT. On IOPs (highlighted in table 2), two launches were performed; at 700 and approximately 1300 CDT.

Table 2. Ozonesonde launches from UH campus during August/September 2006

Date	Time (CDT)	IOP?	Comments
1-Aug-06	1355	No	
2-Aug-06	1305	No	
4-Aug-06	1355	No	
7-Aug-06	1343	No	Malfunctioning pressure sensor
9-Aug-06	1332	No	No ozone data collected
10-Aug-06	1322	No	
11-Aug-06	1332	No	
14-Aug-06	1351	No	
15-Aug-06	1436	No	Malfunctioning pressure sensor - data only good up to 18 km
17-Aug-06	721	Yes	Data collected above 4000 m only
	1338	Yes	
19-Aug-06	1307	No	
20-Aug-06	1305	No	
21-Aug-06	1312	No	
22-Aug-06	1302	No	No data collected
23-Aug-06	1302	No	
25-Aug-06	1258	No	
28-Aug-06	1306	No	
29-Aug-06	1303	No	
30-Aug-06	1314	No	
31-Aug-06	701	Yes	
	1330	Yes	
1-Sep-06	700	Yes	No data collected
	1354	Yes	
2-Sep-06	702	Yes	
	1338	Yes	
8-Sep-06	1301	Yes	
13-Sep-06	1245	No	
14-Sep-06	705	Yes	
	1300	Yes	
15-Sep-06	712	Yes	Data collected above 1500 m only
	1304	Yes	
19-Sep-06	1301	No	
20-Sep-06	703	Yes	
	1301	Yes	
25-Sep-06	700	Yes	
	1303	Yes	
26-Sep-06	1040	Yes	
	1417	Yes	
27-Sep-06	1301	No	

Ozone Measuring Package

For the balloon-borne ozone measurements, the University of Houston program utilized aqueous solution Model 2Z electrochemical concentration cell (ECC) ozonesondes manufactured by EN-SCI Corporation of Boulder, Colorado and provided by Valparaiso University through a subcontract. The full ozonesonde launch package is designed for real-time data acquisition and processing and consists of a 600 g rubber meteorological balloon (1.7 m in diameter), a parachute, 36 m of string in a payout reel, a Vaisala, Inc. RS80-15 meteorological radiosonde, a GPS receiver and antenna, and the ozonesonde which is protected during the flight in a molded polystyrene weatherproof box (sized 19 x 19 x 25 cm). Weighing approximately 1000 g, the instrument package ascends at 5-6 m/s. Data parameters captured and transmitted during the flight include ozone concentrations, ambient air pressure, air temperature, relative humidity, and GPS position data as well as several sonde-specific readings. The package generally reached 25 to 30 km above ground level before the balloon bursts and the instruments float back to earth under the parachute.

On the ground, supporting equipment to receive the data signals from the instrument package included an antenna with pre-amplifier, a receiver, a 300-baud modem, and a personal computer with a software package designed for use with this system.

Ozonesonde

This section briefly summarizes details of the design and performance of the ozonesonde instrument according to the documentation of the manufacturer [*EN-SCI Corporation*, 1997]. The ECC ozonesonde is lightweight and compact (sized 7.6 x 7.9 x 13.3 cm), consisting of a motor-driven Teflon and glass air sampling pump, an ozone-sensing electrochemical concentration cell, and an Innovative System Designs' V2C interface circuit board, which links the ozone sensor, the GPS unit, and the radiosonde.

The ozone sensor cell of the ECC ozonesonde has separate Teflon cathode and anode chambers which each contain a platinum electrode. The electrodes are immersed in potassium iodide (KI) sensing solutions of differing concentrations; the anode contains a saturated KI solution and the cathode contains a ½% KI solution. The chambers are linked with an ion bridge, providing an ion pathway between them.

During the flight, ambient air is forced into the sensor by the battery-driven air sampling pump. When ozone is in the sampled air, iodine is formed in the cathode half-cell according to the reaction: $2KI + O_3 + H_2O \rightarrow 2KOH + I_2 + O_2$. The cell then converts the iodine to iodide through the reaction: $I_2 + 2 \text{ electrons} \rightarrow 2I^-$. Electrons subsequently flow in the cell's external circuit and an electrical current is generated proportional to the mass flow rate of ozone through the cell. The analog cell current and other sonde-specific parameters, along with the data measured by the radiosonde (temperature, pressure, and humidity) and the GPS unit (wind speed/direction and sonde position), is formatted into binary packets by the V2C circuitry and sent to the radiosonde transmitter.

On the ground, the antenna/receiver system acquires the data transmission, which is demodulated by the 300-baud modem and sent to the computer/software through a serial port. The low baud rate decreases the possibility of errors that may occur during transmission, but limits the data transmission to one data packet every 1.2 s. A GPS data packet is substituted for a data packet every 5 s [*EN-SCI Corporation*, 2003a].

From the received data, ozone partial pressure and mixing ratio is calculated in real-time by the software algorithms. Through using the volume flow rate and temperature, the algorithms convert the electrical current to an ozone concentration under the assumption that the ozone reaction with potassium iodide is quantitatively known [*Russell III et al.*, 1998].

The ECC ozonesondes require advance preparation ahead of a planned launch. An EN-SCI Corporation Model KTU-2 ozonizer/test unit is used to check the overall performance of the instrument, condition the air intake tubing and pump with ozone, charge the sensor with sensing solution, check the sensor background current with zero ozone air, and check the sensor response time.

One day to two weeks prior to a launch, the sonde goes through an approximate 2-hour preparation in order to attain a low sensor background current. Within 15 hours of a launch, the sonde has an additional preparation of approximately one hour. During this preparation, the sensing solutions are refreshed, air flow rates are measured, and the entire system is checked to ensure that data is being transmitted and received successfully.

The ECC-type ozonesondes has been characterized thoroughly over the last decade [*Russell et al.*, 1998] and intercomparison studies, among them the Jülich Ozone Sonde Intercomparison Experiment (JOSIE), showed that in terms of accuracy and precision ECC-type ozonesondes yield better results than the Brewer Mast and KC79 sondes [*Smit and Kley*, 1996]. While the relative precision is best for all sondes in the middle stratosphere where ozone is at a maximum, the non-ECC type sondes show a considerably lower precision in the troposphere and stratosphere compared to the ECC sondes. Comparison studies with routine lidar measurements made at the Observatoire de Haute Provence during 1990-1995 show that for fifteen simultaneous ECC versus lidar profiles, the mean of the differences observed between 4 and 7 km was 2.5 ± 1.8 parts per billion (4 ± 3%) [*Ancellet and Beekmann,* 1997].

Radiosonde

A 403-megahertz (MHz) frequency-modulated Vaisala RS80-15 radiosonde was used for data collection and transmission for all flights. Radiosonde specifications as detailed by the manufacturer [*Vaisala, Inc.*, 1997] are shown in the following table:

Table 3. Specifications of the Vaisala RS 80-15-GPS Radiosonde

Vaisala RS80-15 GPS Radiosonde Specifications	
Pressure Sensor	BAROCAP® capacitive aneroid
- Measuring Range	1060 hPa to 3 hPa
- Resolution	0.1 hPa
- Accuracy (Reproducibility)	0.5 hPa
- Accuracy (Repeatability of calibration)	0.5 hPa
Temperature Sensor	THERMOCAP® capacitive bead
- Measuring Range	+60 °C to -90 °C
- Resolution	0.1 °C
- Accuracy (Reproducibility)	0.2 °C up to 50 hPa, 0.3 °C for 50-15 hPa, 0.4 °C above 15 hPa level
- Accuracy (Repeatability of calibration)	0.2 °C
- Lag	< 2.5 seconds
Humidity Sensor	HUMICAP® thin film capacitor
- Measuring Range	0% to 100% relative humidity (RH)
- Resolution	1% RH
- Accuracy (Reproducibility)	< 3% RH
- Accuracy (Repeatability of calibration)	2% RH
- Lag	1 second
Sampling Rate	7 samples per 10 seconds for each parameter
Battery	Water activated
Voltage	19 volts

GPS Receiver

Each instrument package that was launched incorporated a Garmin GPS receiver and antenna inside the lid of the flight box for measurements of wind speed and direction as well as the altitude, latitude and longitude of the instrument during flight. As with the radiosonde, the GPS unit is coupled to the V2C interface electronics board of the ozonesonde. According to the manufacturer [*EN-SCI Corporation*, 2003b], the GPS System provides horizontal measurement precision of ± 2 m and vertical precision of ± 10 m. Up to twelve GPS satellites can be detected by the GPS unit simultaneously, but it only requires communication with 4 satellites simultaneously in order to obtain elevation and position data. GPS data packets are received by the sonde package every 5 s. Wind speed and direction are computed from the GPS data by the software and displayed on the computer in 1-min intervals.

2.4 Tethersonde

Tethered balloon ascents were made with a Vaisala, Inc. DigiCora Tethered Balloon Sounding System. The system was used in profile mode consisting of one tethersonde (Vaisala, Inc. TTS-111) and one custom ozone analyzer provided by the University of New Hampshire. The tethersonde system logs data at 1-s intervals and includes pressure, temperature, humidity, winds, and analog voltages. The tethersonde specifications are the same as discussed above for the radiosonde (RS92-GPS) because the same technology and sensor are used.

The ozonesonde (TWS Ozone Sensor) developed by the University of New Hampshire uses UV absorption cell technology to measure the ozone concentration. The instrument is housed in a lightweight styrofoam box and is operated from a rechargeable battery pack. The unit has analog voltage outputs (0-5V) that are recorded from the tethersonde's auxiliary analog inputs. The analog output from the TWS sensor has a minimum average of 10 s while the sampling of the tethersonde inputs is 1 s. Therefore, post-processing is required for all instantaneous data and will be average to 10 s for each profile. This will allow a smoother profile to be calculated.

Ascents were made every half hour up to 250- 300 m AGL throughout the night on selected IOP days beginning at approximately 2100 CDT and ending the following morning at 1000 CDT. Results showed that the development of the nighttime boundary layer was complex.

3. Results

3.1 Relationship between the planetary boundary layer depth, its rate of growth, and observed ground-based pollutant concentrations (Sub-Task 6.1).

The diurnal variation of the planetary boundary layer (PBL) showed quite heterogeneous behavior. A first approach to discriminate specific features is shown in Fig. 1. Figure 1 illustrates the difference between a "Moderate" and a "High" ozone day in the nature of the PBL development. September 02 was rather well-mixed from early in the morning which helped to keep O_3 levels down. Peak O_3 1-hr levels reached 90 ppbv Manvel Croix Park (see Appendix II). August 31 was a high ozone day: at Houston Westhollow peak O_3 1-hr levels reached 147 ppbv and peak O_3 8-hr levels of about 126 ppbv were observed (see Appendix II). The lower PBL height along with the delay in development may have been a factor in increasing Houston's O_3 levels. However, focusing on O_3, the relationship

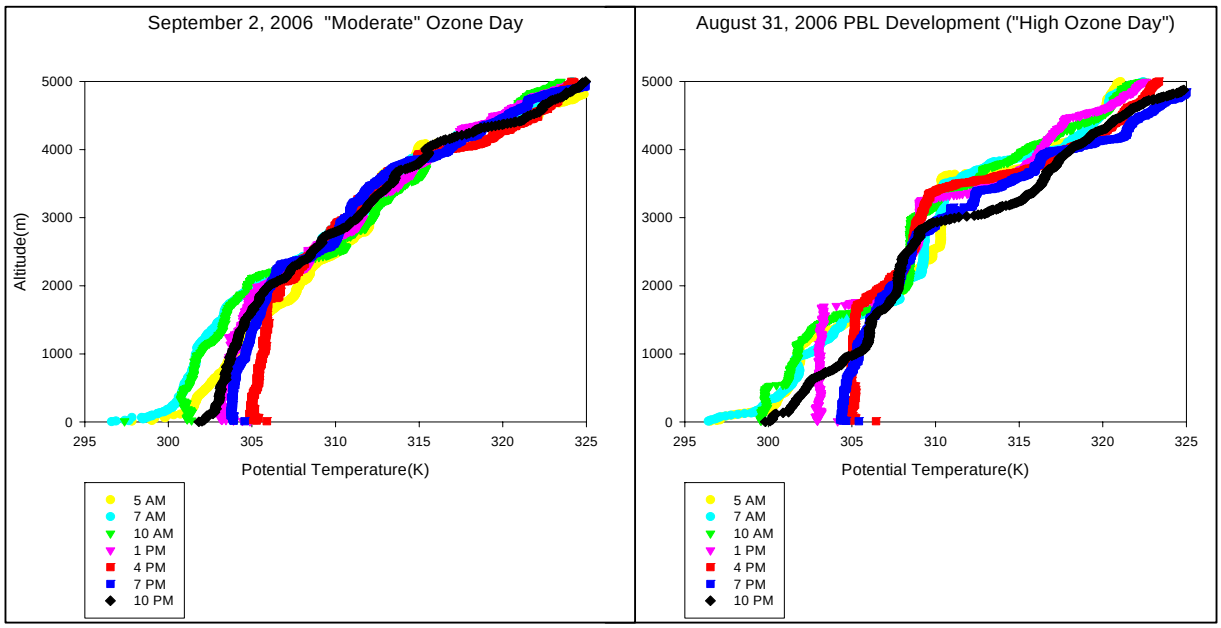

Figure 1. PBL development on September 02 (left) and August 31, 2006 (right). September 02 is considered a "Moderate" and August 31 a "High" ozone day as defined by the TCEQ.

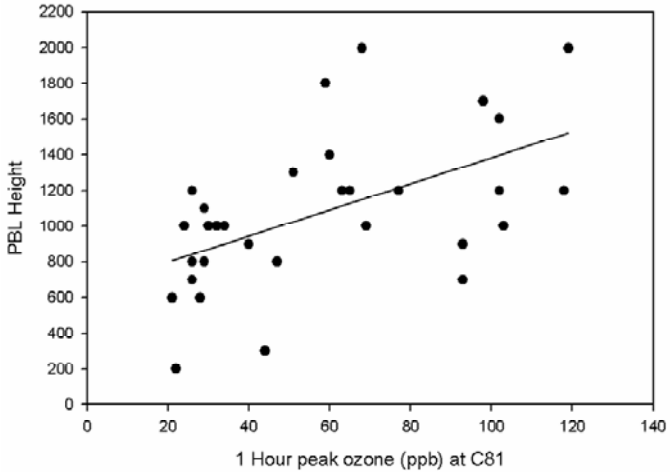

Figure 2. Surface ozone peak vs. PBL height for August 2006.

between the PBL height and surface ozone peak values is not well pronounced. Figure 2 shows the relationship between the PBL height obtained on UH campus at 0700 CDT and the peak O_3 values for the Continuous Ambient Monitoring Site (CAMS) 81 site (Houston Regional Office). There is some slight tendency that higher O_3 values are observed under higher PBL height conditions, whereas low peak O_3 values tend to occur under low PBL height conditions. The critical PBL height between both conditions seems to be around 1000 m AGL. Possible explanation for this finding

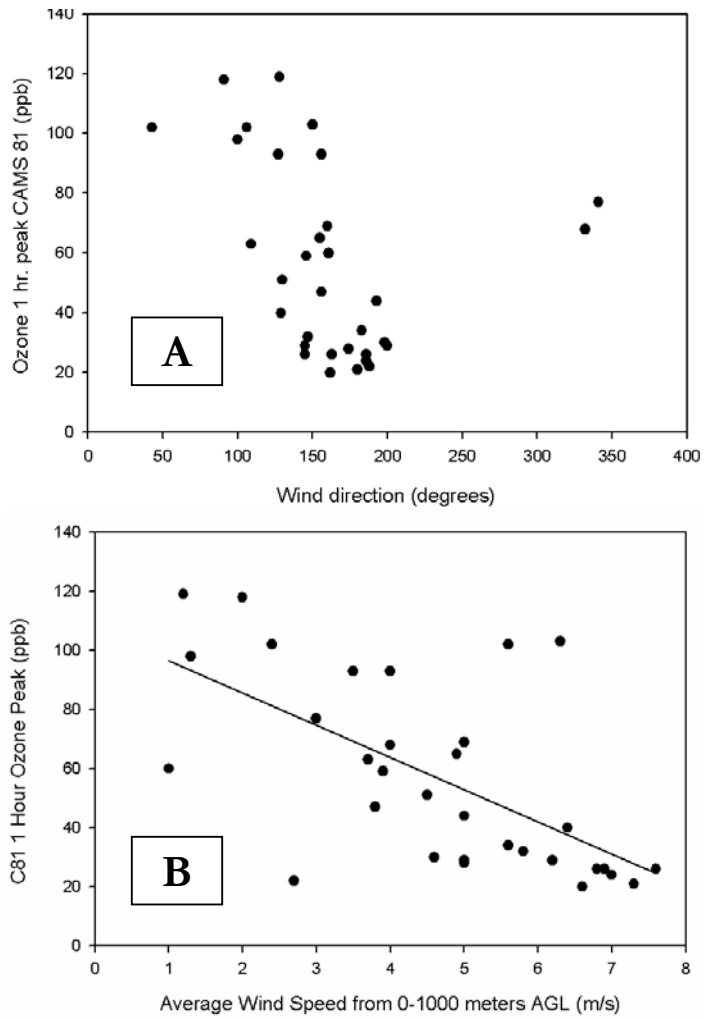

Figure 3. Surface ozone peak vs. average wind direction [A] and vs. average wind speed [B]. Averaging made over 0-1000 m AGL.

might be that low PBL height may also be accompanied by higher mixing ratios of NO and thus keep O_3 at moderate levels due to titration with NO and deposition processes which remove O_3. Higher PBL heights are often associated with stronger convection processes and enhanced mixing. These processes can involve additional ozone from the free troposphere and/or background ozone which can compensate for previously mentioned the removal processes.

Figure 3 demonstrates that also other parameters may bias the results from Figure 2. Figure 3A shows that there is an overall slight dependence on wind direction indicating lower peak ozone values under southwesterly wind conditions, while higher ozone values are associated with southeastery/easterly wind directions. Southwesterly wind directions carry unpolluted marine air masses. Easterly wind directions are closely related to air masses passing the Ship Channel. Apart from this they may also likely carry elevated continental background ozone levels. Figure 3B clearly shows that ozone values decrease with increasing wind speed. Some lower O_3 levels at lower wind speeds may be associated with low PBL heights which will likely support both titration with NO emitted from ground-based emission sources and O_3 deposition processes.

A comparison of radiosonde data obtained on high ozone days vs "non-ozone" days revealed some additional preliminary results. Figure 4 shows as an example the radiosonde launchings on August 31 and September 1. TCEQ labelled August 31 as a "purple" and September 01 as a "red" day (see Appendix II). Both days are characterized by easterly winds within the boundary layer which most likely carry polluted air masses from the Ship Channel areas and are probably superimposed by elevated continental background ozone levels. In addition, these days show dry layers aloft.. Both features were frequently observed on high ozone days, whereas "non-ozone" days were only seldom associated with easterly wind direction (if they were, wind speeds were high thus suppressing high ozone values) and the soundings in the free troposphere did not reveal dry layers.

The results so far indicate that PBL effects on ozone levels cannot be considered as an isolated process. Various effects likely superimpose and require further analysis. In particular, the contribution from ozone in the residual layer, free troposphere and from the continental/marine background may be important. Synoptic-scale impacts as evident in the humidity conditions in the free troposphere will also likely play a major role.

At this point only PBL effects on ozone have been considered. Primary precursors which are emitted close to the surface and most likely trapped within the PBL, and do not have significant levels in the residual layer need have not been included in this analysis.

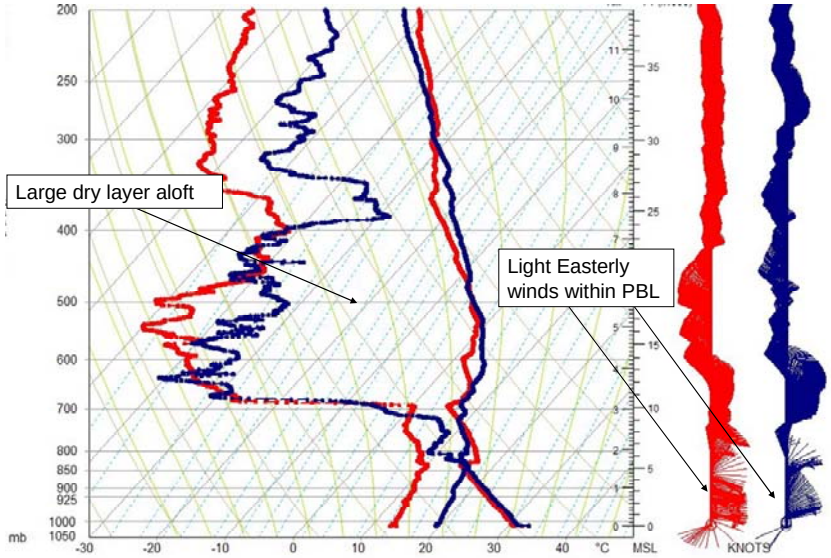

Figure 4. Dewpoint and ambient temperature as obtained in radiosonde launchings on August 31 (red lines) and September 01 (blue lines).

Planetary Boundary Layer Height Calculation

When compared to other methods under similar meteorological conditions (those that are favorable for high ozone), the rawinsonde seems to yield the most accurate results when compared to wind profiler and lidar data [*Marsik et al.*, 1994]. Also, many boundary layer studies that utilize remote sensing techniques to determine the PBL height use rawinsonde data as a standard for comparison [*Marsik et al.*,1994; *Grimsdell and Angevine*, 1998; *Berman et al.*, 1999; *Eresmaa et al.*, 2006].

Seemingly, the best method to use in determination of the boundary layer height would be through tracking certain atmospheric constituents such as carbon monoxide or light aerosols [*Berman et al.*, 1999]. However, it is not practical to get vertical in-situ measurements of atmospheric species with the exception of ozone, which is a secondary pollutant.

For this study, soundings were separated into morning and afternoon/evening times. It has been shown that temperature and water mixing ratio profiles can reveal the location of the top of the boundary layer [*Wiegner et al.*, 2006]. For the morning soundings, the height of the morning inversion was used to determine the mixing layer height [*Eresmaa et al.*, 2006]. The mixing layer height in the mornings was defined as the first location where temperature began to decrease with height (through visual inspection). For the remaining soundings, the boundary layer was estimated using graphical representations of each sounding. Potential temperature was calculated for every sounding and water mixing ratio was taken from the sounding data itself. The mixing layer height was determined in a subjective manner by finding the point where there is a sharp increase in potential temperature [*Senff et al.*, 2002; *Yi et al.*, 2000], and a sharp decrease in water mixing ratio. These parameters were plotted for every sounding. An example sounding is shown below in Figure 5.

Another technique is determining the mixing layer height by using the first inversion height, assuming the potential temperature profiles meet two criteria [*Marsik et al.*, 1994] :

1) $\Delta\theta/\Delta Z > .005$ K/m

2) $\theta_{top} - \theta_{base} > 2K$

This technique was developed by *Heffter* [1980]. The height of the boundary layer is taken to be the top of the 2K difference [*Marsik et al.*, 1994].

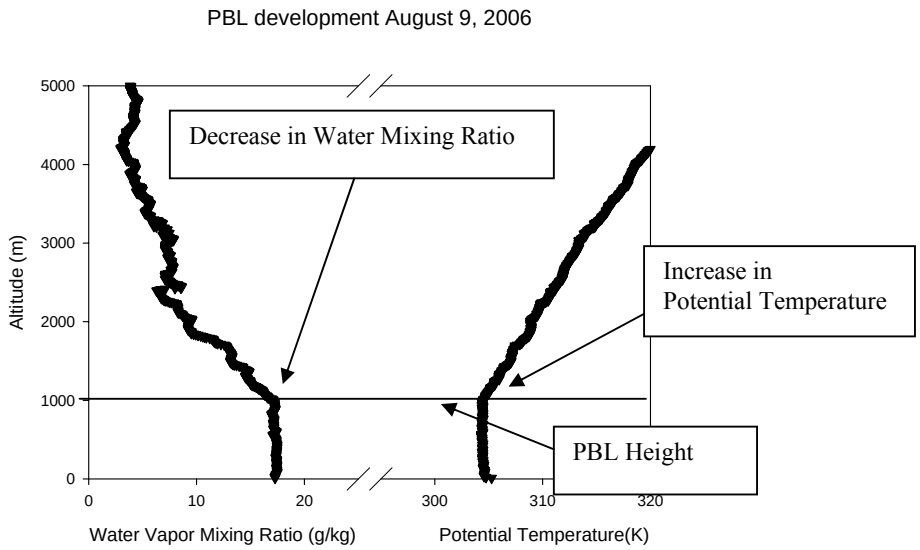

Figure 5. Water mixing ratio and potential temperature taken from rawinsonde launch at 7 PM CDT August 9, 2006.

Although H*effter's* technique was investigated in this study, this technique seemed to overestimate the boundary layer. It did not follow the height where the water mixing ratio began to decrease, which has been shown to be an indicator of the boundary layer height [*Berman et al.*, 1999]. For an example, an obvious under-estimation of the PBL height occurred on August 09, 2006. A time series of PBL heights based on potential temperature and water mixing ratio are shown below in Figure 6. It can be seen from this example that the approximate height of the boundary layer is 1000 m. However, the height estimated from *Heffter's* method [1980] is 1900 m. This is likely the result of moisture not being taken into account in *Heffter's* method.

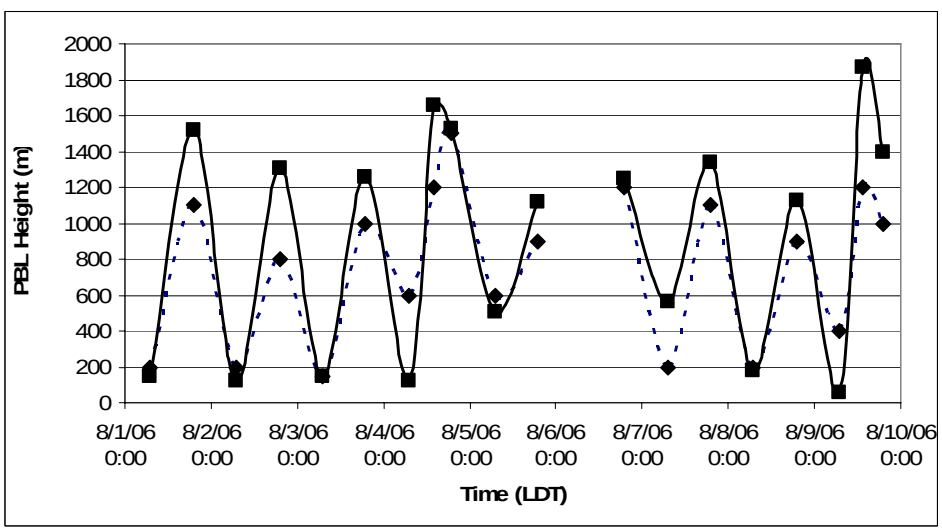

Figure 6. Comparison of subjective method (dashed line) vs. Heffter (1980) method (solid line).

The Effect of the Morning Inversion Height on Houston's 8 Hour Ozone Peak

It has been hypothesized that the role of the morning inversion height and strength has an effect of concentrating ozone precursors and may lead to higher hourly ozone peaks during the day [*Berman et al.*, 1999]. This occurs during a typical morning rush hour, when mixing layer heights are low and ozone precursors are being emitted at a rapid rate [*Berman et al.*, 1999]. This can slow the development of the mixing layer height in the mid-morning hours and lead to higher observed ozone levels in the afternoon [*Berman et al.*, 1999]. This can occur by a downward vertical mixing of the residual layer in the mid-morning hours as the morning inversion breaks up, which has been shown to increase the hourly concentration of ozone [*Zhang and Rao*, 1999]. Since these previous studies have analyzed the growth rate of the boundary layer in the morning hours, it should be determined whether or not the strength of the morning inversion is linked to the afternoon ozone peak. Figure 7 shows the morning inversion strength compared to the 8 hour peak ozone in the afternoon. Figure 8 shows the rate of temperature increase with height compared to the peak 8 hour ozone in the afternoon.

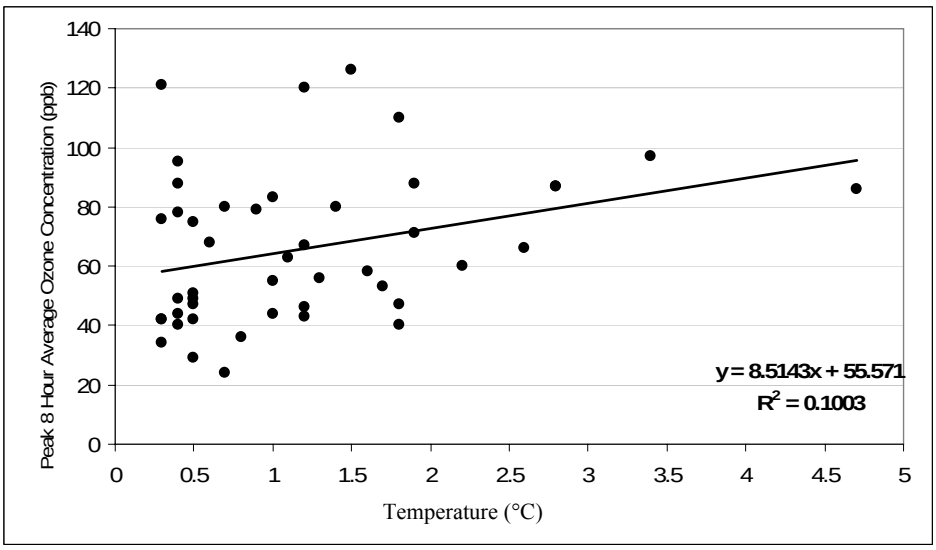

Figure 7. Strength of morning inversion (°C) compared to 8-hr peak ozone.

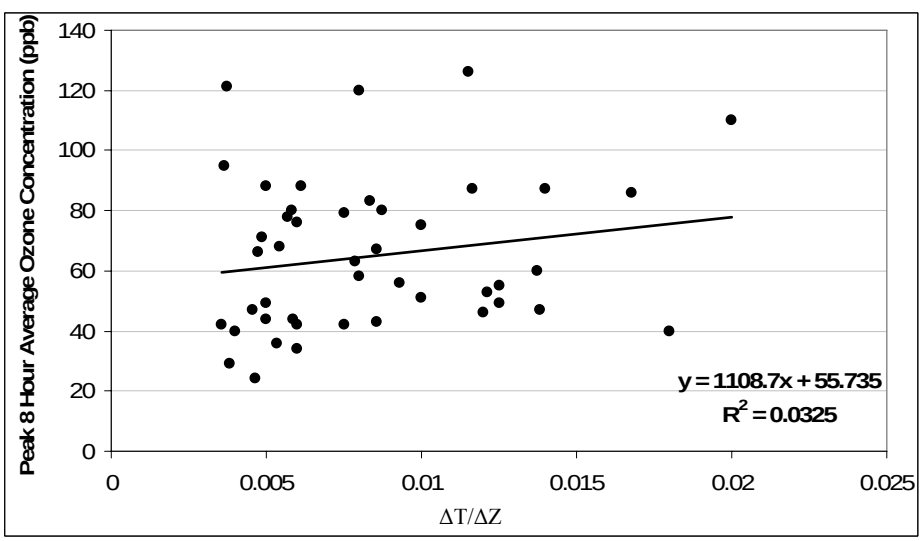

Figure 8. Strength of morning inversion (°C) compared to 8-hr peak ozone rate of change of temperature with height (°C/m) compared with 8-hr peak ozone.

The above figures show that there is very little correlation between morning inversion strength/rate of change and afternoon peak ozone. There are certainly also other factors that dictate the afternoon ozone peak including the amount of stagnation, solar radiation, wind direction, presence/absence of precipitation, and temperature. For instance, cool temperature in the morning hours could lead to a strong morning inversion, however these days are not necessarily ozone episode days since the northerly flow is usually too strong and background levels are initially too low.

The Effect of the PBL Height on the Average 8 Hour Ozone Peak

This rawinsonde study is limited for the purposes of determining the PBL height's relation to ozone peak. Soundings were taken daily at 0700 and 1900 CDT. Although the strength of the morning inversion was captured well from the 0700 CDT soundings, the development of the PBL height in the morning hours was not always captured. Also, the afternoon PBL peak was not always observed due to a lack of data in the afternoon hours. Only on intensive days, i.e. ozone episode days, soundings were taken every 3 hours. Figure 9 shows the average rate of PBL development on episode vs non-episode days. These results closely match those found in *Berman et al.* [1999].

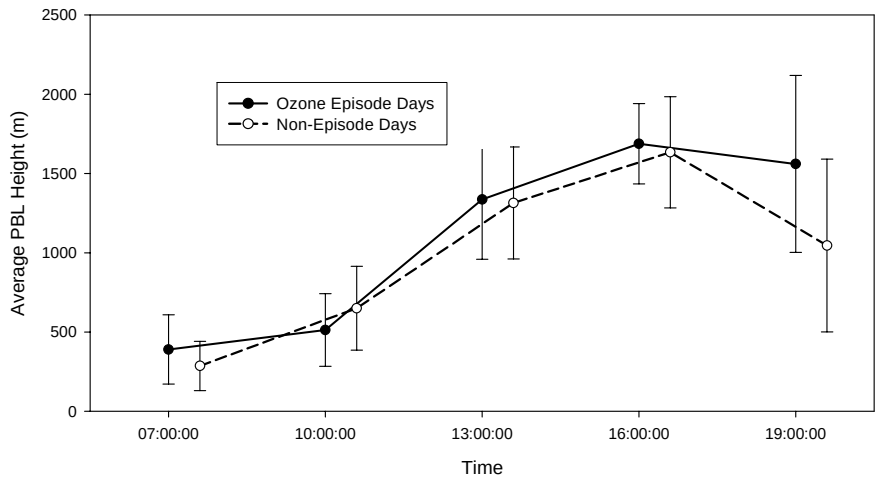

Figure 9. Development of the boundary layer on ozone episode days and non-episode days.

It can be seen from this graph that the development of the PBL in the morning may be slower on episode days. This is likely due to the fact that most of the episode days within this study period occurred in a post-frontal environment with relatively cool temperatures in the morning. This may result in a delay of the boundary layer development.

It should be noted that there are many more soundings at 0700 CDT and 1900 CDT (e.g. see Table 1). As discussed previously, there is little correlation between the height and/or strength of the morning inversion when comparing episode and non-episode days. However, the average PBL height at 1900 CDT on non-episode days is actually about 400 m lower than on episode days. Possible explanations for this phenomenon include the presence of cloud layers on non-episode days, precipitation, and/or southerly flow lowering the PBL in the evening (either from synoptic forcing or onset of the sea breeze). However, this is also within one standard deviation which is approximately 550 m at 0700 CDT.

Time	Episode Days	Non-Episode Days
7:00	10	46
10:00	8	4
13:00	11	6
16:00	8	3
19:00	10	45

Table 1. Number of data points used in Figure 9.

The Role of Elevated Inversions on Houston's Ozone Peak

In the post-frontal environment, it was noted that the soundings on ozone days had several features in common. One of these features was a strong elevated inversion, indicating an extremely stable atmosphere in the post-frontal environment. There was also evidence of advected continental air both at the surface and aloft, providing favorable conditions for an ozone episode day (e.g. clear sky) along with subsidence. This subsidence may increase the entrainment effect of the residual layer aloft, as is described in *Zhang and Rao* [1999]. Since an elevated inversion was present during most of the high ozone days (especially in September), different characteristics of the air mass associated with this inversion were analyzed. Figure 10 shows the skew-t plot on the morning of August 31, 2006. A very strong elevated inversion can be noted.

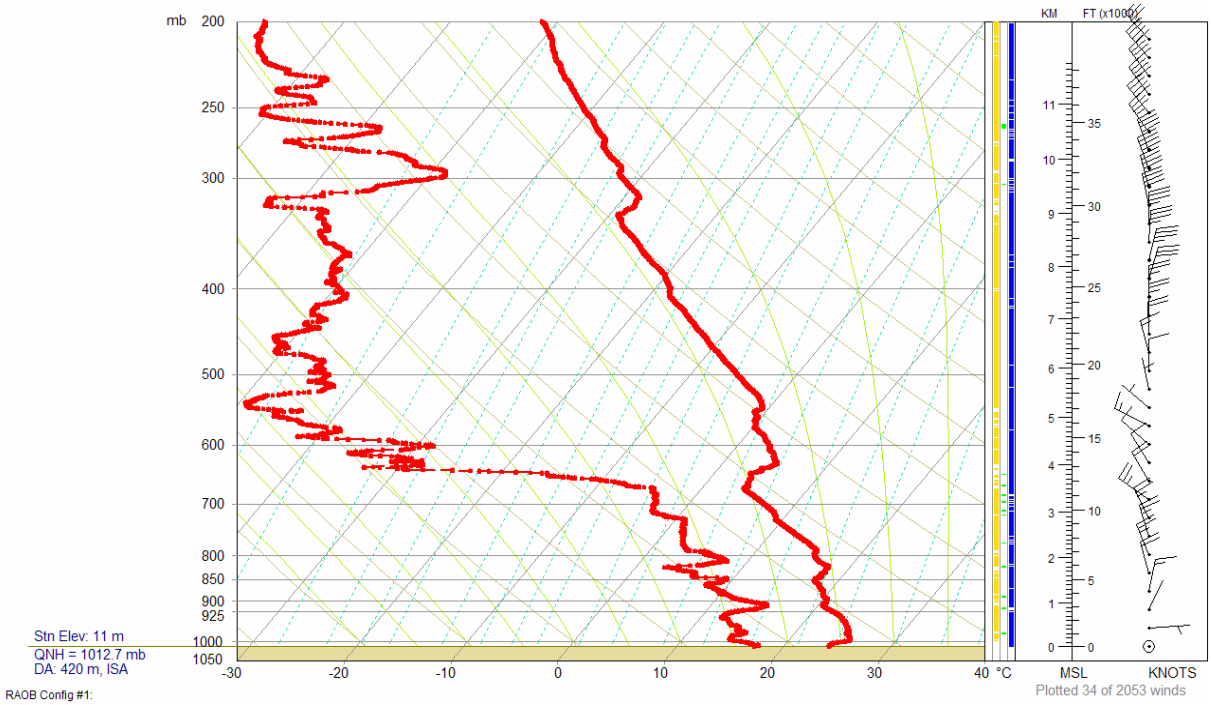

Figure 10. Skew-t plot at 0700 CDT August 31, 2006.

To find the possible role that inversions play on Houston's 8 hour ozone peak, inversions for each sounding at 0700 CDT and 1900 CDT were categorized by strength of inversion (by amount of temperature increase), moisture, and height. Inversions that were less than 0.3°C were ignored. The results of the 0700 CDT analysis are shown in Figure 11. This figure shows that the strongest elevated inversions are not necessarily correlated with the highest ozone values. However, the dry air masses aloft (see back corner of the diagram) are associated with frontal passages which occurred in the days preceding ozone episodes. The diagram shows that the highest ozone averages occurred when the relative humidity of the air mass was rather low, but the inversion itself may not have been very strong. This is evidence that although the inversion still exists, it is getting weaker as instability gradually increases in the post-frontal environment. Figure 7 also shows that moist inversions typically do not occur on episode days. This is because these moist inversions are usually associated with cloud layers, which help prevent higher ozone levels from occurring due to a lack of photochemistry. Figure 7 summarizes the vertical temperature and moisture structure observed during most of Houston's ozone episodes in August and September 2006. Directly behind a cold front the northerly flow would be too strong for an episode to occur, but these days are associated with the driest air masses aloft. As the front departed the area and high pressure settled in, background levels would increase and ozone

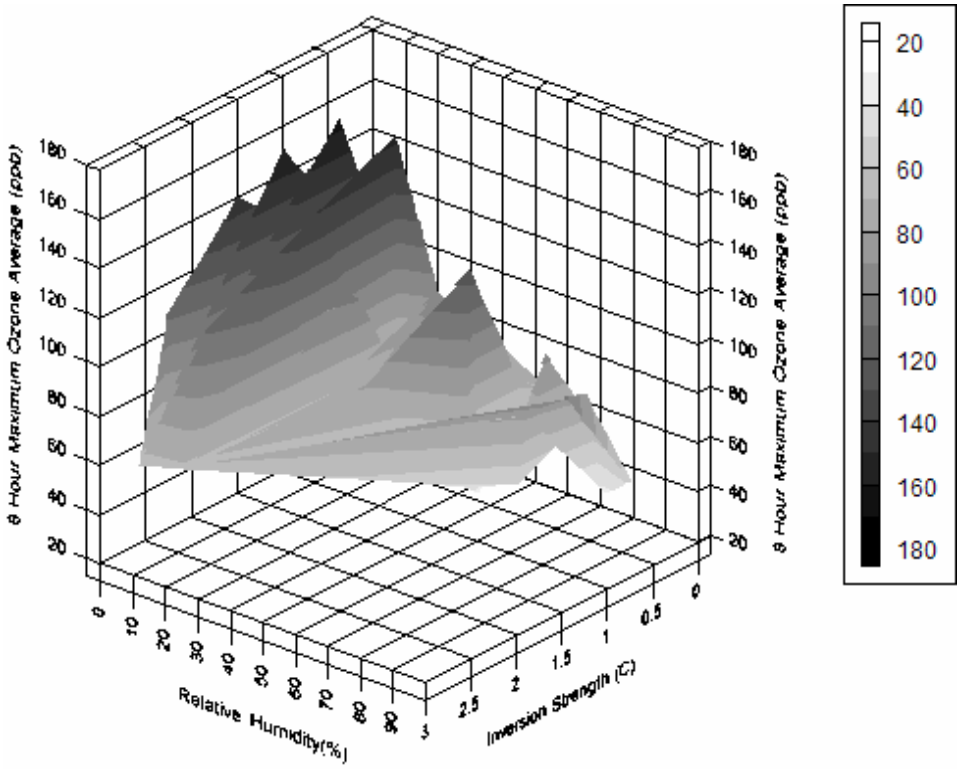

Figure 11. 8-hr average ozone peak compared with elevated inversion strength (°C) and relative humidity (%) at the top of the inversion.

episodes were more likely to occur. This is shown in Table 3 later in this report, where only one of the post-frontal episodes occurred the day after a frontal passage.

Composite soundings of 2006 Ozone Episodes

Composite skew-t diagrams were produced to gain a better perspective of the vertical profile of the atmosphere during August and September 2006. The composite skew-t for August ozone episodes is shown in Figure 12, and the composite skew-t for September ozone episodes is shown in Figure 13. The soundings were based on the 0700 CDT launch time. The only exception was when one 1000 CDT sounding was used for the episode on August 17, since no 0700 CDT sounding was available.

There is little difference in the skew-t diagrams between episode and non-episode days in August, with the exception of the wind direction and speed in the boundary layer. Strong southerly winds reveal the prevailing wind tendency, whereas episode days reveal increased stagnation. A similar analysis for the month of September is shown in Figures 14 and 15.

The morning inversion for the September episode days is much stronger, and the elevated inversion is also more noticeable in the September episode composite. This is again due to the frequent frontal passages that occurred during the month of September. August soundings also contain more moisture than September, again due to the lack of northerly flow bringing in dry continental air to Houston. The non-episode composite sounding of September reveals more moisture present in the atmosphere, along with a stronger southerly wind.

The lower level winds are also quite different. August soundings tend to have more of a southerly component, which is due to the prevailing wind. September soundings on episode days seem to have a northeasterly component. This shows both a tendency for northerly flow increasing background levels, and easterly flow bringing in precursors from the Ship Channel.

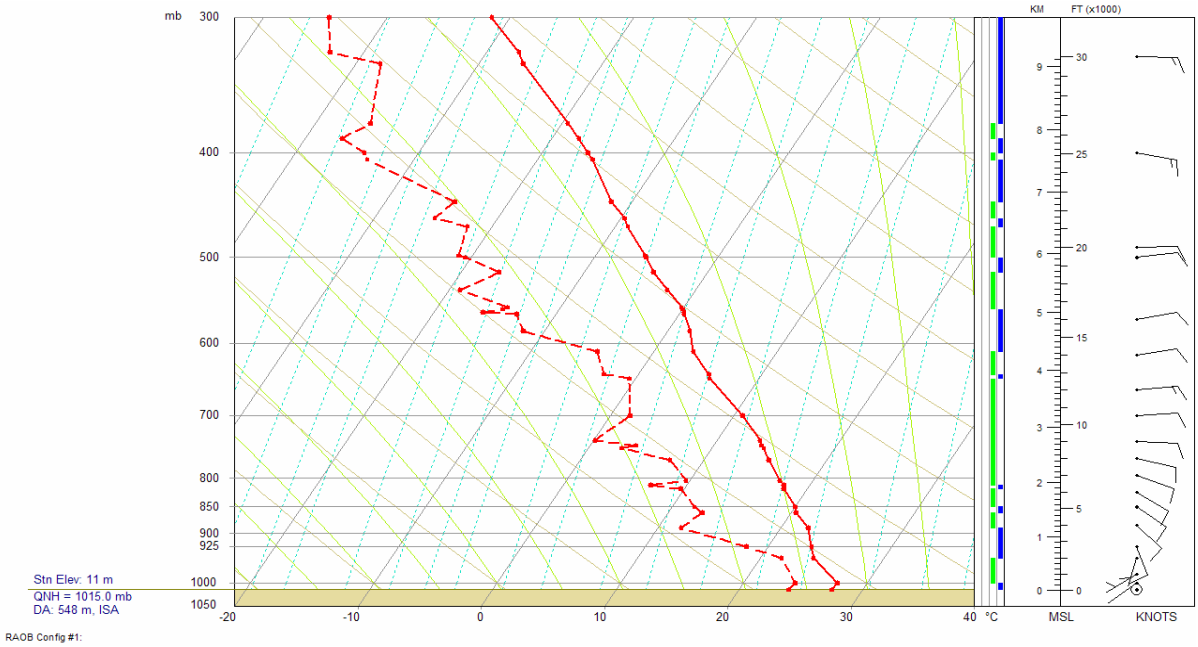

Figure 12. Composite skew-t diagram for August episode days at 0700 CDT (4 days).

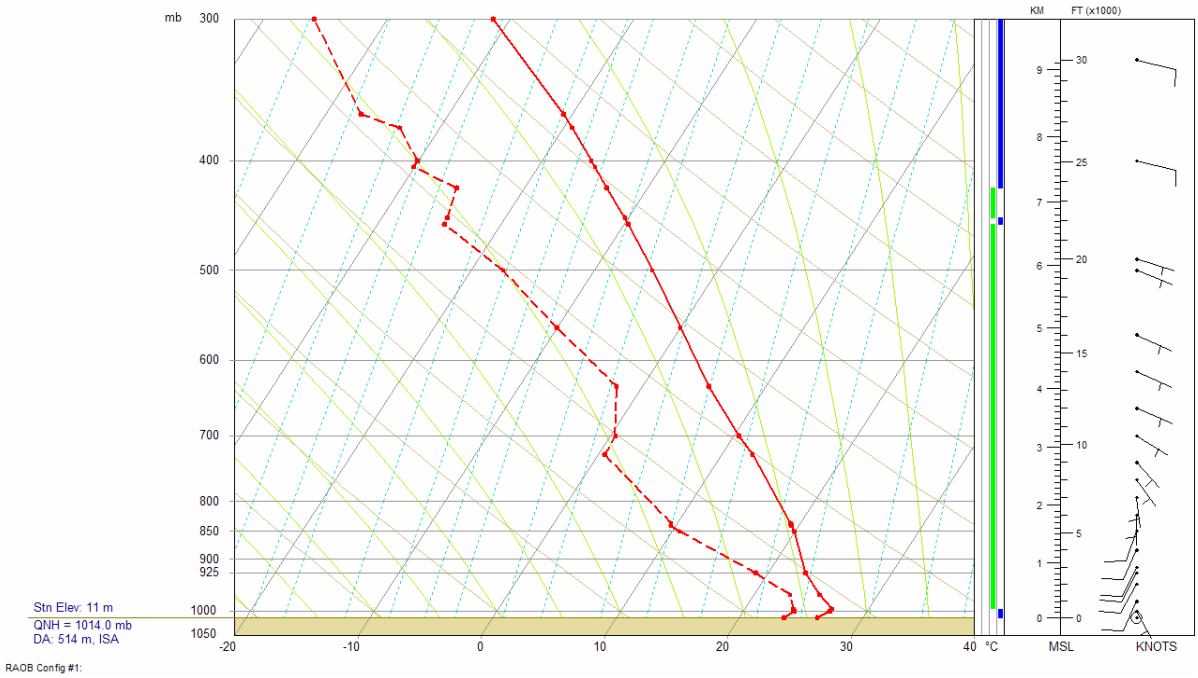

Figure 13. Composite skew-t diagram for August non-episode days at 0700 CDT (25 days).

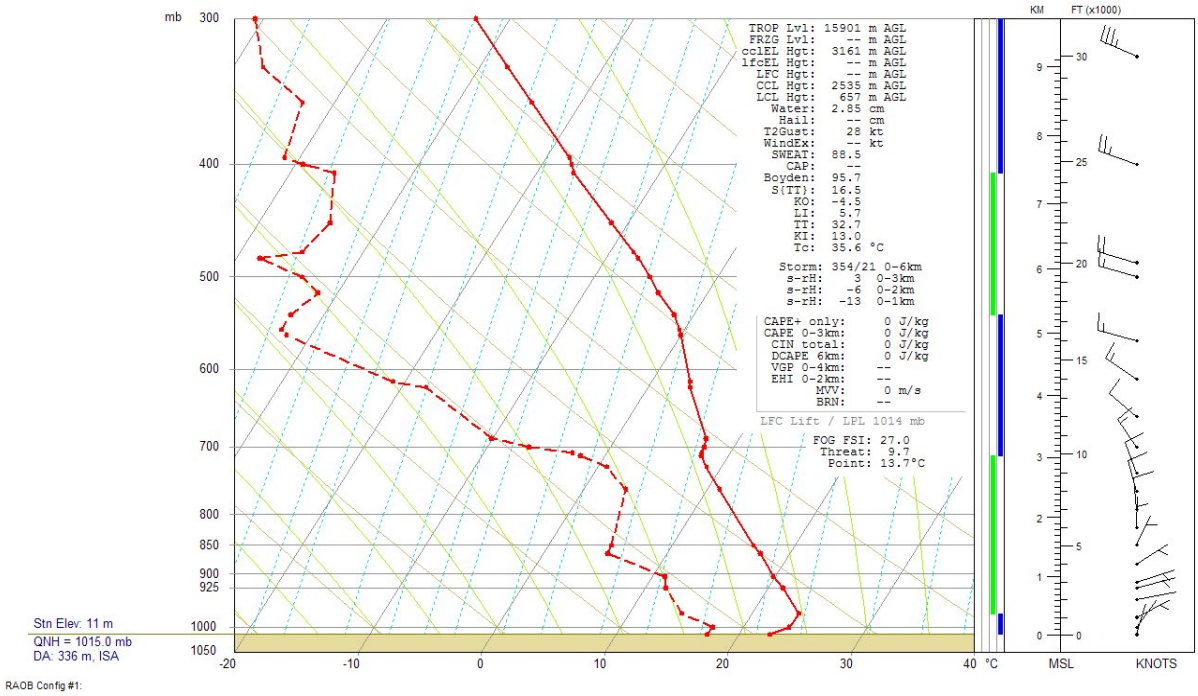

Figure 14. Composite skew-t diagram for September episode days at 0700 CDT (9 days).

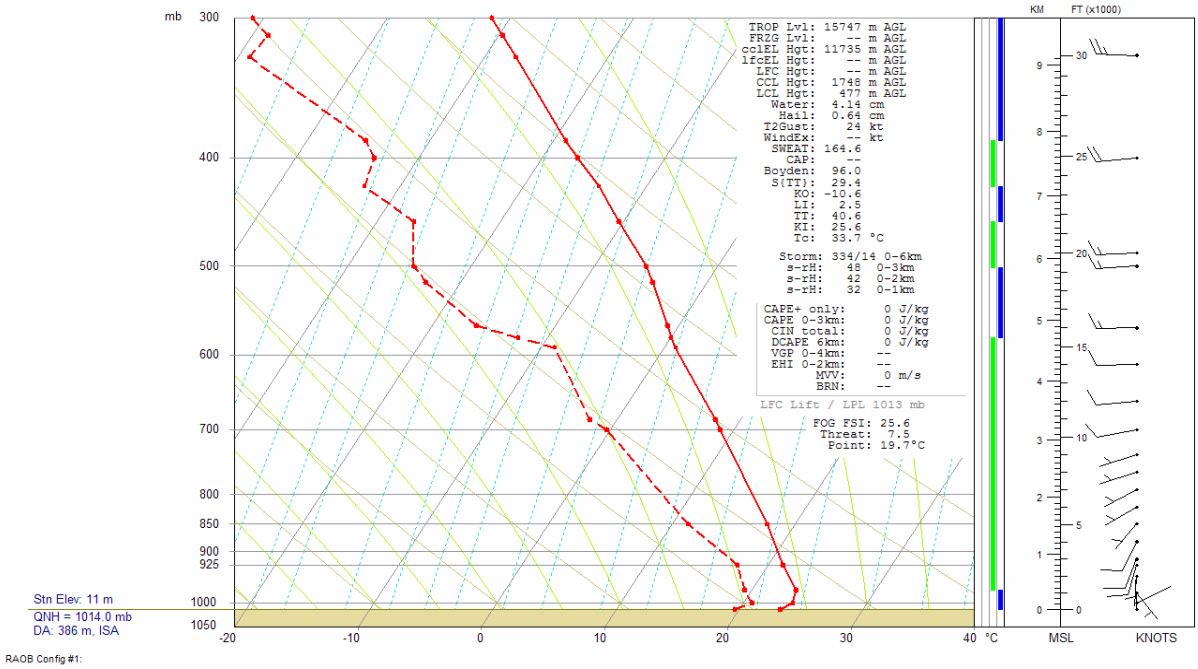

Figure 15. Composite skew-t diagram for September non-episode days at 0700 CDT (21 days).

3.2 Land-sea-bay breeze interaction with planetary boundary layer growth, depth, and observed ozone concentrations (Sub-Task 6.2).

In order to elucidate the interaction of the land-sea-bay breeze interaction with the PBL various CAMS sites were included in this study to account for special coverage. Figure 16 shows the locations of all CAMS sites within the Greater Houston area. The selection of the CAMS sites followed the following criteria:

1) Apart from meteorological parameters wind direction and wind speed the sites should also report ozone
2) Most of the sites should be located along a virtual line from the coastal areas, including the bay area, towards Houston downtown and a little bit beyond, e.g. downwind of the downtown area. The UH campus site with its vertical soundings should be located along this virtual line.

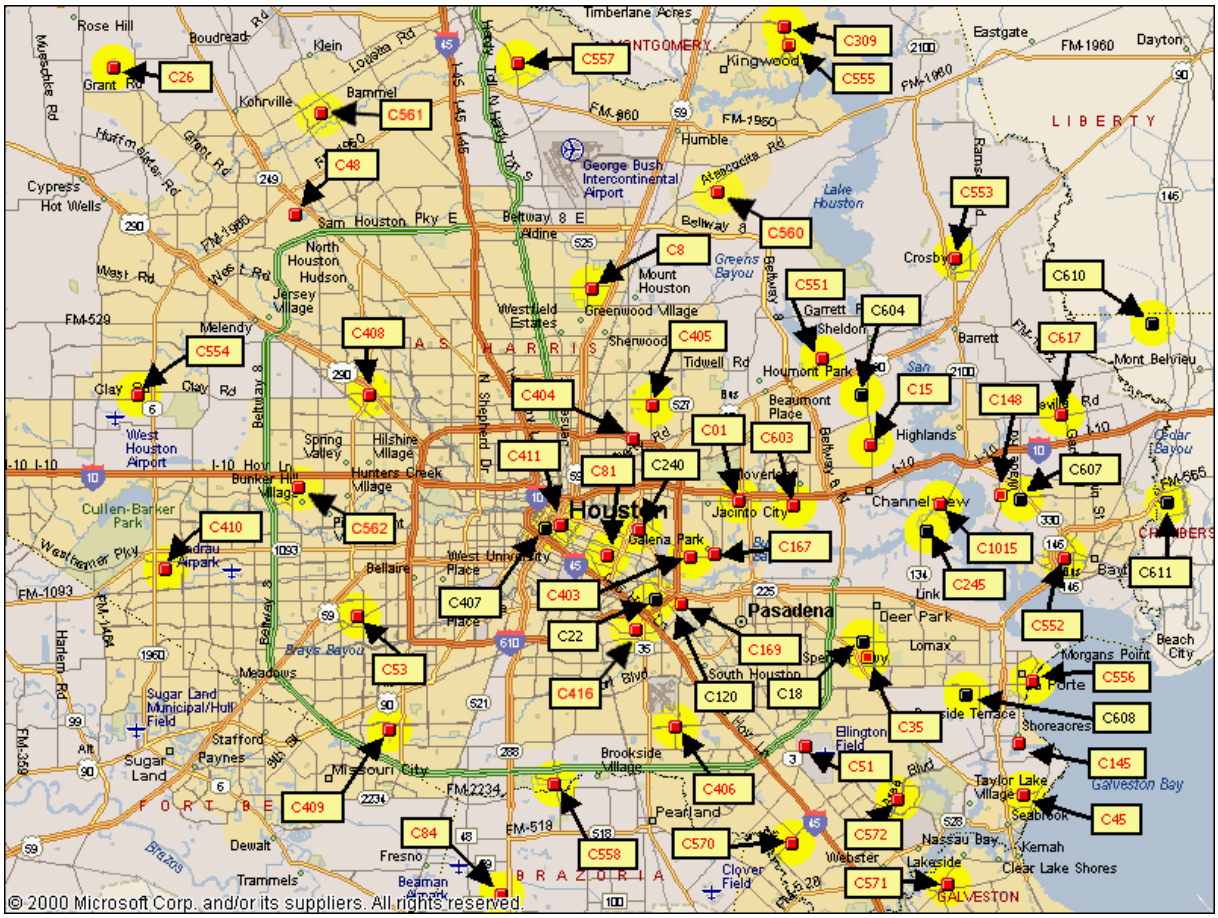

Figure 16. Location of CAMS sites.

The final selection included the following CAMS sites, ranked among their different CAMS code:

1) Aldine (C8)
2) Galveston (C34)
3) Deer Park (C139)
4) Milby Park (C169)
5) Clinton Rd (C403)
6) Kirkpatrick (C404)
7) Croquet ((C409)
8) Westhollow (C410)
9) Park Place (C416)
10) La Porte (C556)

In order to complement this data set, also the corresponding data sets obtained at the Moody Tower on UH campus was included. Unfortunately, for the sites Milby Park (C169) and Kirkpatrick (C404) no ozone data was available.

Figure 17 gives an overview about the temporal variation of the PBL height. This time series is based on regular two radiosonde launches per day and multiple radiosonde launches on IOP days. As can be seen from this figure PBL heights vary significantly and can range from less than 100 m AGL during nighttime up to 2700 m AGL during daytime. However, it should be noted that most of the daytime PBL heights are found between 1000 – 1500 m AGL.

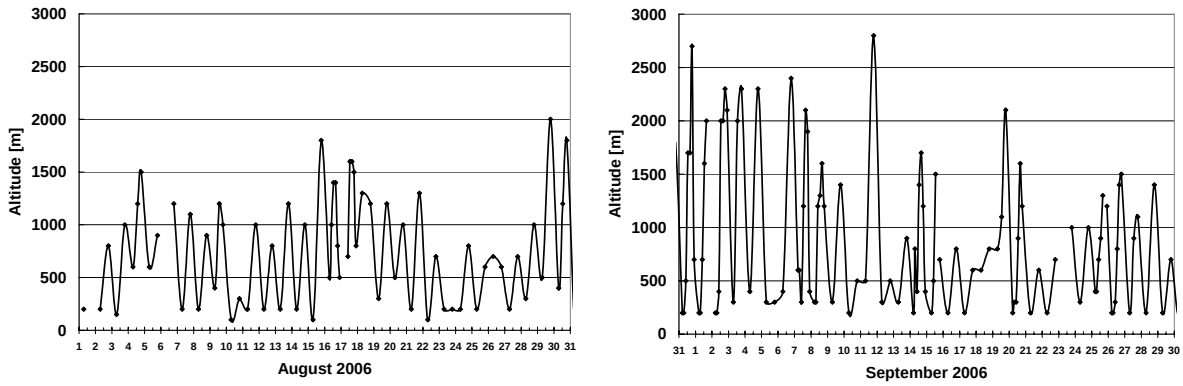

Figure 17. Time series of PBL heights during August and September 2006.

The following discussion will focus on selected IOP days, because multiple radiosonde launches give a more comprehensive insight into the diurnal variation of the PBL. In addition, IOP days were selected which have the most complete O_3 sonde data coverage

<u>August 31 – September 02, 2006</u>

Figures 18-20 describe these three days in some greater details. On August 31, 2006, ozone levels measured "Very Unhealthy". This was based on the 8-hr average of 126 ppbv measured at the Westhollow site. This measurement rated level purple, "Very Unhealthy", based upon the EPA's Air Quality Index (AQI) scale. On September 01, 2006, ozone levels were also measured "Very Unhealthy", this time based on the 8-hour average of 129 ppbv measured at the LaPorte site. High ozone levels were also initially forecasted for September 02, but actually did not occur. Figure X show that maximum ozone levels on September 02 reached about 80 ppbv, whereas ozone levels during the preceding days reached up to around 160 ppbv. As shown in the diurnal PBL heights, maximum PBL height was observed at the 1900 CDT radiosonde launching on August 31 and was about 2700 m AGL . In a layer between 2700 m AGL and 3500 m AGL a background ozone concentration level around 60 ppbv was found throughout this 3 day episode. Above this altitude the ozone profile showed more variations, possibly due to long range transport events which actually did not penetrate into lower tropospheric levels. The layer between 2700 AGL - 3500 m AGL altitude was always associated with northerly wind directions, with a more distinct shift towards northeastern on the last day, September 02. As can be seen from Figures 18-20 land-sea breeze conditions clearly occur on the first two days and are confined to the PBL. The first two days are basically characterized by strong wind shear at the top of the PBL, a feature which is only present in the early morning hours of September 02. Usually, the impact of the land-sea breeze system can be best identified looking into the wind pattern at Galveston. In addition, this site allows to characterize the marine background conditions under onshore wind conditions. On August 31, the Galveston site has about 60 ppbv during daytime under onshore wind conditions which also coincides with the tropospheric background conditions between 2700 AGL – 3500 m AGL altitude. The corresponding values on September 01 are approximately

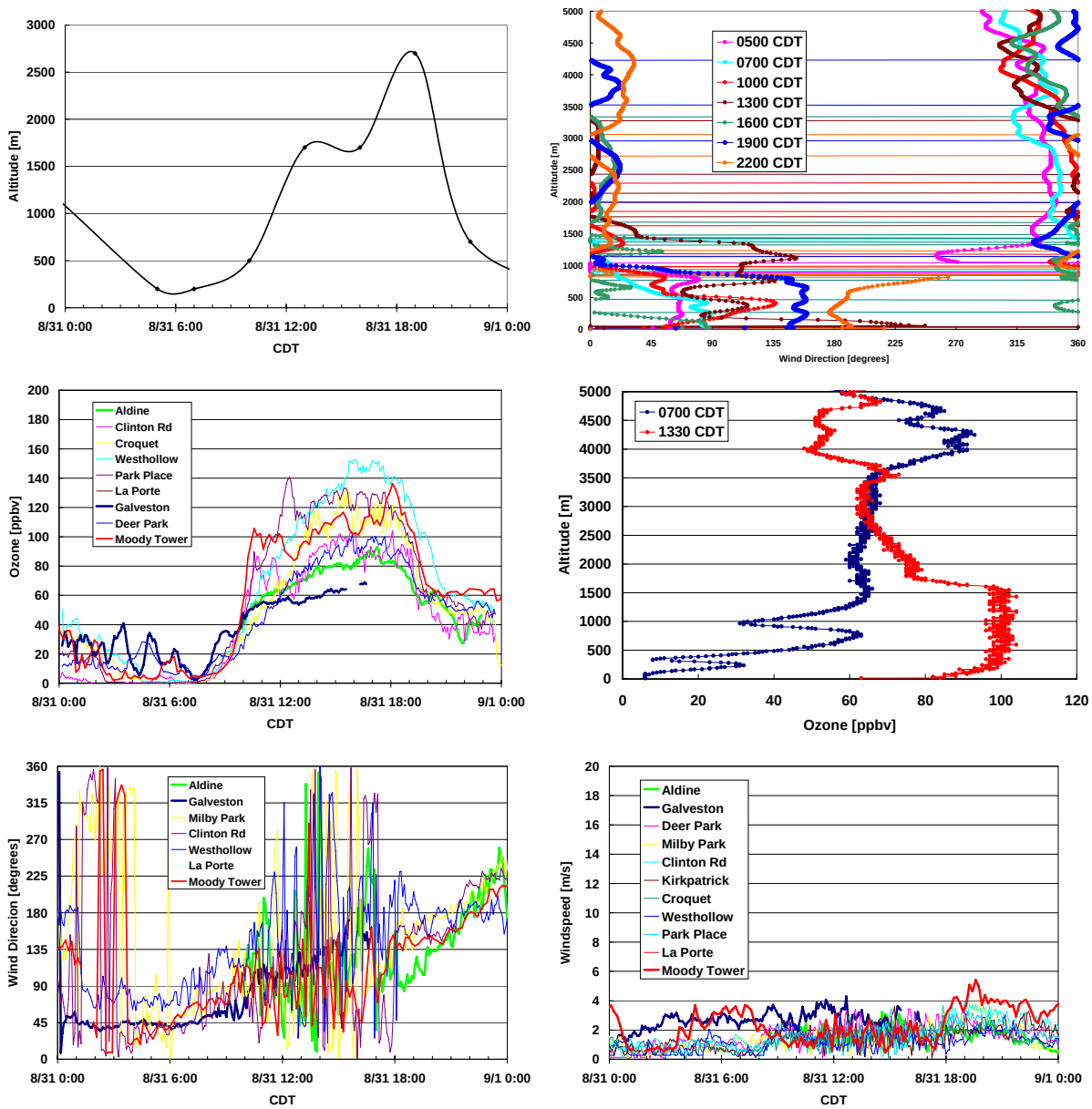

Figure 18. PBL characteristics for August 31, 2006. Left column: Diurnal variation of the PBL height (uppermost plot) based on UH radiosondes, of surface ozone (central plot), and of surface wind direction (lowermost plot) for selected CAMS sites. Right column: vertical profiles of wind direction (uppermost plot) and ozone (central plot) based on UH radiosondes and ozonesondes, and diurnal variation of surface wind speed (lowermost plot) for selected CAMS sites.

20 ppbv higher indicating the impact of recirculating air masses which under land sea breeze condition will likely lead to higher regional background ozone levels. These higher background levels are also reflected in the overall increase of the ozone levels in the afternoon ozone sonde launches which rise from about 100 ppbv in the PBL up to 1500 m AGL on August 31 to slightly below 120 ppbv on September 01. Strong increases in ozone levels at the individual sites are usually associated with wind directions which shift through easterly directions, also coinciding with bay breezes at this time. The strong increases in ozone levels around 10 am CDT on August 31 are closely related to these conditions, whereas on September 01, corresponding increase in ozone levels occurs slightly later which coincides with a rapid shift from NW conditions to NE and E wind patterns. As discussed

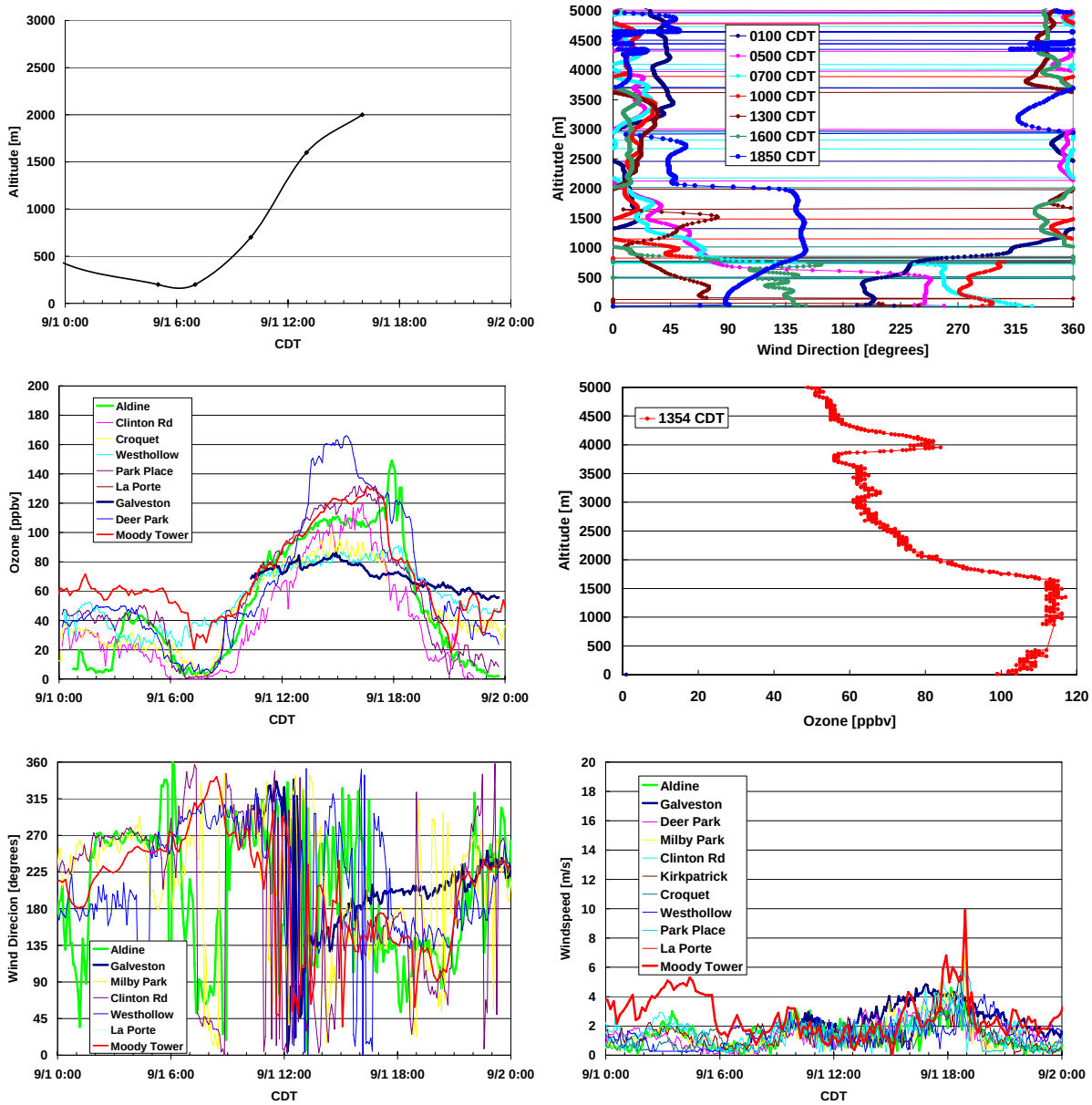

Figure 19. PBL characteristics for September 01, 2006. Left column: Diurnal variation of the PBL height (uppermost plot) based on UH radiosondes, of surface ozone (central plot), and of surface wind direction (lowermost plot) for selected CAMS sites. Right column: vertical profiles of wind direction (uppermost plot) and ozone (central plot) based on UH radiosondes and ozonesondes, and diurnal variation of surface wind speed (lowermost plot) for selected CAMS sites.

earlier, September 02, is influenced by a breakdown of the land-sea breeze condition and the wind shear on top of the PBL. Only at Galveston, there is some tendency towards a land-sea breeze occurs with SE wind conditions. All other sites report NE to E winds. It seems that a couple of factors help to keep ozone levels at a moderate level on September 02. The weakening of the land sea breeze system leads to less recirculation. The weakening of the wind shear at top of the PBL may lead to a weaker inversion strength (see Appendix I). An important factor seems to be that (i) under distinct land-sea-bay breeze conditions E wind flow conditions occur which bring Ship Channel emissions into the Houston area and that (ii) these conditions occur during late morning hours at relatively low PBL heights, but already at a time where fast photochemistry occurs, in particular formaldehyde (HCHO)

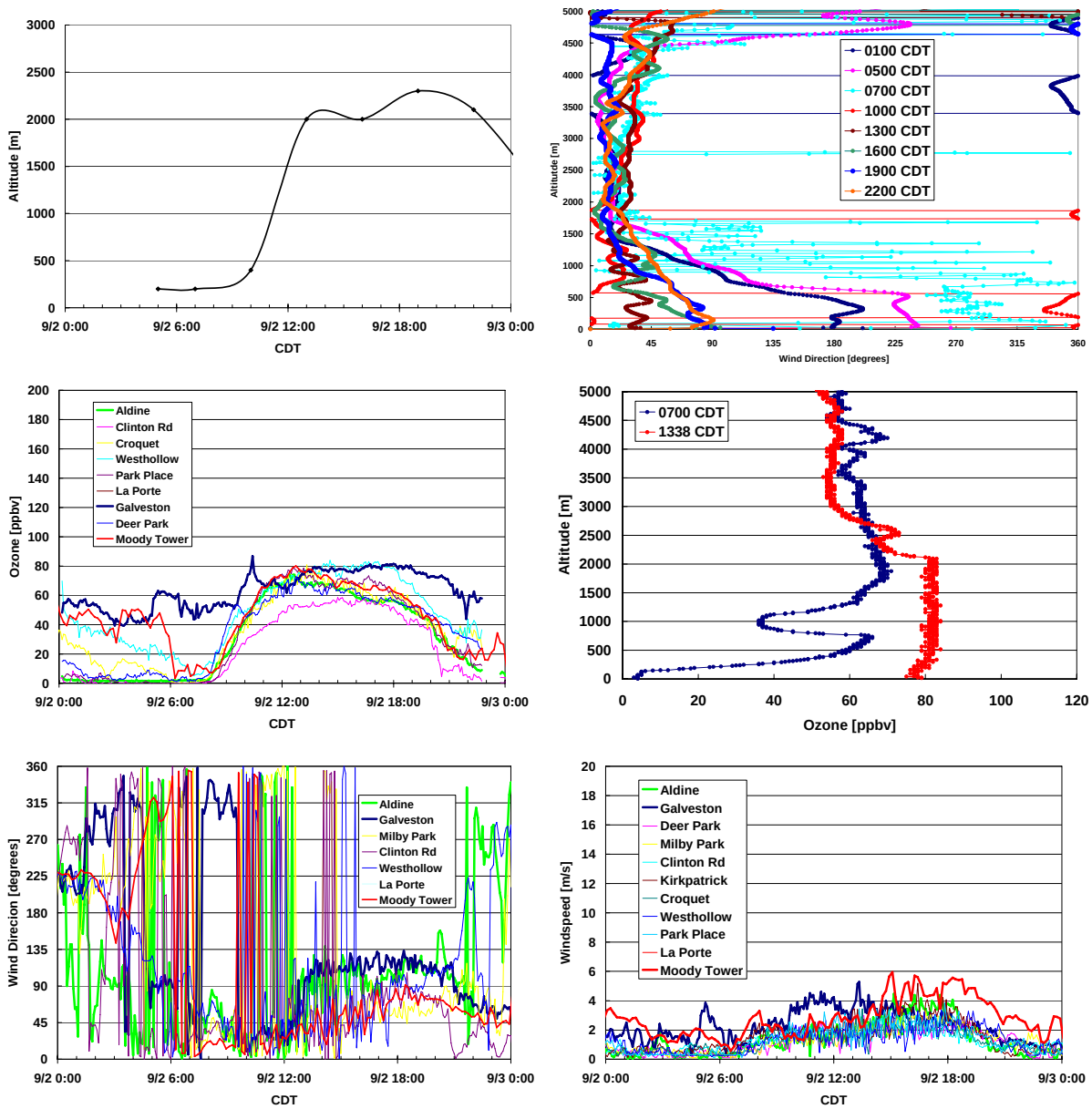

Figure 20. PBL characteristics for September 02, 2006. Left column: Diurnal variation of the PBL height (uppermost plot) based on UH radiosondes, of surface ozone (central plot), and of surface wind direction (lowermost plot) for selected CAMS sites. Right column: vertical profiles of wind direction (uppermost plot) and ozone (central plot) based on UH radiosondes and ozonesondes, and diurnal variation of surface wind speed (lowermost plot) for selected CAMS sites.

photochemistry. Low PBL heights at this time will also lead to a volume effect leading to higher concentrations.

Figure 21 reflects these findings overlaying diurnal ozone variations with the corresponding PBL variations. On August 31 and September 01 increase in PBL height is significantly delayed compared to September 02, when the PBL rapidly increases up to around 2000 m AGL from 1000 CDT to 1300 CDT. It appears that on August 31 delayed PBL increase and E wind patterns at this time of the day lead to ozone levels higher than 80 ppbv at various sites already at around 10 am CDT, i.e. earlier than on September 01 which can also enhance the overall probability for an 8-hr ozone exceedance.

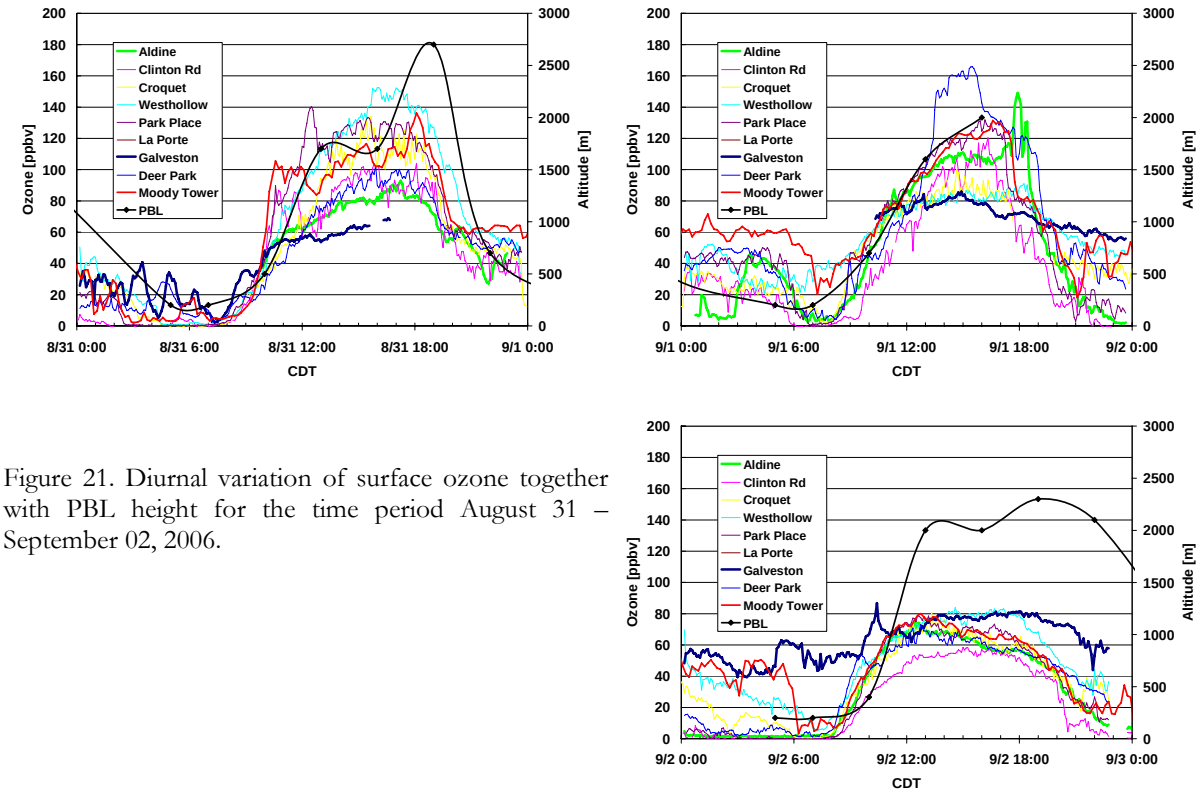

Figure 21. Diurnal variation of surface ozone together with PBL height for the time period August 31 – September 02, 2006.

September 14 and September 20, 2006

September 14, 2006, was labelled as a "level red" day and September 20, 2006, was classified a "level orange" day. Figures 23 – 24 show the overall conditions on these two days. Both IOP days reflect similar conditions as for the period discussed previously: (i) wind shear at top of the PBL and land-sea-bay breeze conditions confined to the PBL, (ii) background tropospheric ozone levels between top of the PBL and about 3500 m AGL are about 60 ppbv and coincide marine background conditions at Galveston under onshore wind conditions (note: these are 1-day episodes with limited recirculation), (iii delayed increase of PBL height, and (iv) E-wind conditions during time period when PBL increases.

As shown in Figure 22 enhanced ozone levels already occur during the period when the PBL height increases. Note that on September 14 maximum formaldehyde levels were observed at Moody Tower around 11:30 am under E wind conditions. Elevated formaldehyde levels were also observed on September 20, however at around 12:45 pm, but still under increasing PBL height conditions. Again, it seems likely that these conditions enhance the probability for 8-hr ozone exceedances.

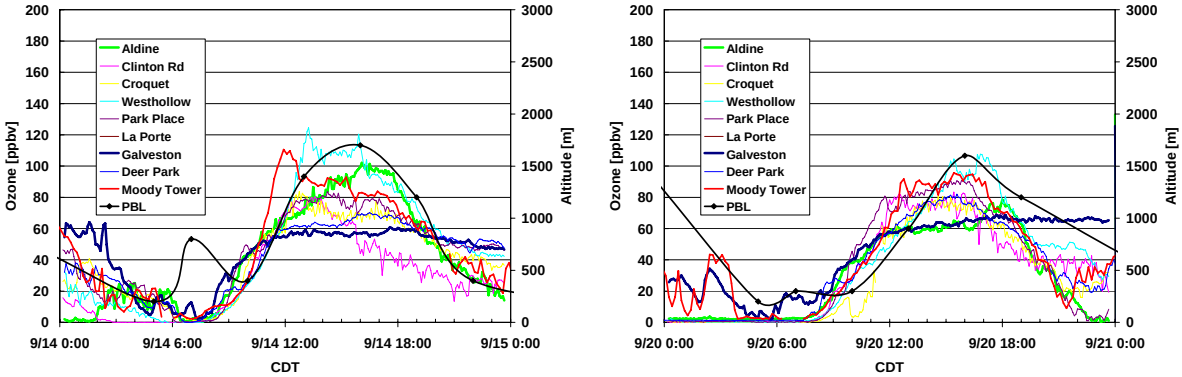

Figure 22. Diurnal variation of surface ozone together with PBL height for September 14 and 20, 2006.

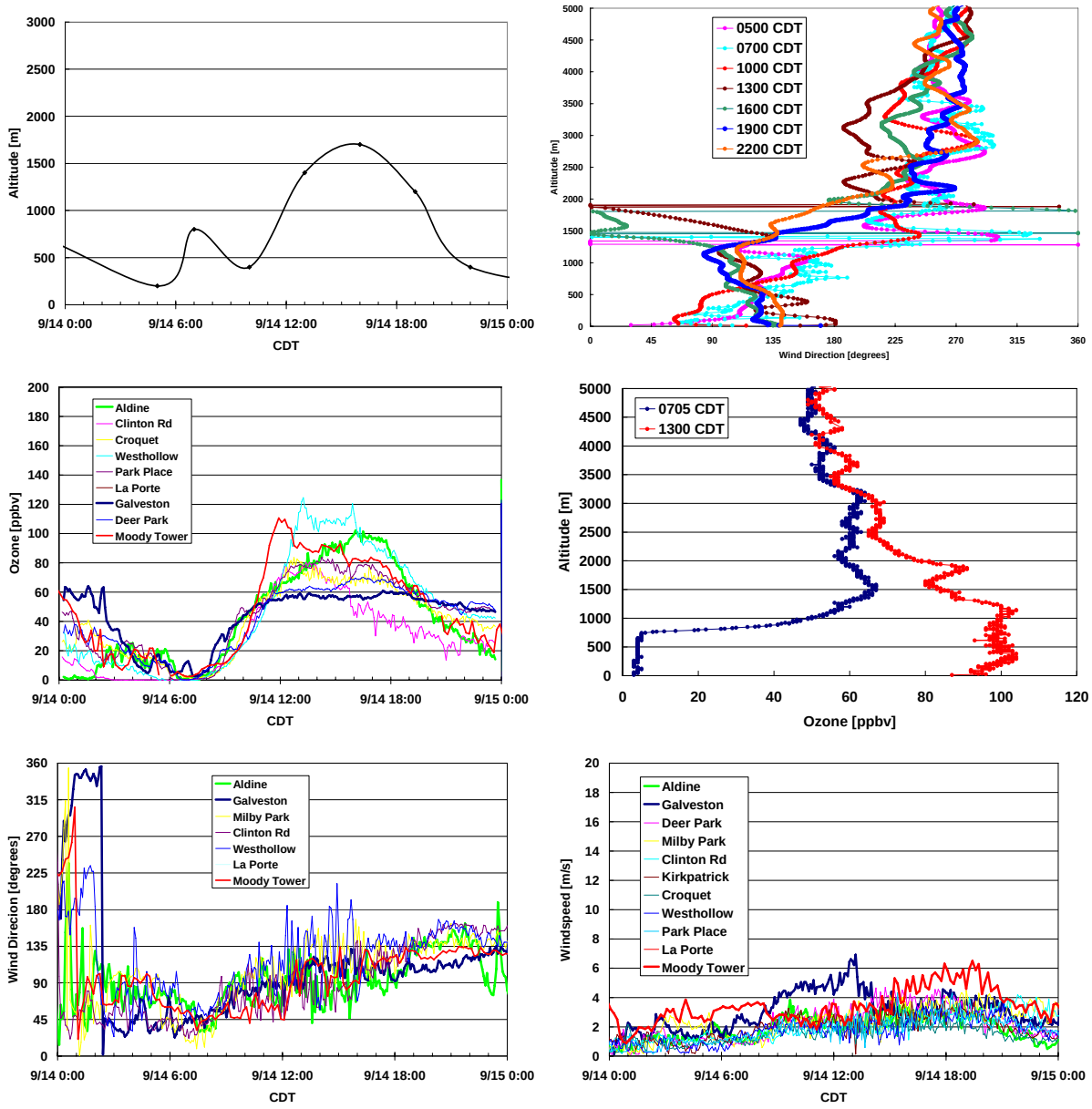

Figure 23. PBL characteristics for September 14, 2006. Left column: Diurnal variation of the PBL height (uppermost plot) based on UH radiosondes, of surface ozone (central plot), and of surface wind direction (lowermost plot) for selected CAMS sites. Right column: vertical profiles of wind direction (uppermost plot) and ozone (central plot) based on UH radiosondes and ozonesondes, and diurnal variation of surface wind speed (lowermost plot) for selected CAMS sites.

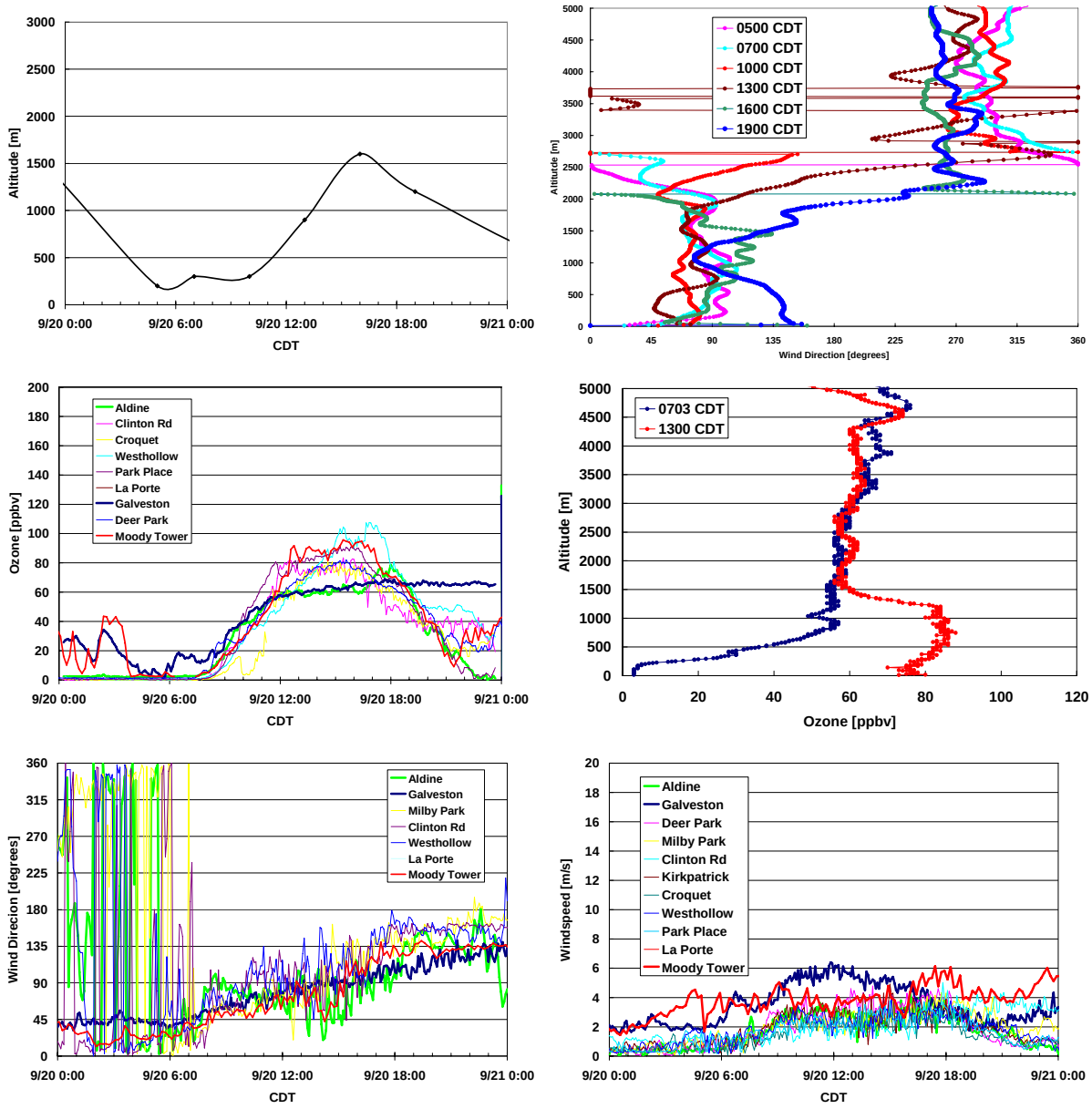

Figure 24. PBL characteristics for September 20, 2006. Left column: Diurnal variation of the PBL height (uppermost plot) based on UH radiosondes, of surface ozone (central plot), and of surface wind direction (lowermost plot) for selected CAMS sites. Right column: vertical profiles of wind direction (uppermost plot) and ozone (central plot) based on UH radiosondes and ozonesondes, and diurnal variation of surface wind speed (lowermost plot) for selected CAMS sites.

3.3 PBL observations vs. the MM5-modeled PBL dynamics, and the parameterization of vertical mixing in photochemical grid modelling (Sub-Task 6.3).

Comparison with CMAQ/MM5

Figure 25 shows a comparison of MM5 PBL results vs observations for the days August 30 – September 03, which includes the IOP days August 31 - September 02. From this plot it seems that MM5 consistently under-forecasts the PBL development during the morning hours. On September 02 the agreement is rather good. However, this day was not a high ozone day. Figure 26 is another example for a comparison between the MM5 forecasted PBL and the actual PBL.

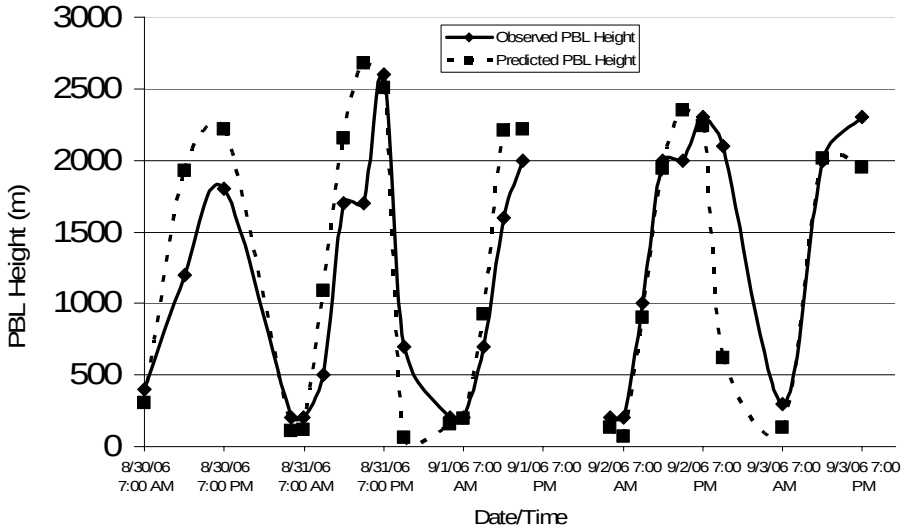

Figure 25. MM5 PBL comparison with sounding observations for period of August 30 – September 3, 2006.

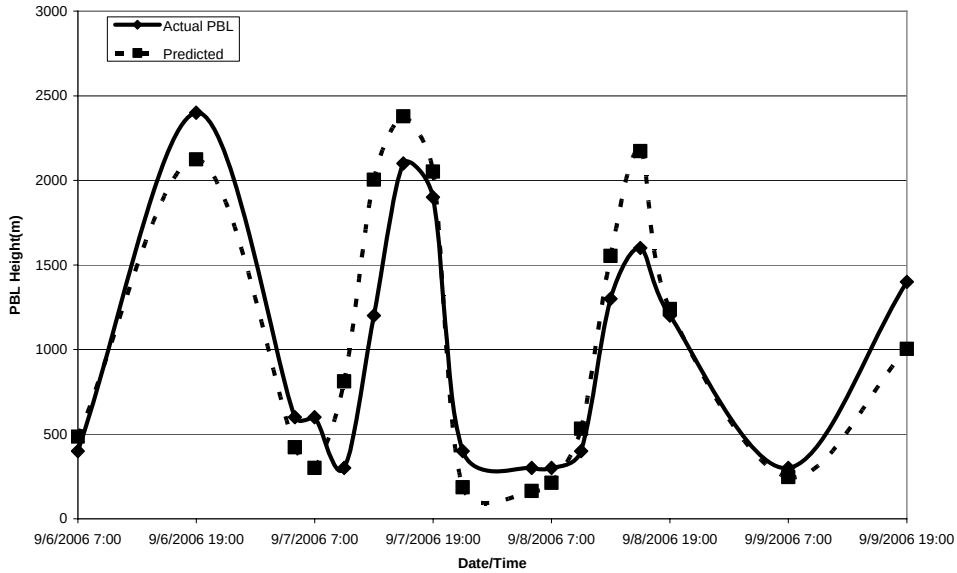

Figure 26. Comparison of MM5 predicted PBL with the actual PBL derived from rawinsonde soundings.

As can be seen from Figure 27, CMAQ under-forecasted the maximum O_3 for the episode of September 07 by 65 ppb. This could have been related to a number of factors, in particular incorrect forecasting of PBL height as demonstrated in Figures 25 and 26. Not surprisingly, the wind speed and direction at the surface are also much different than were forecast (Figure 28). CMAQ forecasted the winds to be out of the NE at about 5 m/s. The actual winds were from east and were under 5 m/s. This could also be the reason why the model over-forecasted the PBL height for this particular day.

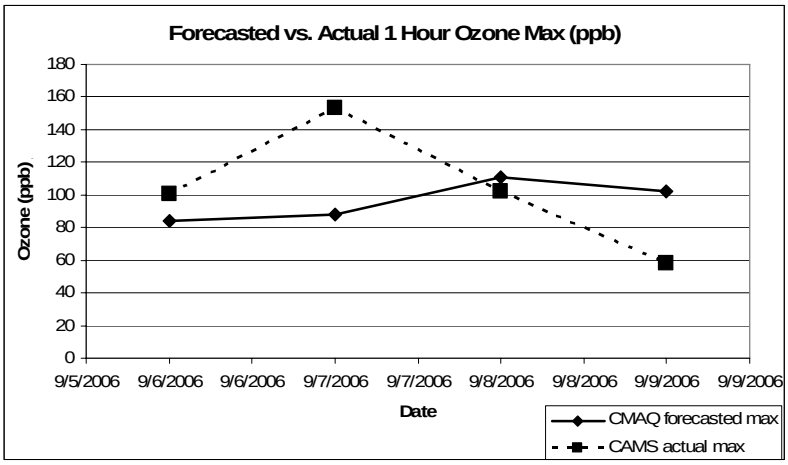

Figure 27. Comparison of CMAQ forecasted ozone maximum to observed ozone maximum.

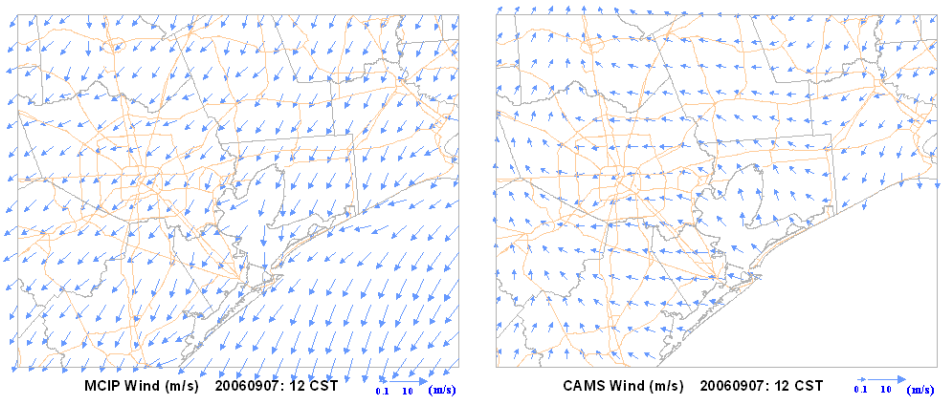

Figure 28. Forecasted surface wind speed/direction compared with actual wind speed/direction.

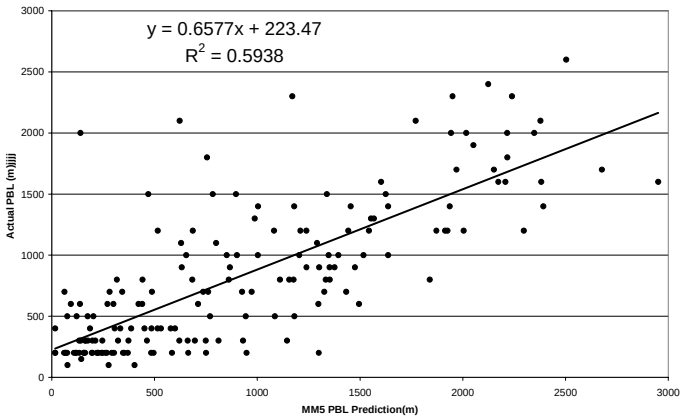

Figure 29. Scatter plot of MM5 predicted PBL vs observed PBL.

Figure 29 displays a scatter plot of MM5 predicted PBL heights compared to observational data for the entire period where sounding data was obtained. The R^2 value is approximately 0.59 and emphasizes the need for further refinements, presumably in twofold aspects: (i) progress in the experimental determination of the PBL heights and (ii) advances in parameterizations in MM5.

3.4 Vertical ozone structures variations over a typical diurnal cycle and the relation of the diurnal variation in ozone structure to the evolution of boundary layer dynamics and thermodynamic structure (Sub-Task 6.4).

This chapter focuses on selected IOP days which also provide insights into small scale variations as obtained by tethersonde launchings on UH campus which were performed complimentary to the radiosondes required for this task. The case study August 31 – September 01 has be chosen, because tethersonde measurements were performed during the nighttime period from August to September 01, whereas the case of September 26 was included, since on this first day of the Vertical Mixing Experiment (VME) tethersondes were launched during the daytime.

3.4.1 Case Study August 31 – September 01, 2006

As mentioned earlier, ozone levels on August 31 and September 01, 2006, measured "very unhealthy", i.e. "purple level", based upon the EPA's AQI scale. Figure 30 shows a summary of ozone time series on both days along with the diurnal variation of the PBL height. For discussions concerning land-sea-bay breeze impacts on these days see Chapter 3.1.

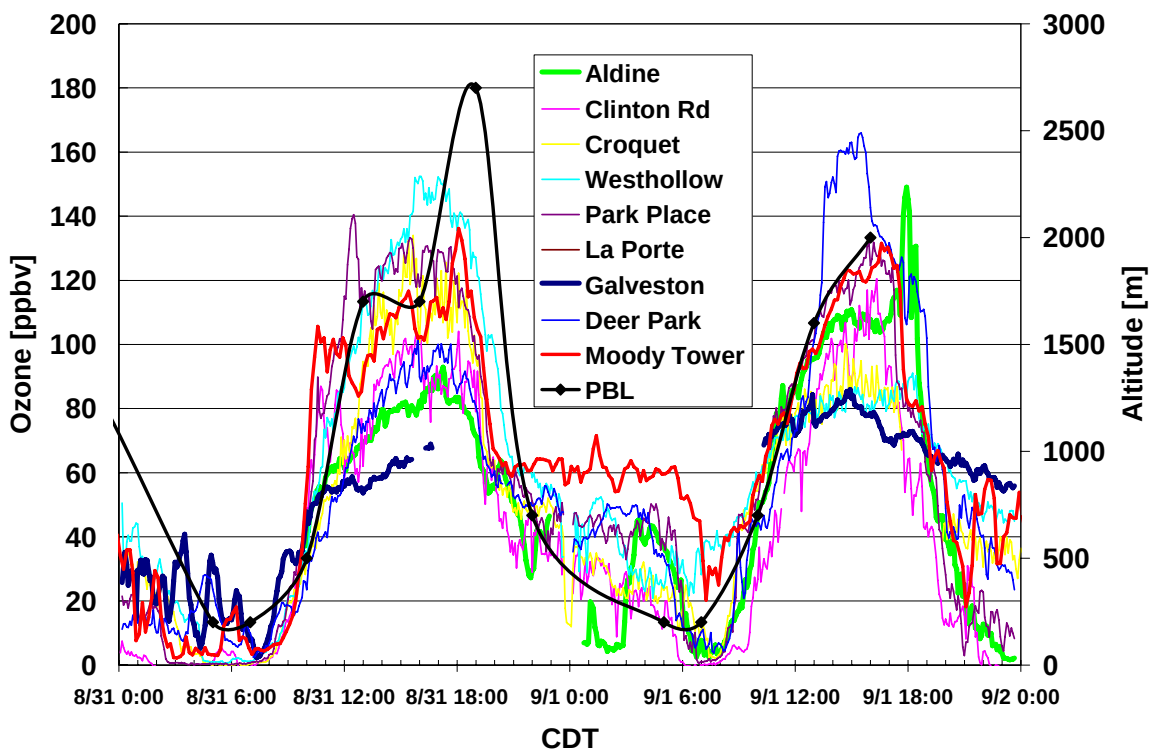

Figure 30. Ozone mixing ratios at various CAMS sites and at the Moody Tower for 8/31/06-9/01/06 along with PBL heights determined by UH radiosondes.

On August 01, 2006, a High center was located to the west of Houston at 850 hPa, making the upper-level winds over the Houston area north/northeasterly throughout the day. A front had passed through the city two days prior. The 0700 CDT morning inversion height was 150 m AGL, and the mean wind speed and direction in this inversion layer was 82° at 4.9 m/s (Figure 31). The ozone sounding at this same time revealed an increase in ozone mixing ratio underneath the inversion layer (Figure 31). In the residual layer above the inversion, ozone concentrations initially decreased and then

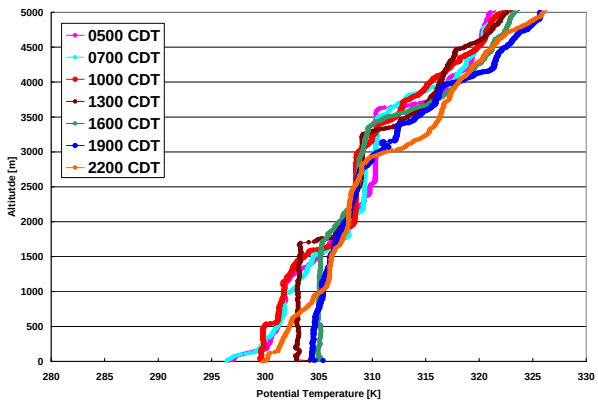

Figure 31. Left above: radiosonde profiles obtained at various times on August 31, 2006. Central plots: vertical profiles of windspeed (left) and wind direction (right). Lowermost plots: ozoneprofiles (left) and radiosonde profiles obtained at 0700 and 1330 CDT on August 31, 2006.

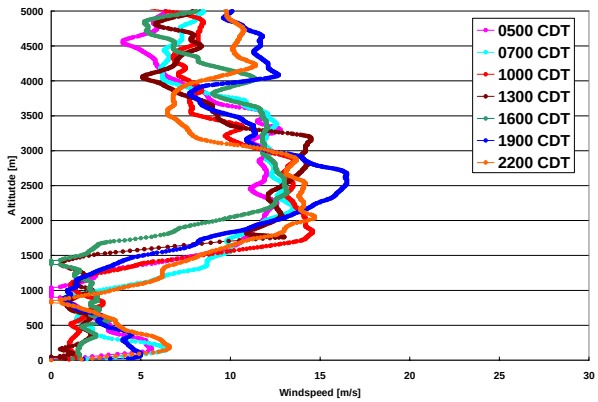

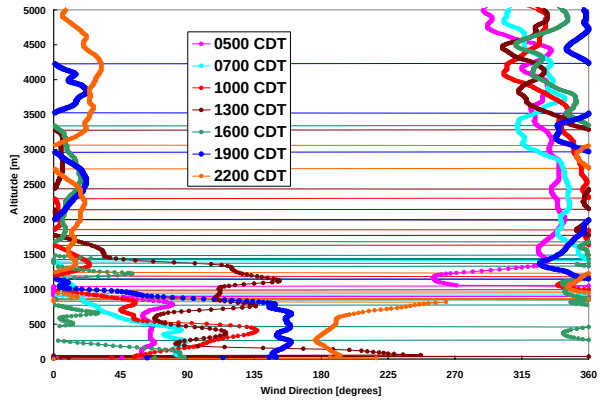

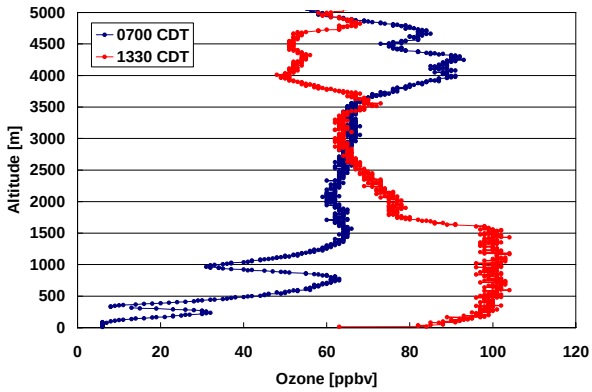

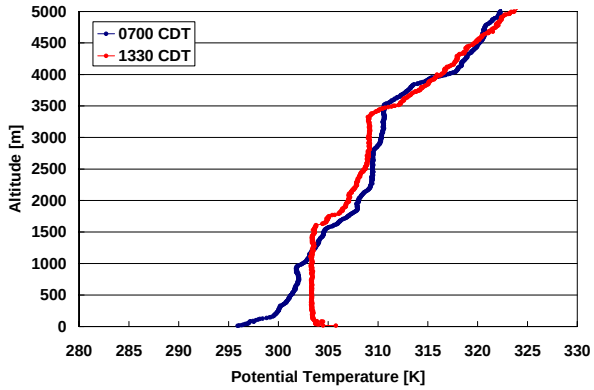

then rose to 63 ppbv at 800 m AGL, before decreasing rapidly to 31 ppbv at an altitude of 1000 m AGL. The likely cause of this decrease was a shift in the wind direction from east to north. A strong temperature inversion was observed at 3500 m AGL, with dry continental air coming from the north and a dew point depression of about 42°C (about 2-3% relative humidity). This inversion also corresponded with a sharp increase in ozone mixing ratio, which is seen in the 0700 CDT ozone profile.

The 1330 CDT vertical ozone profile (Figure 31) shows a well-mixed layer, with ozone concentrations up to 104 ppbv, between the ground and an inversion at approximately 1600 m AGL. This inversion can clearly be seen on the 1300 CDT radiosonde profile (Figure 31). Ozone concentrations decreased above the inversion due to its "capping" effect, and the winds shifted to northerly and increased in speed. At 3500 m GL, an increase in ozone is observed again underneath the higher inversion.

In the mid-afternoon, the atmosphere was well-mixed with easterly winds continuous from the surface to 150 m AGL. The sea-breeze from distinct SE-S wind directions was evident in the 1900 CDT sounding, with a height of approximately 1000 m AGL. The 2200 CDT sounding revealed stronger southerly winds up to 1000 m AGL. The strong inversion aloft was still present but had fallen to 2800 m AGL.

On September 01, 2006, the High at the 850 hPa level had moved closer to southeast Texas and had intensified. The morning inversion began with a height of 125 m AGL at 0100 CDT, and increased to 140 m AGL at 0500 CDT (see Figure 32). Surface temperatures were very similar (26.5°C and 26.7°C, respectively), but wind patterns of the two soundings revealed some difference. The mean wind in the morning inversion layer at 0100 CDT was 203° with a wind speed of 3.4 m/s, and the mean wind in the layer at 0500 CDT was 239° with a wind speed of 3.0 m/s. Technical difficulties with the ozonesonde launch at 0700 CDT led to a loss of ozone data for the morning sounding.

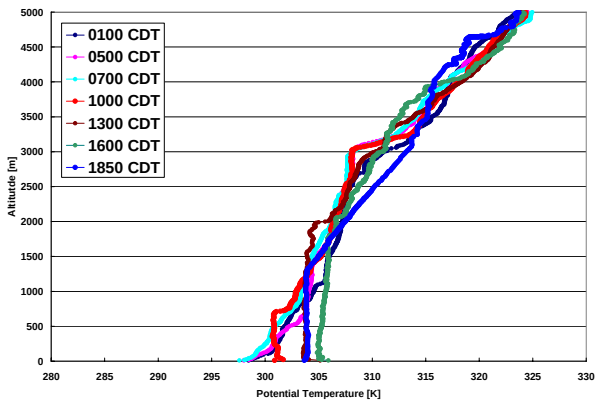

Figure 32. Left above: radiosonde profiles obtained at various times on September 01, 2006. Central plots: vertical profiles of windspeed (left) and wind direction (right). Lowermost plots: ozoneprofiles (left) and radiosonde profiles obtained at 0700 and 1330 CDT on September 01, 2006.

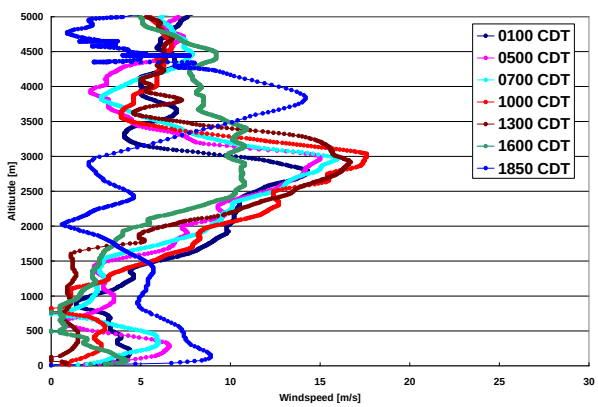

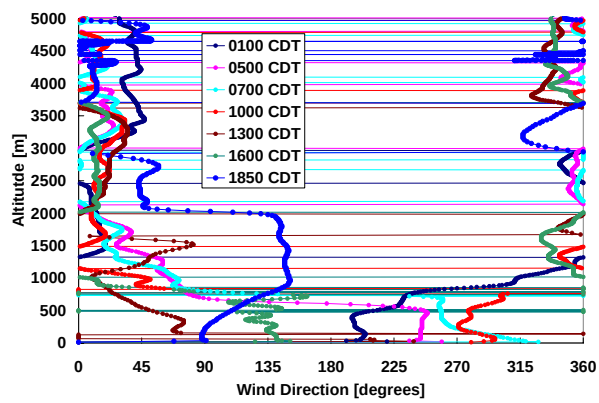

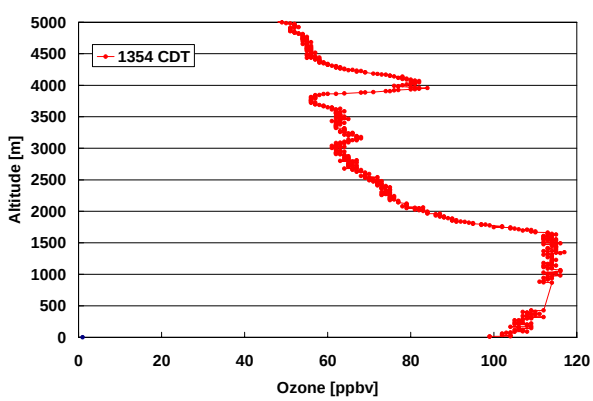

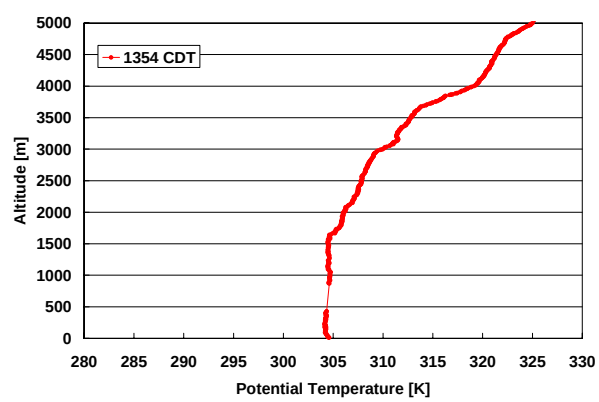

The afternoon ozone sounding at 1354 CDT was successful (except for less than one minute of data loss). The data showed a well-mixed layer up to approximately 1800 m AGL which corresponds to an inversion seen in the radiosonde profile (Figure 32). High ozone concentrations between 100-117 ppbv were observed in this layer (Figure 32). Above this layer, ozone levels decreased significantly to 56 ppbv, possibly due to an increase in wind speeds or due to a cloud layer which is evident on the radiosonde profile (Figure 32). This cloud layer was approximately 200 m thick, existing between 1800-2000 m AGL. The remainder of the ozone decrease seems to occur at a "normal"/slower pace above 2000 m AGL. At 3800–4000 m AGL, a sharp increase in ozone to 84 ppbv occurred in the vicinity of the strong inversion remaining in place from August 31. The sea-breeze from SE directions became evident on the 1600 CDT sounding with a height of 700 m AGL and an average speed and direction of 136° and 1.9 m/s, thus being very weak. Data was not available for the 1354 CDT soundings.

Boundary Layer Evolution

The evolution of the boundary layer development for the days of August 31 to September 1 is shown in Figure 33. The height of convective boundary layer (CBL) was 1700 m AGL at 1600 CDT. At 1900 CDT a slight increase in stability occurred throughout entire profile with slight cooling below 700 m AGL and warming above. This may be due to the increase in windspeed that occurred above 1000 m AGL. By 2200 CDT a stable layer formed quickly up to almost 1000 m AGL. Shallow mixed layers where observed near the surface at ~100 m AGL at this time. During the period from 2200-0700 CDT low level jets were observed with maximum winds of ~ 5–6.5 m/s at 200-350 m AGL. A minimum in wind speed (~0 m/s) was observed at 600-850 m AGL indicating the top of the low-level jet. Wind direction changed from southeasterly to southwesterly during this period up to heights of 750 m AGL.

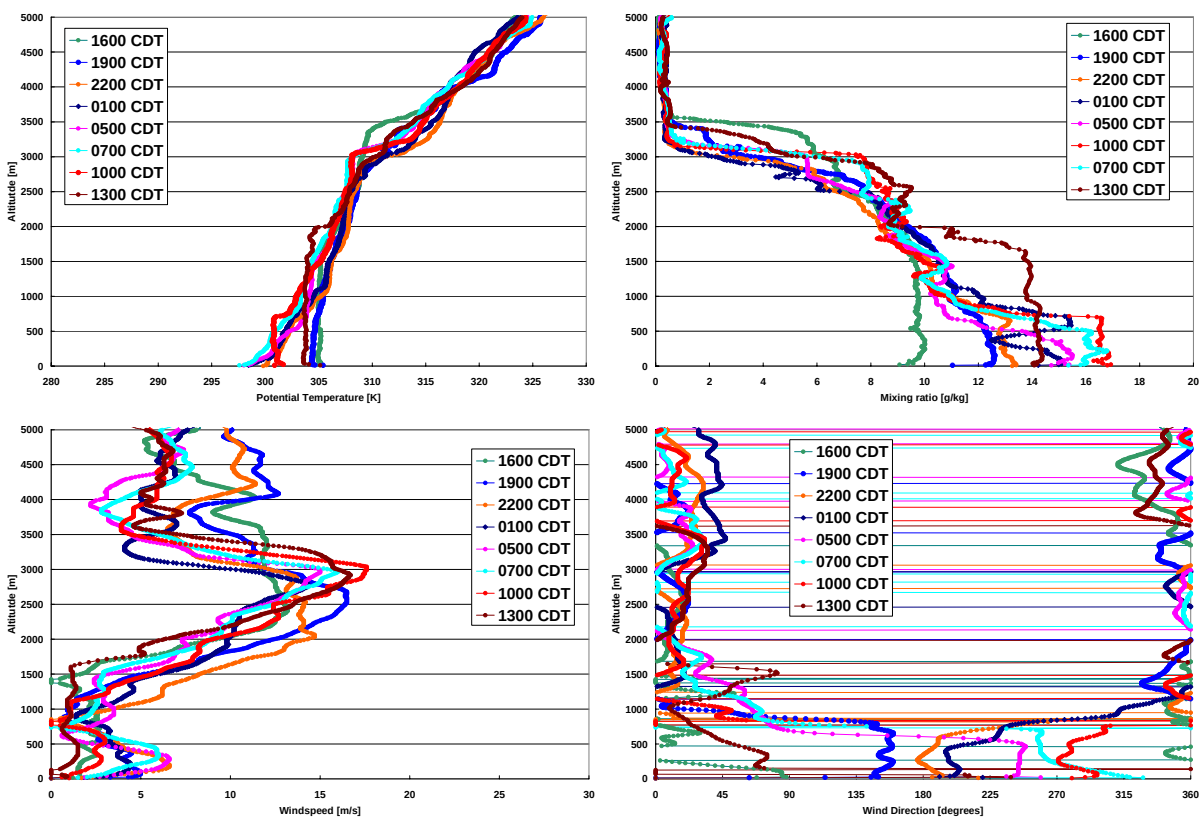

Figure 33. Radiosonde results obtained at various times from August 31, 2006, 1600 CDT – September 01, 2006, 1300 CDT for potential temperature (left above), mixing ratio of water vapour (right above), windspeed (left below), and wind direction (right below).

Above this level winds are from the north. This change in low-level winds is associated with the local scale flows such as the sea/land breeze circulations. Inversion strength was fairly weak overall with potential temperature gradients $\Delta\theta/\Delta z$ = 0.006 K/m for the first 1000 m AGL at 2200 CDT. By 0700 CDT (September 1) $\Delta\theta/\Delta z$ =0.007 K/m for depth of inversion up to 500 m AGL. These weak temperature gradients were most likely due to the complex nature of the surrounding urban landscape. By 1000 CDT the mixed layer grew to 700 m AGL indicated by the strong capping inversion in the 1000 CDT profile. Note sharp discontinuity of mixing ratio at this height and the low-level winds from the west-southwest. By 1300 CDT the mixed layer grew to 2000 m AGL as indicated by constant potential temperature profile. Winds were constant throughout the depth of the mixed layer as expected, but have shifted back to the east-northeast. Overall, water vapor mixing ratios increased from August 31 to September 1. Above the mixing layer height (2000 m AGL, 1300 CDT) the atmosphere was weakly stable. This layer was the free atmosphere, but at 3000 m AGL there existed a stronger capping inversion. This layer was associated with larger scale structure and not the boundary layer. The sequence of profiles shows the continued weakly stable region above the nocturnal boundary layer and below the free atmosphere. This weak stability is most likely the residual layer that forms above the nocturnal boundary layer; in this case, above 700-900 m AGL (0500 and 0700 CDT). Typically, the residual layer is more neutral than it is stable. This upper-level stability may be associated with advection or synoptic-scale forcing. Therefore, a definition of the residual layer may be difficult to determine at this preliminary stage, however, a first approximation would suggest that the residual layer is anywhere between 700 to 2000 m AGL at night.

Tethersonde Results

Results from the tethersonde data are shown in Figure 34. The profiles show the very detailed structure of the nocturnal boundary layer near the surface. Times listed in Figure 34 are in CDT . These profiles are instantaneous values and have not been averaged.

Initially at 2045 CDT the atmosphere was well mixed. Cooling did not begin until approximately 2330 CDT or just before that and happened quickly. The strongest temperature gradient occurred at 2330 CDT, but eventually became weaker as cooling occurred in the layers above 100 m AGL. The near surface atmosphere continued to cool throughout the evening and the temperature inversion started to break by 0850 CDT. Winds near the surface were weak, but were approximately

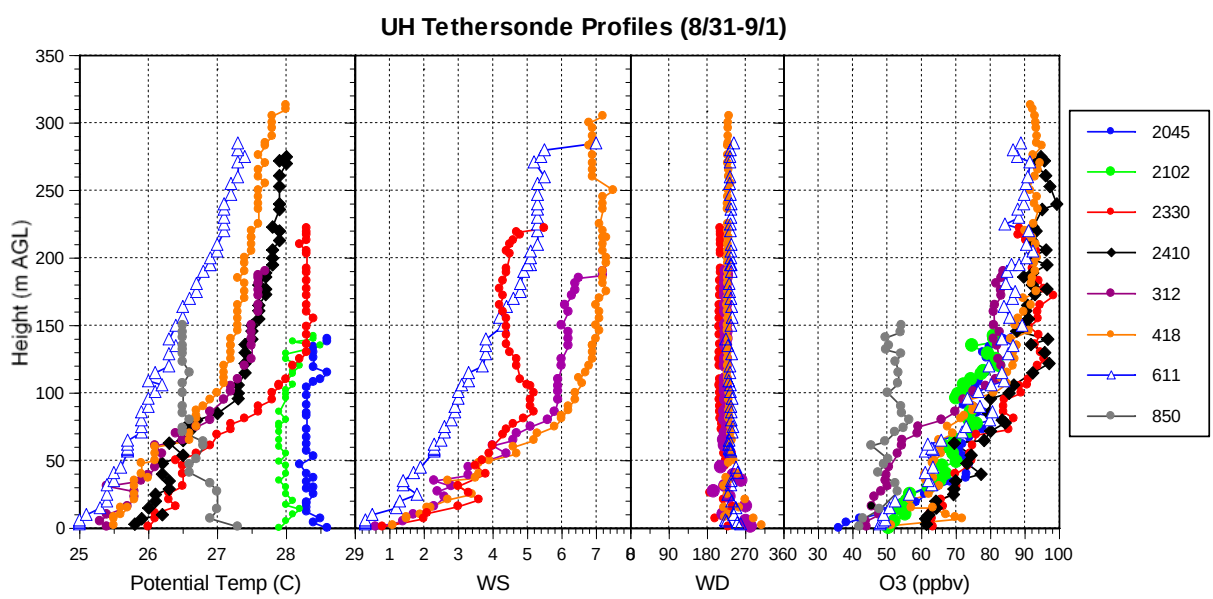

Figure 34. Tethersonde data profiles showing potential temperature [°C], wind speed [m/s], wind direction [°], and ozone mixing ratio [ppbv] for 8/31/06-9/01/06.

6-7 m s^{-1} at 100 m AGL and above. The direction of the flow changed with height. Winds above 50 m AGL were from the south-southwest. Ozone profiles indicated much higher ozone concentrations above the temperature inversion than near the surface. At 2410 CDT ozone was near 100 ppb above 100 m AGL. Throughout the night ozone concentrations stayed above 90 ppb. At the surface concentrations were on the order of 50 ppb and most likely due to titration and/or dry deposition at the surface caused by the formation of a stagnant air mass below the stable layer. As the morning CBL developed ozone concentrations decreased to 50 ppb due to the mixing of cleaner air near the surface.

3.4.2 Case Study September 26, 2006

On September 26, 2006, ozone levels were not reported to be in exceedance in the Houston-Galveston area, however, ozone levels were reported to be in the "orange level" in Conroe, C78, and at Danciger site, C618, (see Appendix II). Figure 35 shows a summary of ozone time series on both days.

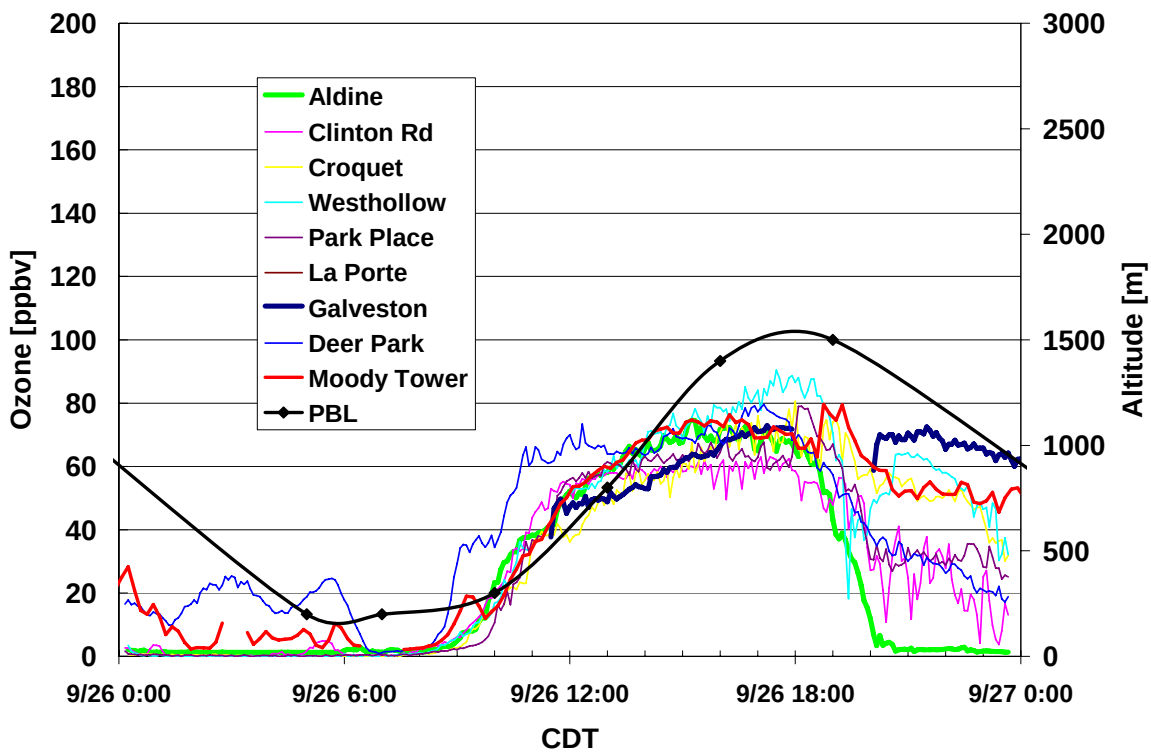

Figure 35. Ozone mixing ratios at various CAMS sites and at the Moody Tower for September 26, 2006, along with PBL heights determined by UH radiosondes.

Boundary Layer Evolution

The evolution of the boundary layer development for September 26 is shown in Figure 36. The PBL in the early morning hours (0500 CDT and 0700 CDT) is very shallow and the inversion strengths are very strong compared to the August 31 – September 01 case. As can be seen in the ozone time series of Figure 35 ozone values at around 0700 CDT are pretty low throughout the Houston-Galveston area, most likely due to high NO traffic emissions during rush hour. The low level jet is only evident in the 0500 CDT sounding and reaches windspeeds up to 8.9 m/s. This low level jet is associated with easterly wind flows. The low level jet eventually breaks down and in the 1000 CDT radiosonde launching very low windspeeds of around 1 m/s are observed in the first 200 m AGL. This

is basically due to the rapid heating of this shallow layer from the ground which eliminated the strong temperature gradient throughout this layer. Note that on the other hand thermal inversion at 1000 CDT at 1000 m AGL becomes stronger and the layer up to 1000 m AGL becomes well mixed by 1300 CDT. In the afternoon hours the PBL eventually grows up to 1500 m AGL and winds become more constant throughout the PBL. Starting with the 0700 CDT launching wind direction eventually turns from E to NE and finally to N. Above the boundary layer winds are consistently from NW. Land-sea breeze circulation is not that evident on this day like on other days, but both profiles of the water vapour mixing ratio and the wind direction indicate that the 0500 CDT launchings were influenced by the bay breeze, whereas the 1900 CDT launch was impacted by the sea breeze.

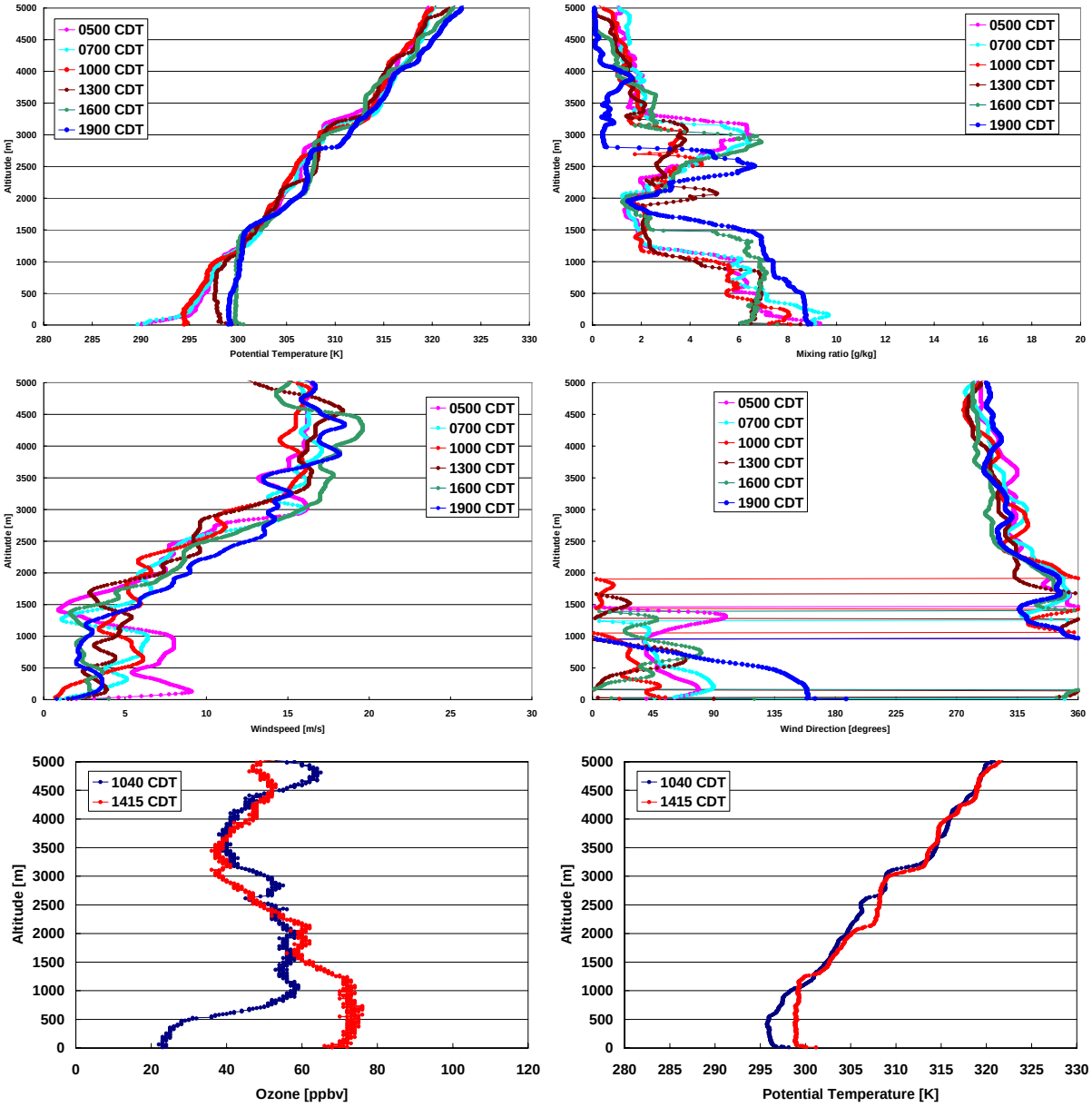

Figure 36. Radiosonde and ozonesonde results obtained at various times on September 26, 2006. Uppermost plots: potential temperature (left) and mixing ratio of water vapour (right). Central plots: vertical profiles of windspeed (left) and wind direction (right). Below: Ozoneprofiles (left) and radiosonde profiles obtained at 1040 and 1415 CDT.

As it can be seen in the ozone profiles (Figure 36) the 1040 CDT profile shows a sharp increase of O_3 from 20 ppb at the surface up to 60 ppbv at around 1000 m AGL, the top of the PBL at that time. In the layer above 1000 m AGL up to 2500 m AGL constant ozone levels of 60 ppbv are present, which can be considered the lower tropospheric background levels with continental air masses. Comparing with the surface ozone time series in Figure 35 it seems that with increasing PBL height also O_3 levels have increased from very low values up to the 20 ppbv range. This increase is most likely due to increasing photolysis of NO_2 which has been produced in previous titration reactions of NO with O_3 and downmixing of background ozone. This downmixing process is supported the strong wind speed gradients in the layers above the PBL. The 1415 CDT ozone profile nicely shows constant ozone levels of about 75 ppbv throughout the PBL which is approximately at 1200 m at this time. Above this layer an ozone gradient is visible which indicates that ozone production is eventually penetrating to layers reaching the final maximum PBL height of 1500 m AGL. It can be assumed that the difference between 75 ppbv observed in the PBL during the afternoon hours and the background O_3 levels of about 60 ppbv has been caused by additional photochemical production of ozone in the Houston area.

Tethersonde Results

Results from the tethersonde data for September 26 are presented in Figure 37. They show data up to 250 m during the time frame 0812 CDT to 1240 CDT, i.e. they include the break up of the morning inversion layer in a better temporal resolution. The data has been averaged into 5 m layers.

As mentioned before the 0500 CDT and 0700 CDT radiosonde launches revealed a shallow PBL with a very strong inversion. The first tethersonde data at 0812 CDT shows that this layer shrank even more and the PBL height decreased to slightly above 100 m AGL. Ground level ozone data was about 20 ppbv coinciding with ozone surface data in Figure 36. Above the inversion there was a tendency towards increasing ozone levels. As time progresses the virtual potential temperature increases first close to the surface and eventually the entire PBL experiences increasing virtual potential temperature. It seems that between the 0903 CDT and 0930 CDT tethersonde launch there is a significant increase of the virtual potential temperature by about 2 K which almost eliminates the inversion. The final break down of the inversion occurs sometime in between 0941 CDT and 1108 CDT tethersonde launchings, most likely shortly before the 1000 CDT radiosonde launch which indicates a PBL height of about 300 m AGL and thus above the tethersonde scale of 250 m AGL. It is interesting to note that the start of ozone increases in Figure 35 vary from 0830 CDT (Deer Park) to 0950 CDT (Park Place). At the Moody Tower some variations occur between 0830 CDT and 0930 CDT most likely indicating small scale turbulent mixing close to the inversion layer. Finally, overall increase starts around 0945 CDT which coincides with the recent assumptions of the inversion layer breakup sometime between 0941 CDT and 1000 CDT. Winds (not shown) were moderate, with minimum wind speed values around the time of the break up of the morning inversion layer. Until the break up of the inversion winds close to the surface winds tended to come from N directions, whereas above the inversion wind shifted towards E. The break up of the inversion led to a rapid mixing and consequently increase of ozone levels close to the surface from initially 20 ppbv to about 70 ppbv at around noon.

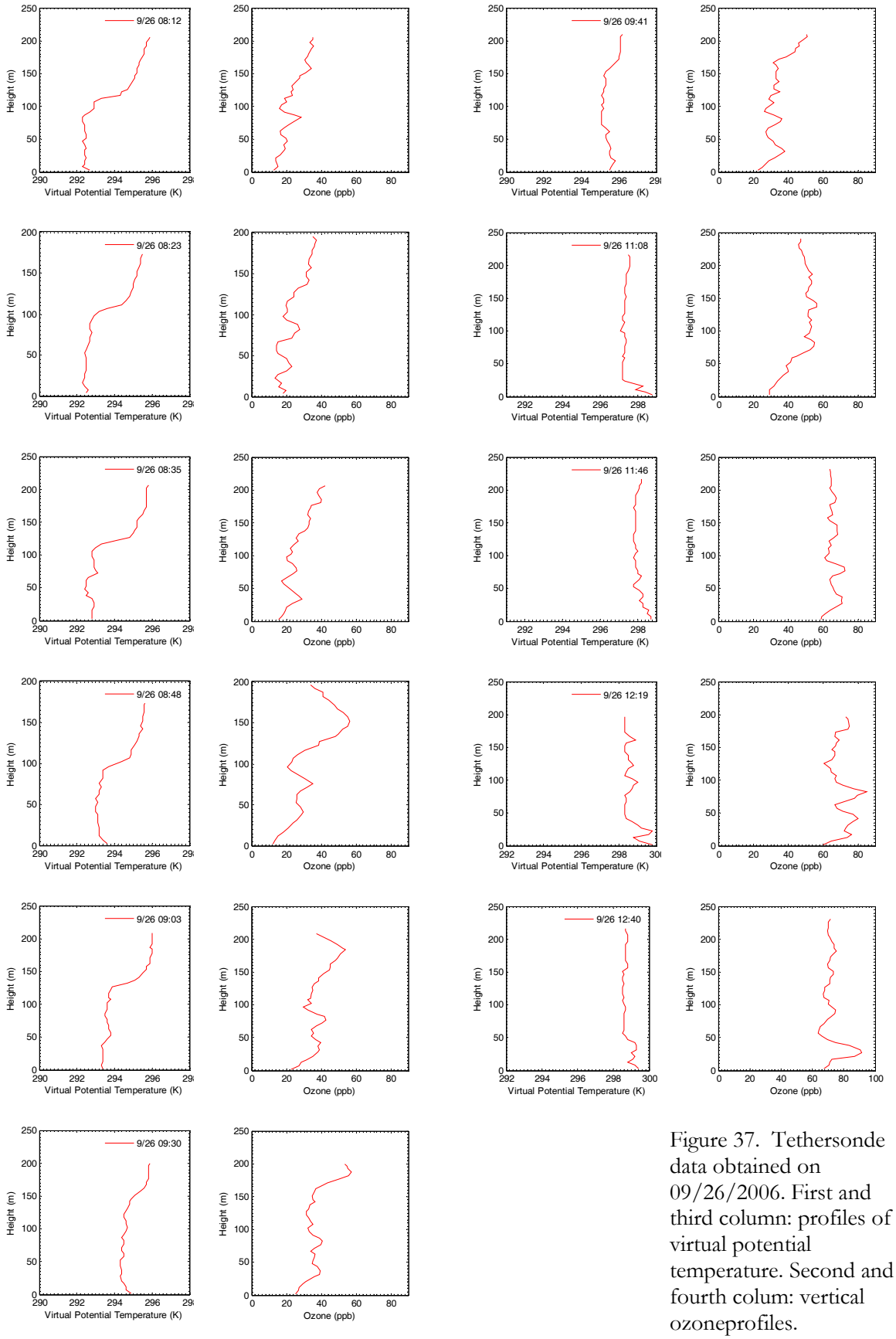

Figure 37. Tethersonde data obtained on 09/26/2006. First and third column: profiles of virtual potential temperature. Second and fourth colum: vertical ozoneprofiles.

3.5 The relation of the vertical ozone structure to surface ozone observations, including to what degree the ozone concentration in the residual layer contributes to the next morning concentration as a result of convective boundary layer growth (Sub-Task 6.5).

Ozone is always present in the free troposphere. This is partly due to downward mixing from the stratosphere, in particular in the upper free troposphere region. Ozone however can also be stored in the residual layer in the lower troposphere. The residual layer is a layer which is exposed to photochemical build-up of ozone during the daytime, but is decoupled from the PBL during the nighttime, due to radiational cooling of the surface and the formation of shallow PBLs. In the residual layer ozone can be rather stable, since titration processes are negligible, because NO will be trapped in the PBL beneath the residual layer. Also, deposition processes are not present since the air mass in the residual layer is not in contact with the soil.

Figure 38 shows a morning ozone profile revealing a significant residual layer above the morning inversion at about 1000 m AGL. Ozone levels are quite low underneath the morning inversion likely due to deposition to the surface and titration by NO. It is likely that downward mixing of approximately 60 ppbv of this residual layer had a significant effect on the increasing ozone peak values in the afternoon (see Figure 38B). The difference between the maximum ozone values of about 90 ppbv in the afternoon boundary layer and the 60 ppbv originating from the input of the residual layer is most likely due to in-situ ozone formation. September 20, 2006 was declared a "high-ozone" day by TCEQ.

These features occurred were frequently observed. As a second example the results from the two ozonesondes and radiosondes launched on August 31 are shown in Figure 39.

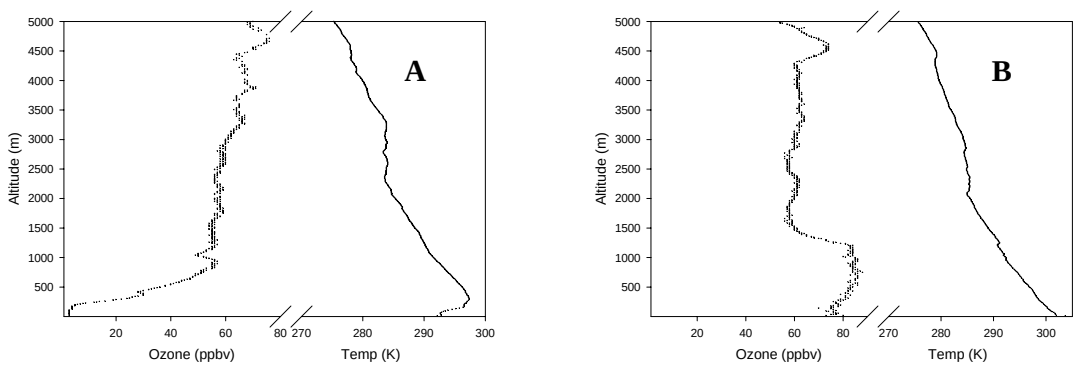

Figure 38. Ozonesonde and radiosonde profiles at 700 CDT [A] and 1300 CDT [B] on September 20, 2006.

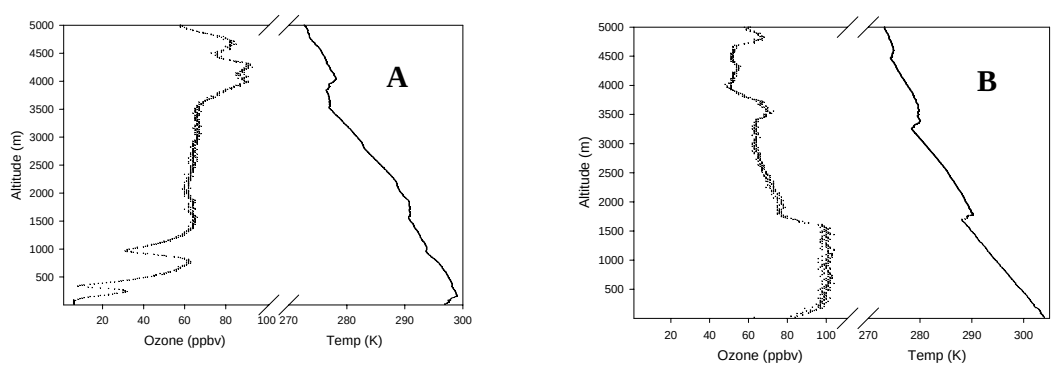

Figure 39. Ozonesonde and radiosonde profiles at 700 CDT [A] and 1300 CDT [B] on August 31, 2006.

Figures 38 and 39 basically demonstrate that ozone in the residual layer may be mixed downward and contribute to surface ozone levels. However, they do not reveal whether the ozone observed in the residual layer is actually ozone left over from the previous day. Figure 40 shows a sequence of three ozonesondes launched at 1300 CDT on September 25 and at 1040 CDT [B] and 1415 CDT [C] on September 26, 2006. On September 15 (Figure 40A) relatively low ozone values of about 40-50 ppbv were measured from the surface up to 2000 m AGL. At about 2300 m AGL a layer with enhanced ozone levels around 60 ppbv were observed. On the subsequent day (Figure 40B) ozone levels between 1000 m AGL (above the morning inversion layer) and 2000 m AGL (shaded area) were about 60 ppbv. There may be two reasons for these higher ozone levels: either (i) transport of air masses or (ii) left over ozone from ozone formation processes which occurred in the afternoon of the preceding day. Anyway, it seems that this residual layer was partly mixed downward during daytime on September 26 when the PBL heights reached 1300 – 1600 m AGL. Figure 40 suggests that about 10 ppbv ozone may be considered as left-over ozone from the previous day. Preliminary analysis show similar values for August 31-September 1 episode.

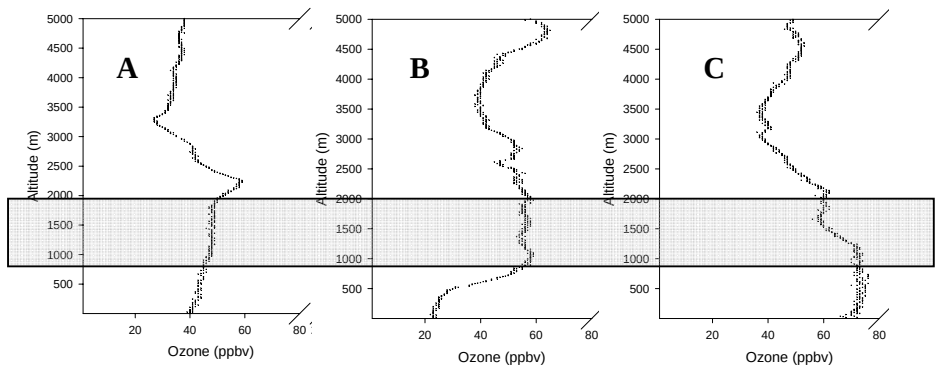

Figure 40. Ozonesonde profiles at 1300 CDT [A] on September 25 and at 1040 CDT [B] and 1415 CDT [C] on September 26, 2006.

3.6 Identify the relative role of regional transport and local concentration in determining the vertical ozone distribution (Sub-Task 6.6).

Preliminary analysis of ozonesonde data shows that also regional-scale transport may have an impact on local ozone levels. Figure 41 shows an example for a sequence of days preceding the ozone events on August 31 and September 01 which were declared "purple" (August 31) and "red" (September 01) by TCEQ. The data for August 28 shows low ozone values around 30 ppbv from the surface up to 3000 m AGL which is in the range of marine background ozone values. Between 3000 and 4500 m AGL ozone increases steadily and reaches almost 50 ppbv. It remains around 50 ppbv up to 5200 m AGL. Above 5200 m AGL ozone steadily rises again up to 70 ppbv. On August 29, the ozone profile remains almost unchanged in the layers above 3500 m AGL. However, below 3500 m AGL background levels rise between 35 and 45 ppbv. Below 1000 m AGL photochemical ozone production in the PBL leads to overall 45 ppbv ozone. Preliminary results from backward trajectories suggest that the peak ozone values of around 45 ppbv ozone have passed southwestern and western parts of Texas prior to arrival in Houston. The August 30 data shows a strong increase in background ozone throughout the troposphere up to 5000 m AGL. On the average the increase is about 30 ppbv ozone. This increase is also present in the surface ozone data, i.e. without the increase of the background ozone levels no high ozone values in the PBL would occur. Backward trajectory analysis suggests increasing inflow of continental air masses from northerly directions. It is interesting to note that the vertical ozone profile changed drastically from August 28 to August 30: August 28: overall increasing ozone values with increasing altitude, August 29: apart from some fluctuations relatively constant ozone values, August 30: overall decreasing ozone values with increasing altitude. It is also

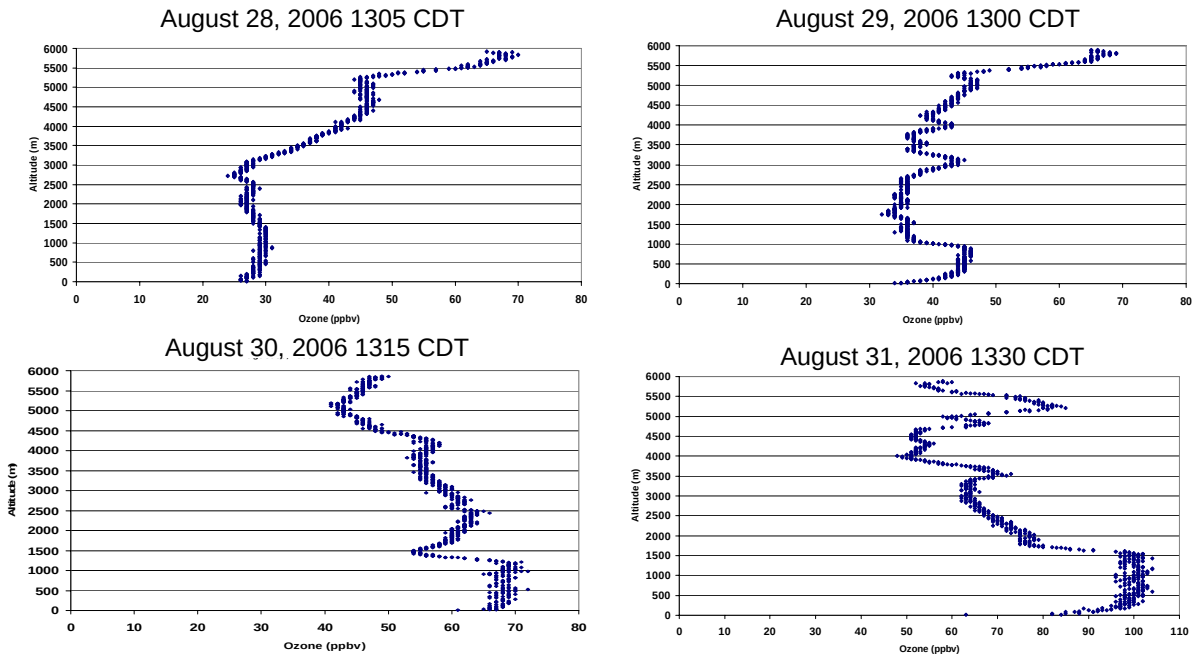

Figure 41. Ozonesonde profiles at around 1300 CDT on August 28, 29, 30, and 31, 2006.

interesting to note that from August 28 until August 31 the PBL height increased and thus with increasing convective processes also more enhanced continental ozone background levels were likely mixed into the photochemically active PBL over the Houston area. August 31, finally, was characterized by (i) a high PBL height of almost 2000 m AGL, (ii) an residual layer which consisted of a combination of high ozone background levels of about 60 ppbv and a probable ozone carry over from the preceding day of about 10 ppbv ozone, and (iii) an additional local photochemical production of about 30 ppbv ozone.

Vertical ozone profiles frequently showed specific layers with enhanced values. Sometimes these profiles revealed rather complex structures. Figure 42 shows a selection of vertical ozone profiles where some layers with significantly enhanced ozone values could be identified. In most cases these layers occur above 3000 m AGL and do not have a vertical extension larger than 500 m. Often, the ozone enhancement is about 10-20 ppbv, but can also reach up to 40 ppbv as it was observed on August 02, 2006. This strong enhancement was associated with transport of air masses over the Gulf of Mexico and an origin in Mexico. Further analysis will be necessary to confirm the possible source regions and in particular the kind of source(s) (biomass burning/urban sources). In most other cases the enhanced ozone values are associated with westerly to northerly wind directions. Since these layers are mostly found in altitudes above 3000 m AGL it is likely that biomass burning, i.e. forest fires in the Canadian or US Rocky Mountains may have contributed to these higher ozone values. So far, the preliminary analyses do not show impacts coming from the industrial areas in the northeast of the US.

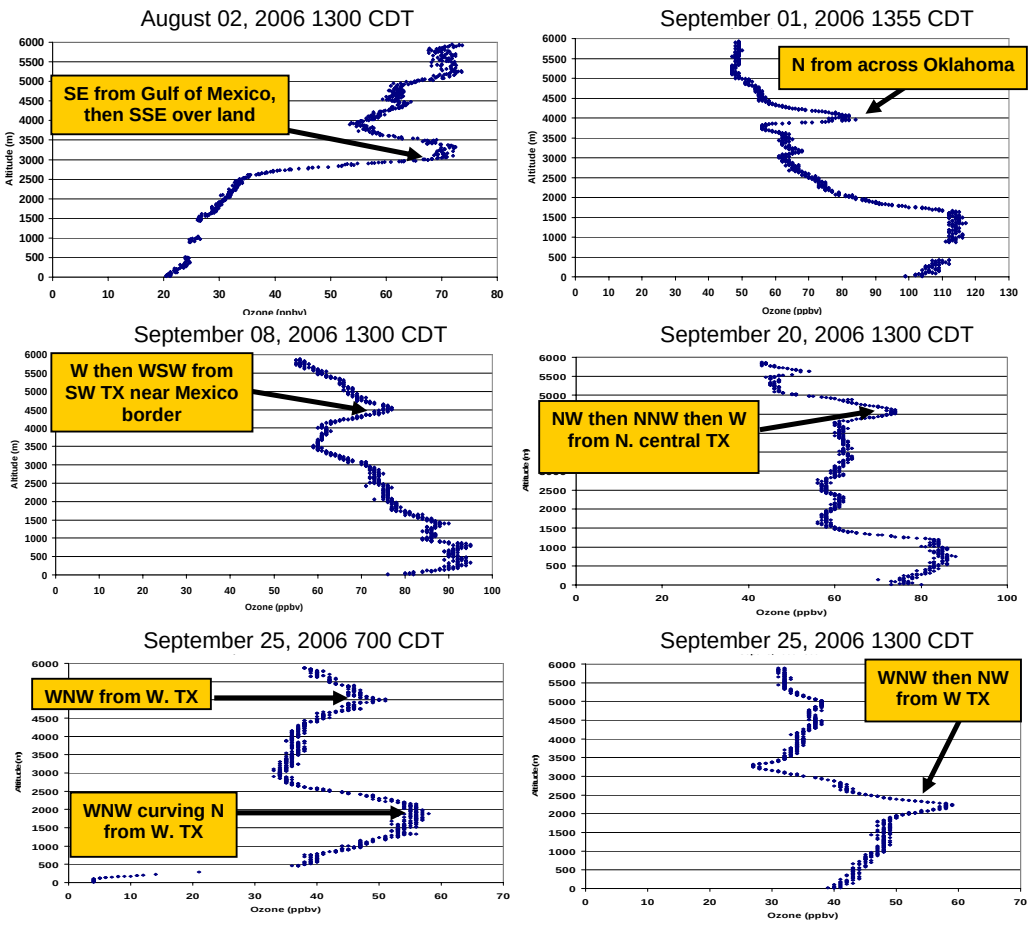

Figure 42. Selected ozonesonde profiles and back trajectory information for specific layers based on NOAA ARL-UH 24-hr back trajectories calculations.

3.7 Describe ozone distribution within the free troposphere, and how it varies with regional transport patterns (Sub-Task 6.7).

It has been well established that the synoptic pattern plays a key role in urban ozone concentrations [*Yu et al.*, 1986; *Banta et al.*, 2005; *Nielsen-Gammon* et al., 2005a]. This study will analyze the common patterns that the ozone episodes have in the late summer of 2006. The months of August and September will typically be considered as separate, since August 2006 saw no frontal passages through the Houston area until late in the month. However, September 2006 was a month of regular frontal passages. It should also be noted that no hurricanes made landfall during 2006, and the tropical activity was far below that of the 2005 season [*Lau et al.*, 2007]. This anomaly could help explain the frequency of frontal passages for the 2006 season, although this phenomenon will not be analyzed further.

It should be noted that there is one exception to the criterion defined for ozone episode days. For most ozone episodes of August and September 2006, the 8-hr average remained above 85 ppb at a minimum of one station in this network. The only exception occurred on August 4, 2006, which was considered an ozone episode but did not exceed the 8-hr standard. However, hourly peaks greater than 140 ppb were measured on this day [*TCEQ*, 2007]. Also, although August 31 was indeed an ozone episode, it was considered a September event since it was associated with the same meteorological conditions as the events of September 01 and 03.

Although several papers have discussed the fact that anticyclonic flow can increase Houston's 1-hr ozone averages [*Darby*, 2005] and 8-hr peak ozone averages [*Nielsen-Gammon* et al., 2005b]; this has only been shown at the local level and not on the synoptic scale. It is well-established that an anticyclonic regime is the cause behind most of Houston's ozone episodes [*Banta et al.*, 2005]. However, composite synoptic maps have not yet been produced in order to more accurately classify synoptic weather conditions for ozone episodes. *Darby* [2005] discussed the idea that flow counteracting the sea breeze can increase the probability that Houston will experience an episode; however the synoptic picture was not discussed. *Nielsen-Gammon et al.* [2005a] used principal component analysis to analyze O_3 background levels; however this was completed on a regional scale. The specifications of the scale were not available, but it included the extreme eastern portion of Texas and Oklahoma, all of Louisiana and Arkansas, and western Mississippi [*Nielsen-Gammon* et al., 2005a].

Thus, composite synoptic maps will be analyzed and related to the bigger picture of Houston's local ozone concentration. Cluster analysis was also performed at the 850 hPa level. An insight will be given into the effect of frontal passages on Houston's ozone concentration.

The Role of Synoptic Forcing in Houston's Ozone Concentration

In order to consider the role of the synoptic picture for Houston's ozone episodes of August and September 2006, composite maps were created using the National Climatic Data Center's composite map web interface. This website can be found at http://www.cdc.noaa.gov/Composites/Day/. Composite maps were produced for episode days and non-episode days for the purpose of providing a possible classification and better forecasting of Houston's ozone episodes in the future. The levels of 500 hPa and 850 hPa will be considered for this upper-level analysis. Although composite maps were created for the 300 hPa level, the results were comparable to the 500 hPa and will not be discussed.

500 hPa Analysis

The 500 hPa composite map for non-episode days of August 2006 (Figure 43) reveals a High center to the northeast of the Houston area. This may have helped support the southeasterly flow that Houston experienced over much of the month of August 2006.

Compared to the non-episode composite, the composite map for ozone episodes in August (Figure 44) shows a stronger than average High system centered over northeastern Texas and Arkansas, giving Houston its northeasterly flow. It should be noted that this is mostly during the episode of August 16-18, since August had relatively few episodes in comparison to other years.

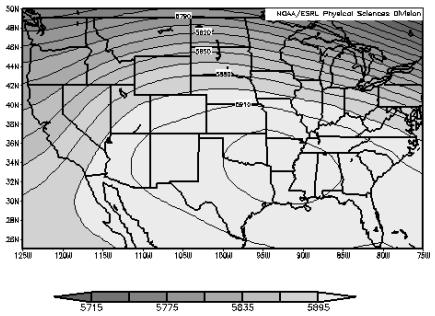

Figure 43. 500 hPa composite map of geopotential heights for non-episode days August 2006.

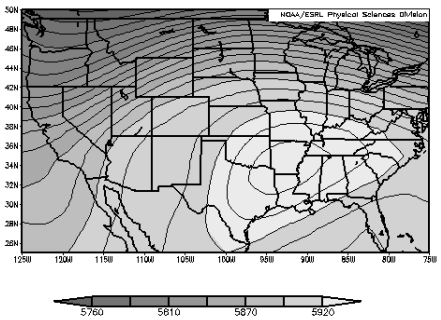

Figure 44. 500 hPa composite map of geopotential heights for August ozone episodes 2006 (4 episodes).

Figure 45 shows the composite map for non-episode days in September 2006. The average flow for the month of September is mostly zonal. Figure 46 shows the average 500 hPa flow for the ozone episodes of September 2006. Note the ridge located to the west of the Houston area, with a trough to the east. This is a typical scenario associated with a recent cold frontal passage and a Low system moving to the east of the Houston area.

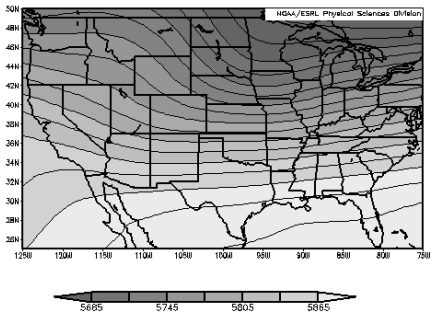

Figure 45. 500 hPa composite map of geopotential heights for non-episode days September 2006.

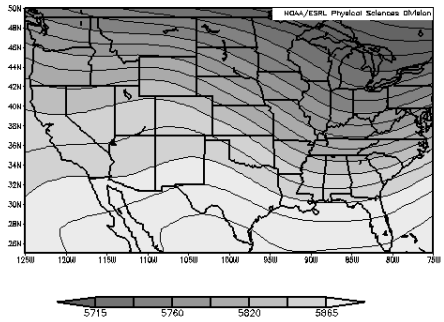

Figure 46. 500 hPa composite map of geopotential heights for September ozone episodes 2006 (10 episodes).

850 hPa Analysis

The composite maps for non-episode days of August 2006 at 850 hPa are shown in Figures 47 and 48. Figure 47 reveals a High system centered to the East of the Houston, possibly contributing to southerly flow which helped to keep ozone levels to a minimum. However, the composite map for the ozone episodes reveals a High system centered to the northeast of Houston, again more indicative of the episode of August 16-18 contributing to the easterly flow over the area. It is this flow which may have contributed to increasing the ozone precursor concentration over the Houston area, since this flow will bring air from the ship channel region into the urban area.

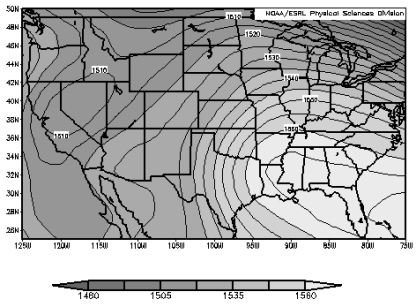

Figure 47. 850 hPa composite map of geopotential heights for non-episode days August 2006.

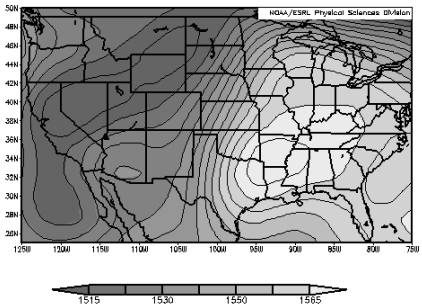

Figure 48. 850 hPa composite map of geopotential heights for August ozone episodes 2006 (4 episodes).

The composite map for non-episode days during September 2006 is shown in Figure 49, and is not very conclusive with the exception of some cold advection occurring over the north-central portion of the country and a tendency for southerly flow over the Houston area.

However, the composite map for September ozone episodes shown in Figure 50 is more conclusive. This shows a High center to the west of Houston, again indicative of a recent frontal passage. This is also the leading cluster for Houston's ozone episodes for September which will be discussed in the next section. The position of this High helps in bringing dry flow from the continent giving Houston a clear sky and an increase in background ozone. This increase is mostly due to the transport of air with higher anthropogenic and biogenic sources of primary pollutants. Also, enhanced ozone concentration within the residual layer could be a factor in increasing the background ozone over Houston. The northerly flow is also associated with increased subsidence which may have a relation to Houston's ozone concentration (high solar radiation, high temperatures). This light northerly flow may contribute to Houston's ozone episodes by acting to counter the sea breeze, resulting in increased stagnation [*Darby*, 2005].

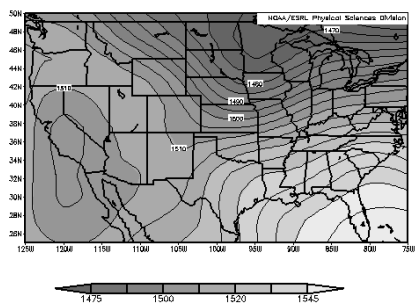

Figure 49. 850 hPa composite map of geopotential heights for non-episode days September 2006.

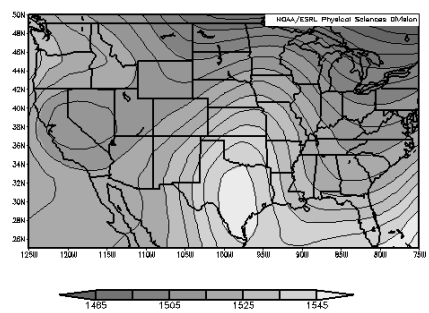

Figure 50. 850 hPa composite map of geopotential heights for September ozone episodes 2006 (10 episodes).

Cluster Analysis of 850 hPa Maps

To observe the weather conditions that create elevated ozone levels in the Houston area, 850 Pa maps were analyzed and placed in "clusters" based upon classifications according to *Ngan and Byun* [2007]. These clusters were created based upon data from May-August of 2005-2006. The cluster classifications were completed by visual inspection of 850 hPa maps and are shown in Figure 51.

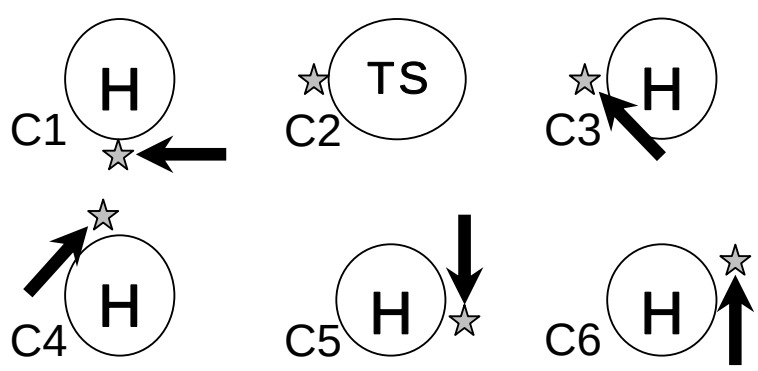

Figure 51. Illustration of different clusters according to *Ngan and Byun* [2007] (H = High Pressure Center, TS = Tropical Storm. Star represents Houston, arrow = wind direction).

The classifications are as follows:

1) Cluster 1 was designated as easterly flow with a High pressure system to the north of Houston.
2) Cluster 2 occurs when Houston is under the influence of a tropical storm (which did not happen in 2006).
3) Cluster 3 is characterized by a High pressure system to the northeast of Houston, providing Houston with southeasterly flow.
4) Cluster 4 occurs when a High is located in the Gulf, and Houston is under southwesterly flow.
5) Cluster 5 is designated as anytime Houston experiences northerly flow with a High to the West. This is otherwise known as the "post-frontal" cluster.
6) Cluster 6 occurs when there is a High to the east of Houston, giving Houston southerly flow from the Gulf [*Ngan and Byun*, 2007].

Table 2 illustrates the frequency of the clusters for ozone episode and non-episode days. It can be concluded from this table that the environments caused by cluster 1 and cluster 5 are the most common scenarios for ozone episodes in August and September 2006. The majority of the scenarios which occurred under cluster 5 are post-frontal and often precede an ozone episode. In fact, it was found that nearly every episode that occurred in September 2006 occurred in a post-frontal environment. This is likely due to the light northerly flow countering the sea breeze, elevated continental background levels, or a combination of the two.

	C1(E)	C2(Trop. Storm)	C3(SE)	C4(SW)	C5(N)	C6(S)
Episode Days	6	0	0	0	5	1
Non-episode Days	6	0	9	12	10	12

Table 2. Cluster frequency during ozone episodes and non-episode days.

Cluster 5 occurred 5 times in episode days and 10 times during non-episode days. This cluster is typical of the post-frontal environment. Once a cold front passed through the Houston area, the northerly flow was typically rather strong, which would help to keep ozone values down due to the higher wind speed ushering pollutants away from the Houston area. Also, precipitation is common with a frontal passage and this could help decrease ozone values due to the enhanced mixing, although the designated cluster for the day falls under a northerly flow category. In order for an episode to occur under cluster 5, the winds need to be weak enough to allow some stagnation to occur.

There are an equal amount of occurrences of Cluster 1 in episode and non-episode days. However, Cluster 1 makes up 50% of the episode days, but only 12% of the non-episode days. In September, cluster 1 was rather common after a frontal passage as High pressure passed to the north of the Houston area. Cluster 1 can result in elevated ozone levels due to winds carrying precursors from the ship channel region. Cluster 1 was also common in August, but if the wind speed was too high it would not result in an episode.

The Role of Frontal Passages on Houston's 2006 Ozone Episodes and their Effect on Background Ozone

September 2006 was unique because nearly every episode occurred in the wake of a frontal passage. This is in contrast to 2005 where a very active tropical season occurred, and the first cold front did not fully make its way past the Houston area until late September. The first major frontal passage occurred on August 29, 2006, which occurred two days before the worst ozone episode that Houston experienced in 2006. The dates of each cold frontal passage are shown below, along with the dates of the ozone episodes.

Frontal Passage	Episode
8/29	8/31, 9/1, 9/3
9/5	9/7
9/12	9/13, 9/14
9/18	9/20
9/24	9/26, 9/27
9/28	none

Table 3. Dates of cold frontal passage in relation to ozone episodes.

There are likely several reasons for the increase of Houston's ozone concentration in the wake of these fronts. These frontal passages were often followed by cooler temperatures which may have helped to increase the strength of the morning inversion (which will be discussed in the next chapter). Also, the fronts ushered in very dry continental air which helped the sky to remain clear, and essentially eliminated any major chance of precipitation on those days. Another major effect of these cold front passages could be to increase the background level of Houston's ozone with the transport of continental air, along with subsidence occurring behind the front.

Table 3 shows that although a cold front passed through the Houston area on September 28, an episode did not occur after this frontal passage. The reason for this is that there was a quick return to southeasterly flow the day following the frontal passage. This is something that did not occur as rapidly in the previous episodes, mainly due to the speed of the Low pressure system that was associated with this particular cold front. Even in the episode several days prior, the High center at 850 hPa remained in place for a couple of days after the frontal passage.

As discussed above, each day was classified using cluster analysis in order to determine the effect of the 850 hPa wind pattern on Houston's average ozone concentration. The background ozone was determined by a method used by *Nielsen-Gammon et al.* [2005a]. Several stations were chosen on the perimeter of the CAMS network that were determined to be representative sites with limited effects of titration by NO, or were not in close proximity to power plants or chemical refineries. The stations chosen are shown in Figure 52 (taken from *Nielsen-Gammon et al.* [2005a]). One station was added on the NE side of Houston (Crosby library). This site was chosen since the analysis done by Nielsen-Gammon did not have a site that represented the east side of Houston. The background ozone was defined as the minimum of the 8-hour mean ozone values among all background stations. This value usually occurs in the CAMS station that is upwind of the Houston area *Nielsen-Gammon et al.* [2005a].

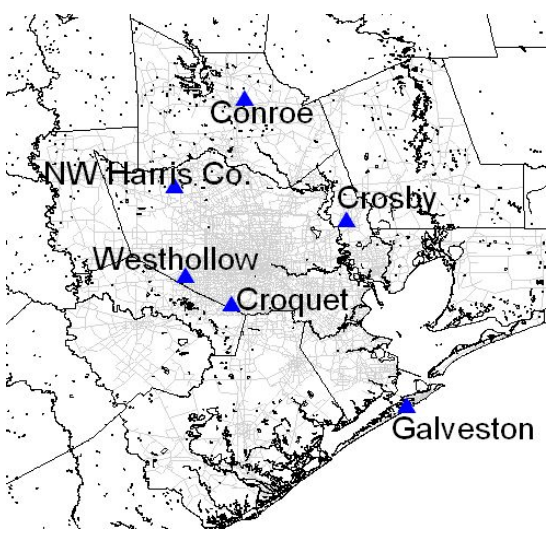

Figure 52. CAMS stations used to determine 8 hour background ozone.

Cluster classifications as shown in Figure 52 were also applied in the post-frontal environment to determine the effect on the background concentration of Houston. Table 4 shows the effect of the synoptic wind on Houston's background ozone level:

Cluster	C1(E)	C2(Trop. Storm)	C3(SE)	C4(SW)	C5(N)	C6(S)
Av. Background O_3 (ppb)	41.6	-------	31	28	52.4	20.6

Table 4. Average background ozone mixing ratio classified by synoptic cluster.

As indicated in Table 4, cluster 5 has the highest background values. This is associated with a High pressure system to the west of Houston, bringing in northerly flow from the continental United States. This cluster is very common in the wake of a cold front. Cluster 1 also has a higher background value, which is typical of easterly flow coming into the Houston area. This cluster can have a slight northerly component which would help to bring in continental air and thus increase the background ozone level. When comparing the backward trajectories for the ozone episodes of September 2006, all trajectories came from either northern Texas or from the northeast in Louisiana. This is evidence that Houston was under the influence of a continental air mass, as would be expected in the post-frontal environment.

As an example for the impact of a frontal passage Figures 53-55 show the time period of August 28-30 which preceded the August 31 ozone episode. In this case, the frontal passage occurred on the evening of August 29. Figures 53 show the ozone sounding for August 28 and 29 (pre-frontal) and August 30 (post-frontal). The figures reveal an increase in ozone in the boundary layer and within a portion of the free atmosphere. The background value above the boundary layer increased from approximately 35 ppb to 55-60 ppb.

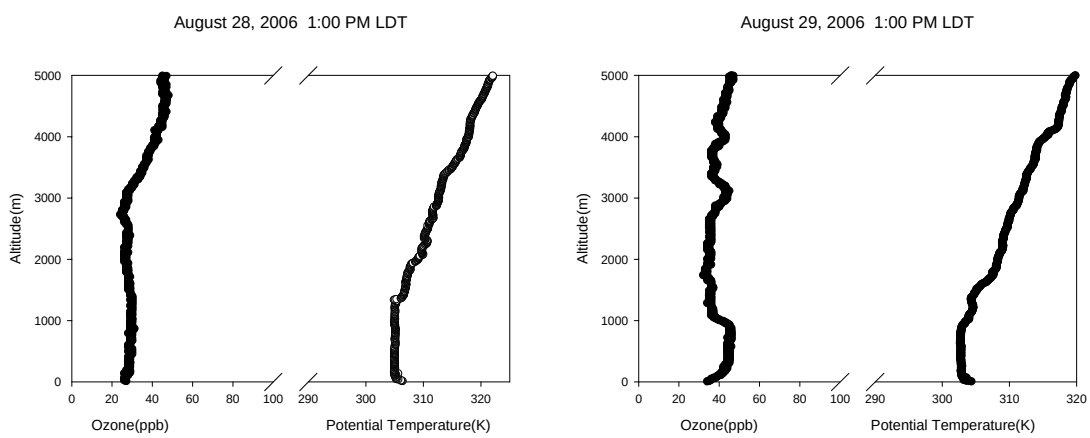

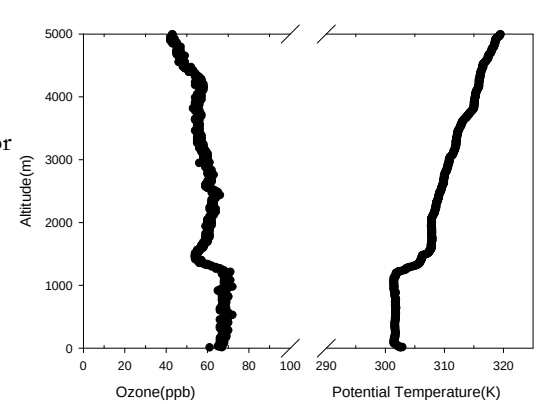

Figure 53: Ozone sounding for August 28, 2006 [pre-frontal] (above left), ozone sounding for August 29, 2006 [pre-frontal] (above right), and ozone sounding for August 30, 2006 [post-frontal] (below right).

This is likely due to the difference in the origin of the air mass, as can be seen from the backward trajectory plots of 54A-B. While Houston was under the influence of a maritime air mass from the Gulf of Mexico on August 28, the background levels in the troposphere up to 2500 m AGL were rather low. After the frontal passage on August 29, the background levels increased to the August 30 levels shown in Figure 53. 2500 m AGL was chosen as an example for these backward trajectories. Other levels from 500-3000 m AGL yielded similar results.

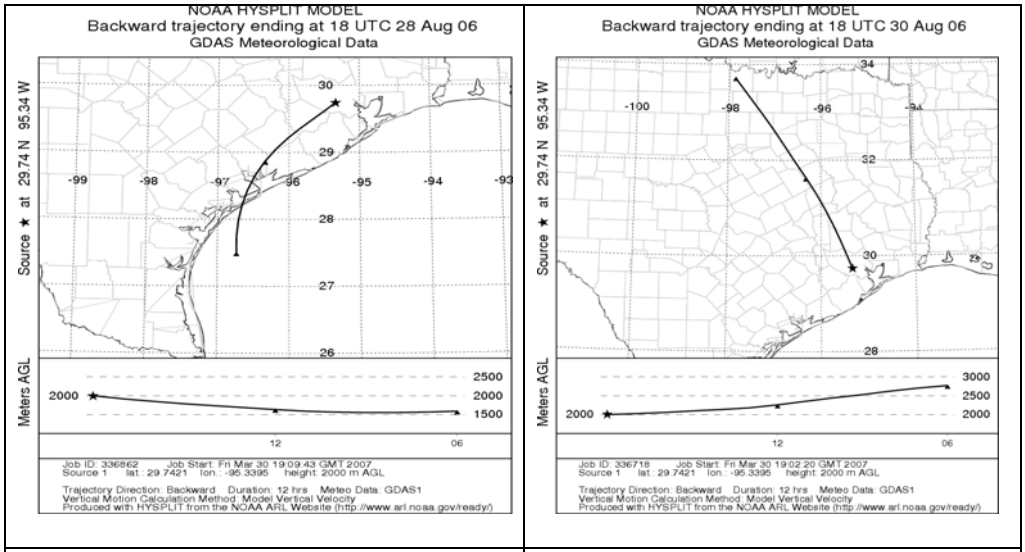

Figure 54A. 12 Hour Backward Trajectory for 1300 CDT August 28, 2006 (pre-frontal)	Figure 54B. 12 Hour Backward Trajectory for 1300 CDT August 30, 2006 (post-frontal)

On the day of the episode, the background ozone in the free troposphere increased to high amounts, as is shown in Figure 55. These graphs also illustrate a large amount of local production occurring below the elevated levels aloft. August 31 was characterized by high solar radiation, high subsidence, and stagnant conditions.

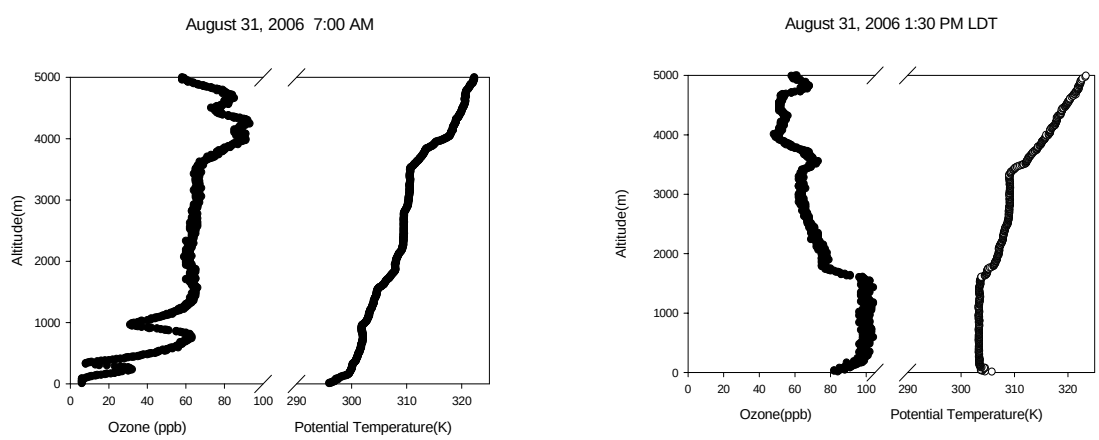

Figure 55. Left: oone sounding for 0700 CDT August 31, 2006 (post-frontal, episode day). Right: ozone sounding for 1330 CDT August 31, 2006 (post-frontal, episode day).

4. Conclusions

During TexAQS-II multiple soundings were launched from UH – Main Campus on forecast episode days, while twice-per-day launches occurred on non-episode days. The data from multiple soundings in a single day was used to determine the rate of mixed layer growth in the morning, an important factor for peak ozone values, as well as the maximum mixed layer heights in the afternoon. Results of the soundings were used for sea-breeze characterization and to determine the structure of the low-level jet and the strength of nocturnal inversions. On particular occasions these rawinsonde launches were complemented by tethersondes to elucidate small-scale structures. Information about vertical profiles of meteorological data were related to surface ozone measurements obtained within the TCEQ network as well as ozonesonde data which were launched twice a day on IOP days. Ozonsonde launchings were performed in a collaborative effort with the University of Valparaiso/IN.

Comparison between "moderate" and "high" ozone days indicated that a delay in the development of the PBL could be associated with higher ozone peaks in the afternoon. There is also some slight tendency that higher ozone values are observed under higher PBL height conditions, whereas low peak ozone values tend to occur under low PBL height conditions. This could be due to cooler temperatures being experienced in the morning hours since most of the episodes in this study occurred in the post-frontal environment. This may have the effect that has been observed in other studies which helps to concentrate O_3 precursors near the surface and could lead to higher peak values in the afternoon (e.g. *Berman et al.*, 1999). Although it was hypothesized that a stronger morning inversion could lead to higher daytime ozone peaks, this was not found to be the case in August-September 2006. Actually this study showed that the morning PBL height had little effect on peak ozone concentration. This could be because the strongest morning inversions occurred right after a cold front passage which was usually 1-2 days before an episode occurred. The northerly flow occurring in the wake of a cold front was usually too strong to gain episode status.

However, also other parameters may superimpose the PBL impact: Important factor seem to be that (i) under distinct land-sea-bay breeze conditions E wind flow conditions occur which bring Ship Channel emissions into the Houston area and that (ii) these conditions occur during late morning hours at relatively low PBL heights (i.e. delayed PBL development), but already at a time where fast photochemistry occurs. Low PBL heights at this time will also likely lead to a volume effect leading to higher concentrations and can also enhance the overall probability for an 8-hr ozone exceedance, but not necessarily lead to higher peak ozone values in the afternoon. These regional flow conditions may also be superimposed by elevated continental background ozone levels as indicated by results from ozonesonde launches.

It was also noticed that many episode days had strong elevated inversions associated with them. This is typical of post-frontal soundings. It was found that higher afternoon ozone peaks occurred where there was an extremely dry air mass aloft, although it was not always associated the strongest inversion observed. Moist inversions (associated with cloud layers) did not produce very high ozone peaks. The strongest and driest air masses aloft did not have extremely high ozone values associated with them, mainly because these episodes occurred right after a frontal passage where the northerly flow was strong enough to keep ozone peaks in check. Based on composite skew-t diagrams it was found that high ozone days in were characterised by a rather moist environment with variable winds in the PBL, whereas high ozone days in September exhibit a slight elevated inversion with PBL winds coming from the east/northeast.

In a synoptical point of view it was found that the upper-level regimes of August included a High centered to the east of Houston over Arkansas, for episode and non-episode days in the upper-levels. However, September's ozone episodes were dominated by an upper-level ridge located over

central Texas and an 850 hPa High sitting just west of the Houston area. This brought dry, continental air into the Houston area and increased background levels of O_3 by as much as 20-30 ppb. Cluster analysis and background level analysis showed that Houston experienced its highest O_3 values under a N or E flow regime at 850 hPa. It was also found that all O_3 episodes in the month of September occurred in a post-frontal environment. Ozonesonde profiles showed an increase in background O_3 within the free troposphere corresponding to transport from the continental United States. This was contrasted with the relatively low values when the back trajectory came from the Gulf of Mexico.

Analysis of ozone profile suggests that about 10 ppbv ozone may be considered as left-over ozone from the previous day and remain in the residual layer. In addition, analysis of ozonesonde data also shows that regional-scale transport may have an impact on local O_3 levels. Depending on the air mass origin background ozone levels may range from 30 ppbv (marine) to close to 60-70 ppbv (continental). These different background patterns are also present in the surface O_3 data, i.e. without the increase of the background ozone levels no high ozone values in the PBL would occur. Vertical ozone profiles frequently showed specific layers with enhanced values. Sometimes these profiles revealed rather complex structures. In most cases these layers occur above 3000 m AGL. and do not have a vertical extension larger than 500 m. Often, the ozone enhancement is about 10-20 ppbv, but can also reach up to 40 ppbv. Possible source areas of these enhancements include Mexico and the Canadian or US Rocky Mountains and may be associated with biomass burning, i.e. forest fires or eventually urban sources. So far, the analyses did not explicitly show impacts coming from the industrial areas in the northeast of the US.

The overall results indicate that PBL effects on ozone levels cannot be considered as an isolated process. Various effects likely superimpose and require further analysis. In particular, the contribution from ozone in the residual layer, free troposphere and from the continental/marine background may be important. Synoptic-scale impacts as evident in the free troposphere will also likely play a major role. It is suggested to implement a way for continuous monitoring of the PBL structure and its impact on ozone. Also, it seems that background ozone (marine vs continental) should be properly addressed in Houston air quality investigation. Experimental approaches may include measurement platforms at high rising constructions (e.g. *Rappenglück et al.*, 2004) and/or the application of LIDAR systems to explore multidimensional behaviour of the PBL and to finally retrieve a PBL climatology for the Houston area.

5. References

Ancellet, G., and M. Beekmann, Evidence for changes in the ozone concentration in the free troposphere over Southern France from 1976 - 1995, *Atmos. Env.* **31**, 2835-2851, 1997

Angevine, W.M., White, A.B., Knupp, K. Coulter, R. Martine, T. Doran, J. C., and White, D., Mixed layer depths variability in the Houston area during TEXAQS2000. Prepr., *4th Conference on Atmospheric Chemistry*. American Meteorological Society, 12-17, January 2002, Orlando, FL, 2002

Banta R.M., C.J. Senff, J. Nielsen-Gammon, L.S. Darby, T.B. Ryerson, R.J. Alvarez, S.P. Sandberg, E.J. Williams, M. Trainer, A bad air day in Houston, *Bull. Americ. Met. Soc.*., **86**, 657-669, doi: 10.1175/BAMS-86-5-657, 2005

Berman, S., K. Jia-Yeong, and S. Trivikrama Rao, Spatial and Temporal Variation in the Mixing Depth over the Northeastern United States during the Summer of 1995, *J. Appl. Meteor.*, **38**, 1661-1673, 1999

Cheng, F-Y, Byun, D. Kim, S., Sensitivity study of the effects of land surface characteristics on meteorological simulations during the TexAQS2000 period in the Houston-Galveston area. Prepr., *13th PSU/NCAR Mesoscale Model User's Workshop*. June 2003, Boulder, CO, 2003.

Ching, J., Dupont, S., Gilliam, R. C., Burian, S., Tang, R., Neighborhood scale air quality modeling in Houston using urban canopy parameters in MM5 and CMAQ with improved characteriza-tion of mesoscale lake-land breeze circulation. *5th Conference on Urban Environment*, American Meteorological Society, 23-26, August , Vancouver. Canada, 2004.

Darby, L. S., Cluster analysis of surface winds in Houston, Texas, and the impact of wind patterns on ozone. *J. Appl. Meteor.*, **44**, 1788–1806, 2005.

EN-SCI Corporation, Information sheet for EN-SCI Corporation model 2Z-ECC atmospheric ozone sounding system, 2003b

EN-SCI Corporation, Instruction manual for EN-SCI Corporation model KZ-ECC atmospheric ozone sounding system, 1997

EN-SCI Corporation, VO3 Reference Manual: Digital ozone and radiosonde data acquisition and processing software (for use with EN-SCI Corporation model 2Z-ECC ozonesonde, incorporating the Innovative Systems Design V2 interface with optional GPS, **Version 5**, 2003a

Eresmaa, N., A. Karppinen, S.M. Joffre, J. Rasanen, and H. Talvitie, Mixing Height Determination by Ceilometer, *J. of Atmos. Chem. and Phys.*, **6**, 1485-1493, 2006

Grell, G., Dudhia, J. and Stauffer, D.R., A description of the fifth-generation Penn State/NCAR Mesoscale Model (MM5). NCAR Tech. Note NCAR/TN-398+STR, 117 pp., 1994.

Grimsdell, A. and W. Angevine., Convective Boundary Layer Height Measurement with Wind Profilers and Comparison to Cloud Base, *J. Atmos. Oceanic Technol.*, **15**, 1331-1338,1998

Heffter, J. L., Air Resources Laboratories Atmospheric Transport and Dispersion Model, *Tech. Memo.* ,**ERL ARL-81**, 24 pp., 1980

Lau, W.K.M. and Kim, K.M. How Nature Foiled the 2006 Hurricane Forecasts, *EOS Transactions, AGU.* **88**, No. 9, February 2007

Marsik, F., K. Fischer, T. Mcdonald, and P. Samson, Comparison of Methods for Estimating Mixing Height Used During the 1992 Atlanta Field Intensive, *J. Appl. Meteor.*, **34**, 1802-1814, 1994

Michalakes, J., J. Dudhia, D. Gill, J. Klemp and W. Skamarock: Design of a next-generation regional weather research and forecast model: Towards Teracomputing, *World Scientific*, River Edge, New Jersey, 117-124, 1998.

Morris G.M., S. Hersey, A.M. Thompson, S. Pawson, J.E. Nielsen, P.R. Colarco, W.W. McMillan, A. Stohl, S. Turquety, J. Warner, B.J. Johnson, T.L. Kucsera, D.E. Larko, S.J. Oltmans, J.C. Witte, Alaskan and Canadian forest fires exacerbate ozone pollution over Houston, Texas, on 19 and 20 July 2004, *J. Geophys. Res.*, **111**, D24S03, doi:10.1029/2006JD007090, 2006

Ngan, F. and Byun, D., Trajectory Analysis for Source-receptor Relation of High O_3 events over Houston/Galveston Area, *Proc. 9th Conference on Atmospheric Chemistry*, San Antonio/TX, Amer. Meteor. Soc., 2007

Nielsen-Gammon, J., Tobin, J., McNeel, A., Li, G., A Conceptual Model for Eight-Hour Ozone Exceedances in Houston, Texas Part I: Background Ozone Levels in Eastern Texas, *Technical report prepared for the Houston Advanced Research Center, Texas Environmental Research Consortium, and the Texas Commission on Environmental Quality*, 2005a

Nielsen-Gammon, J., Tobin, J., McNeel, A., Li, G., A Conceptual Model for Eight-Hour Ozone Exceedances in Houston, Texas Part II: Eight-Hour Ozone Exceedances in the Houston-Galveston Metropolitan Area, *Technical report prepared for the Houston Advanced Research Center, Texas Environmental Research Consortium, and the Texas Commission on Environmental Quality*, 2005b

Rappenglück B., Forster C., Jakobi G., and M. Pesch, Unusually high levels of PAN and ozone over Berlin, Germany, during nighttime on August 7, 1998, *Atmos. Environ.*, **38**, 6125-6134, doi:10.1016/j.atmosenv.2004.08.009, 2004

Russell III J.M., H.G.J. Smit, D. Hofmann, C. Rodgers, Stratospheric processes and their role in climate (SPARC): Assessment of trends in the vertical distribution of ozone, World Climate Research Programme, 1998

Senff, C., R. Banta, L. Darby, W. Angevine, A. White, C. Berkowitz, and C. Doran, Spatial and Temporal Variations in Mixing Height in Houston, *Technical Report prepared for the TCEQ*, 2002

Smit, H.G.J. and D. Kley, Jülich ozone sonde intercomparison experiment (JOSIE), *World Meteorological Organization Global Atmosphere Watch*, **130**, 1996

TCEQ [Texas Commission on Environmental Quality], "2006 Air Pollution Events" http://www.tceq.state.tx.us/compliance/monitoring/air/monops/sigevents06.html, (accessed March 2007)

TCEQ website: http://www.tceq.state.tx.us/compliance/monitoring/air/monops/naaqs.html

TCEQ, http://www.tceq.state.tx.us/compliance/monitoring/air/monops/naaqs.html (accessed October 2006)

Vaisala, Inc., RS80 Radiosonde technical information sheet, 1997

Vaisala, Inc., RS92 Radiosonde informational brochure, 2005

Wiegner, M., S. Emeis, F. Volker, B. Heese, W. Jundermann, C. Munkel, K. Schafer, M. Seefeldner, and S. Vogt, 2006: Mixing Layer Height over Munich, Germany: Variability and Comparisons of Different Methodologies, *J. Geophys. Res.*, **111**, D13201, doi: 10.1029/2005JD006593.

Yi, C., K. Davis, and B. Berger, Long-Term Observations of the Dynamics of the Continental Planetary Boundary Layer, *J. Atmos. Sci.*, **58**, 1288-1299, 2000

Yu, Chang-Han and Pielke, Roger., Mesoscale Air Quality under Stagnant Synoptic Cold Season Conditions in the Lake Powell Area,. *Atmos. Environ.*, **20**, 1751-1762, 1986

Zhang, J., and S.T. Rao, The Role of Vertical Mixing in the Temporal Evolution of Ground-Level Ozone Concentrations, *J. Appl. Meteor.*, **38**, 1674-1691, 1999

Appendix I – Plots of Radiosonde and Ozonesonde Launches on IOPs

August 17, 2006, "Level Red"

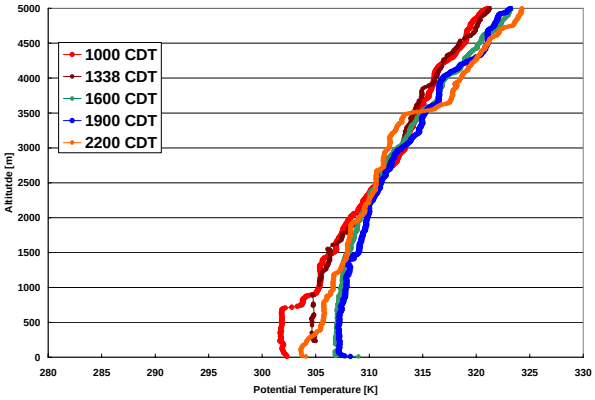

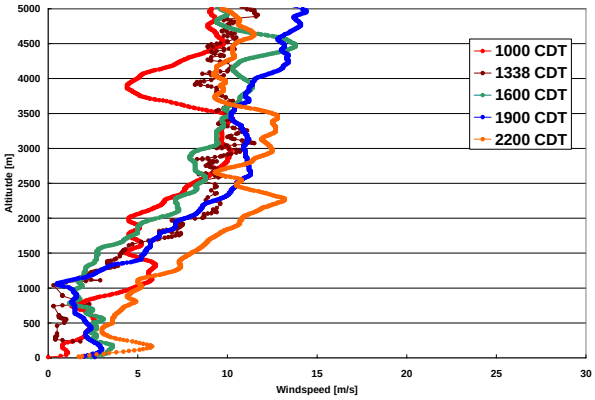

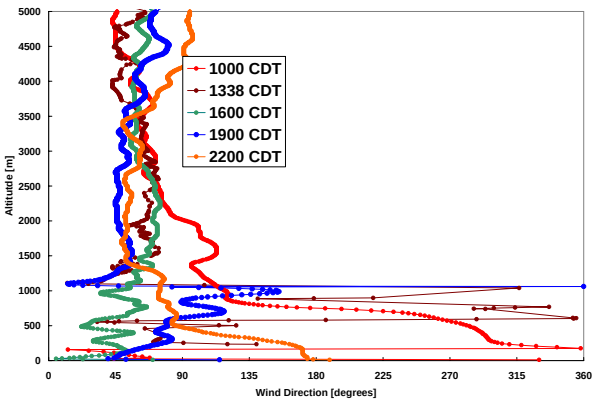

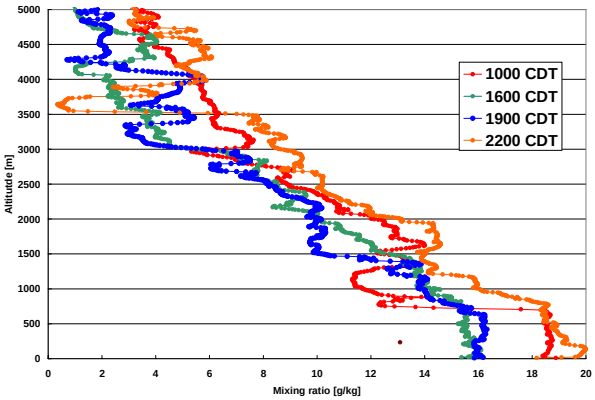

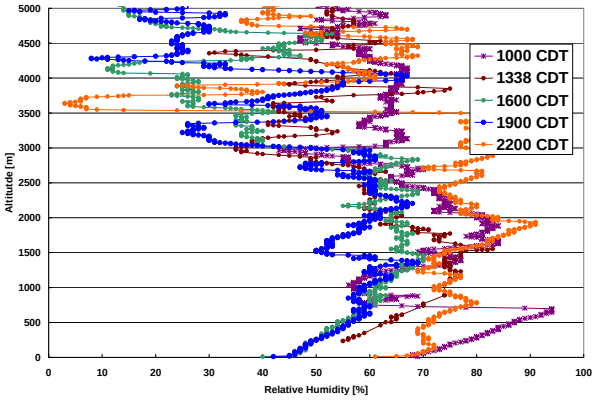

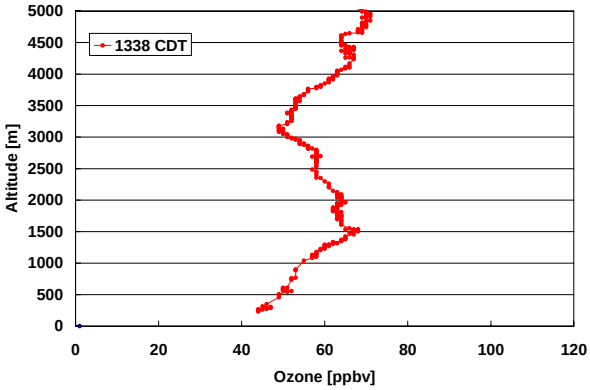

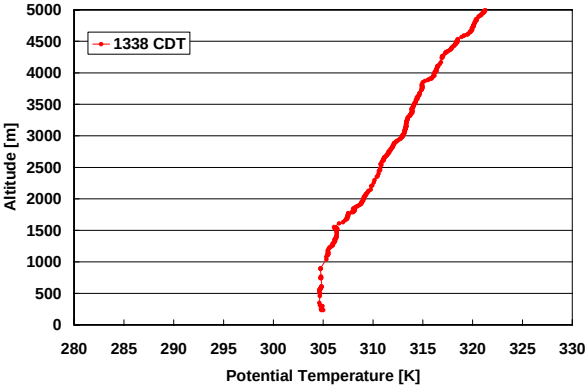

August 31, 2006, "Level Purple"

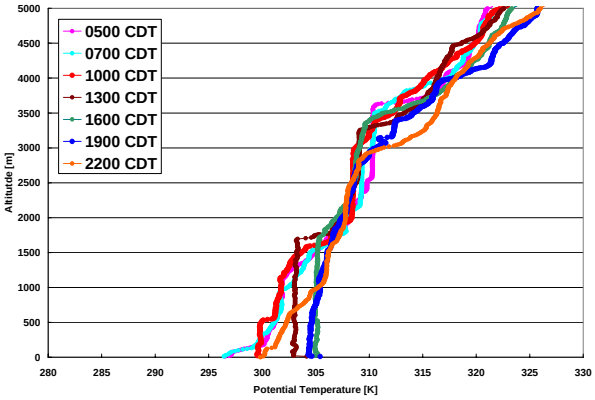

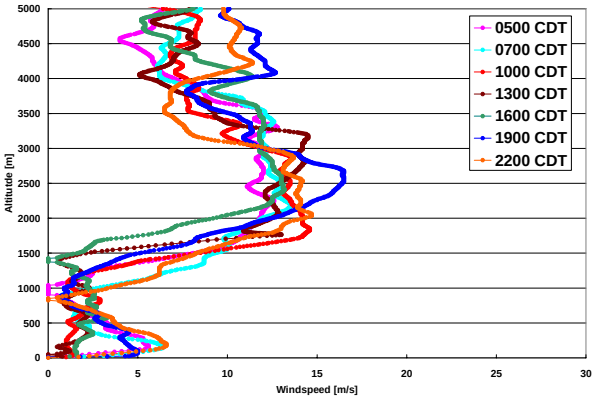

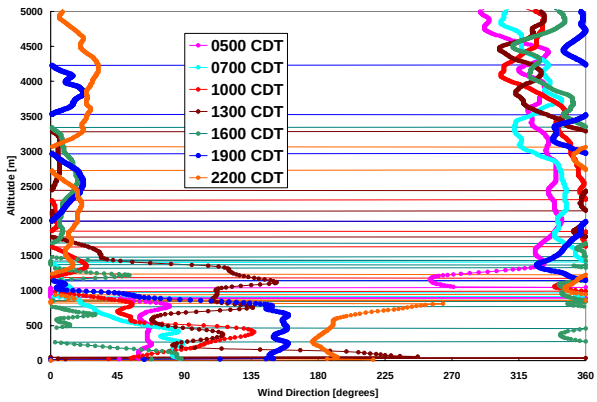

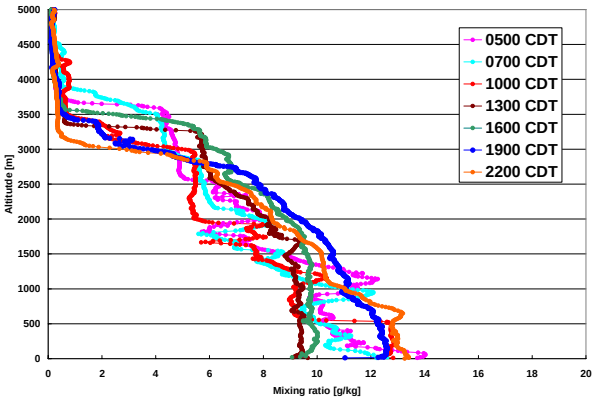

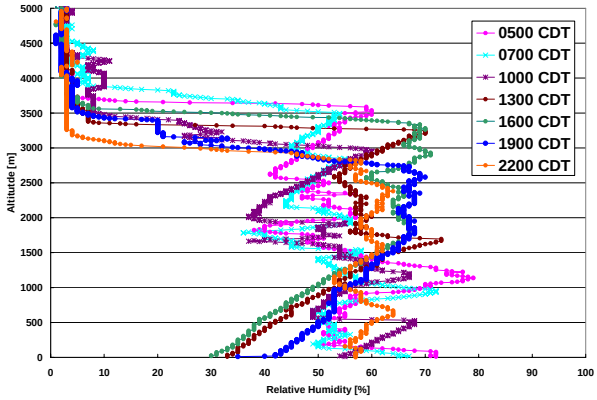

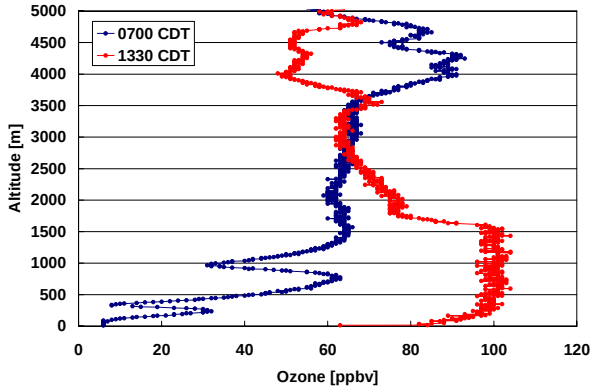

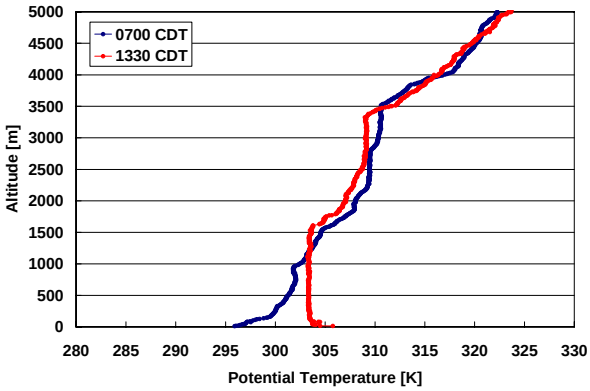

September 01, 2006, "Level Red"

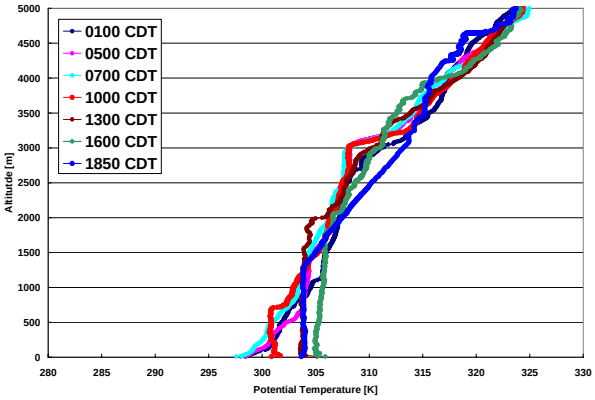

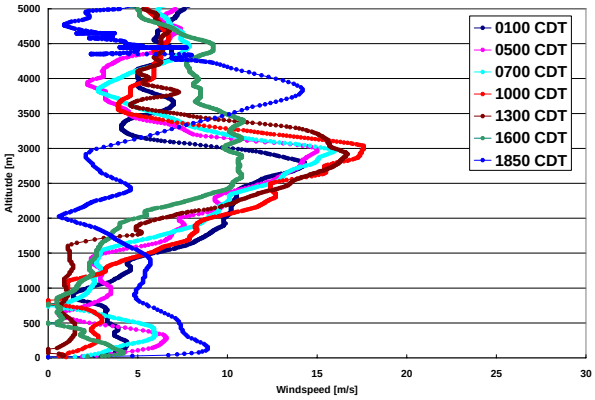

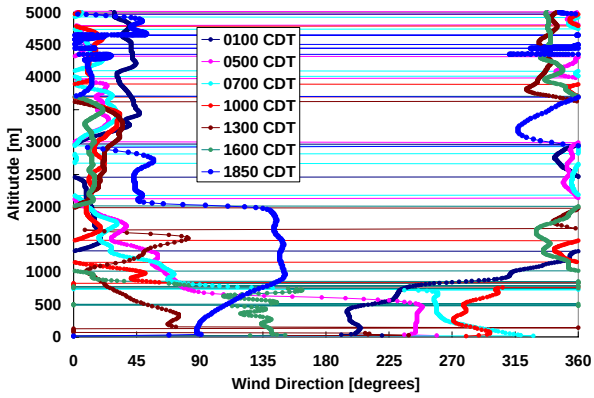

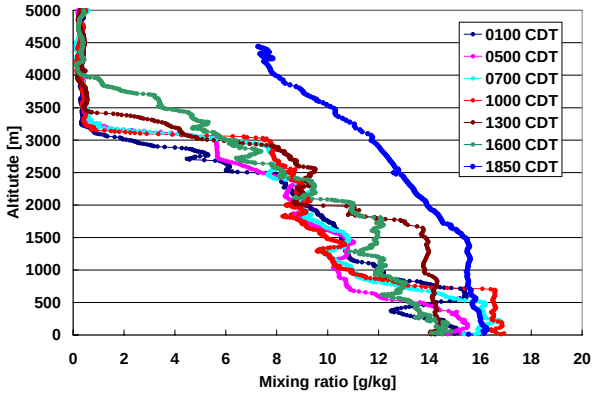

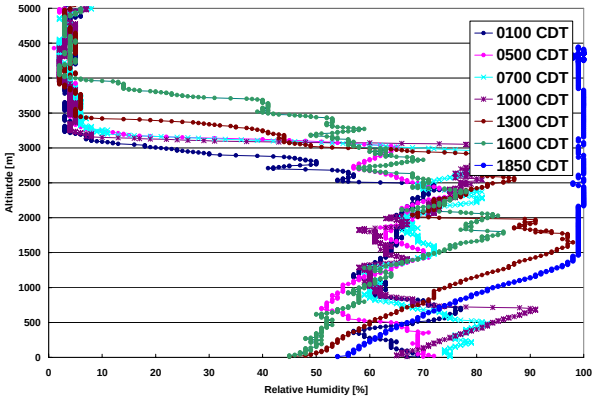

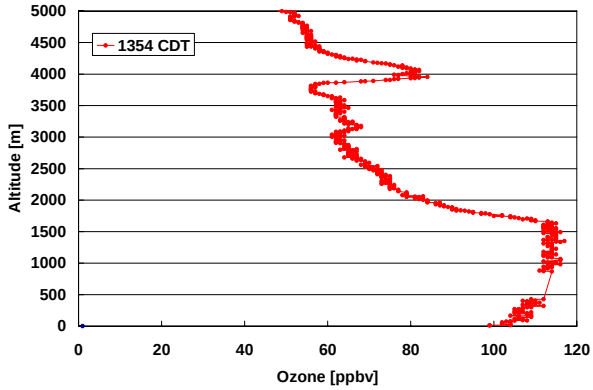

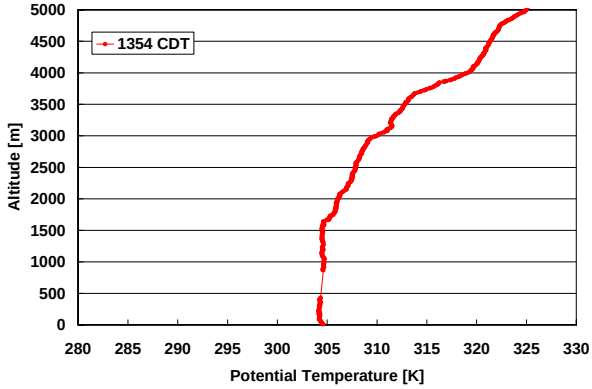

September 02, 2006, Forecasted high Ozone – but did not occur

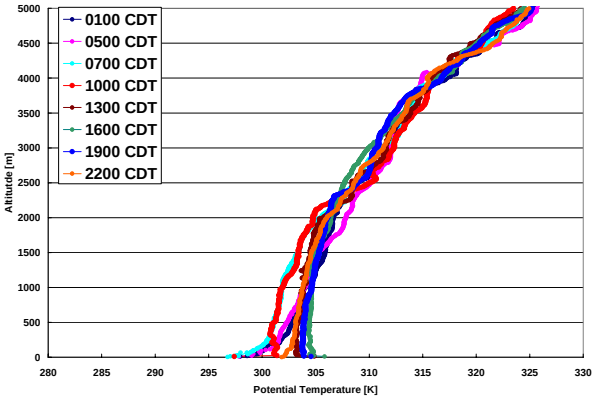

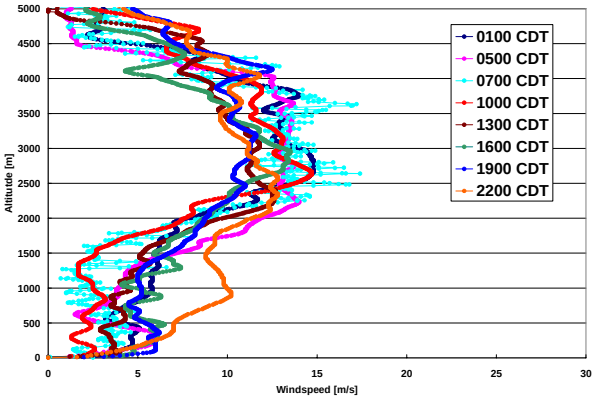

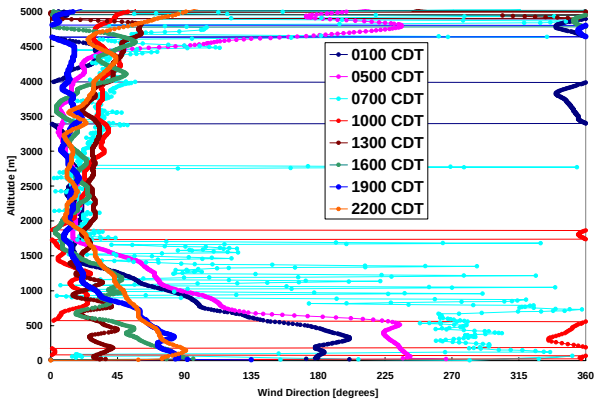

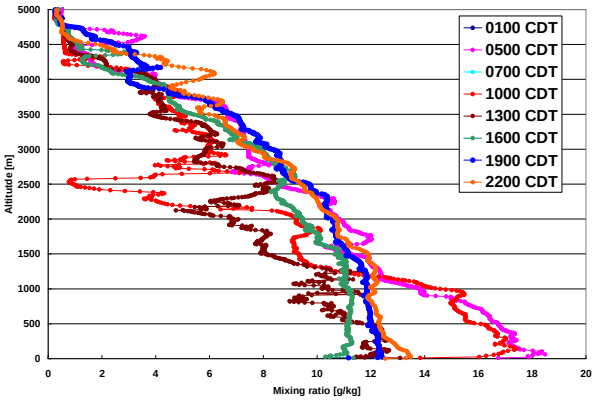

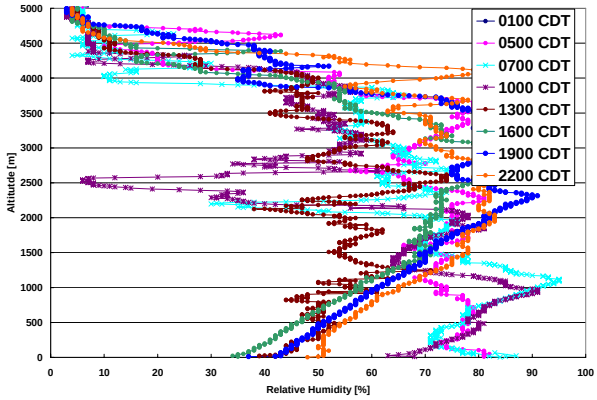

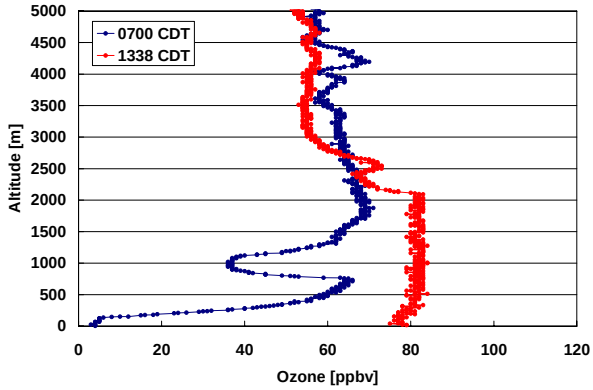

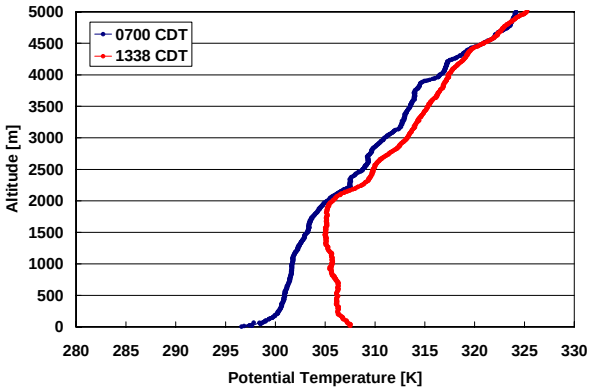

September 07, 2006, "Level Red"

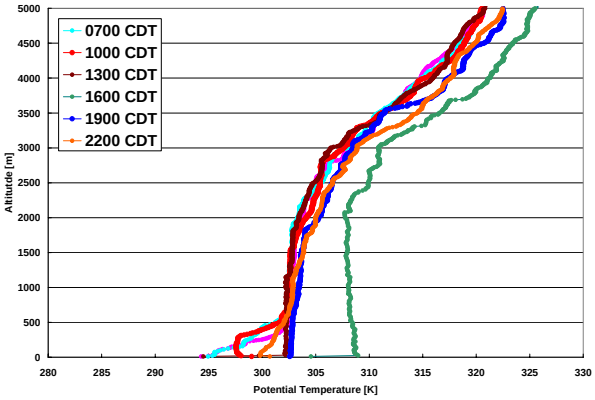

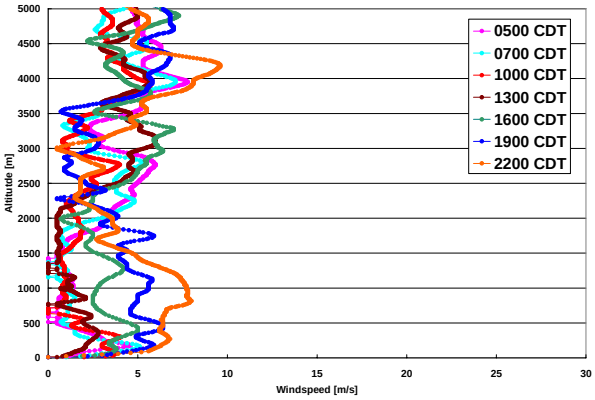

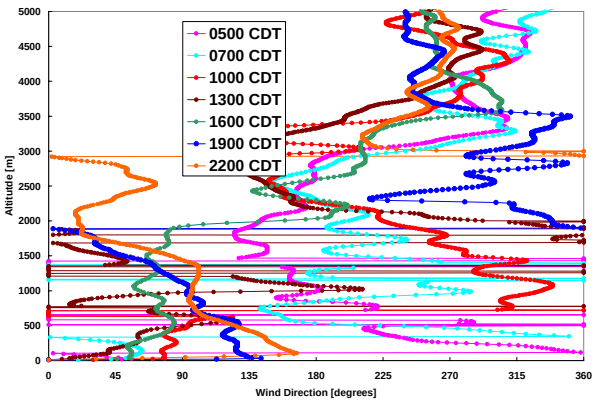

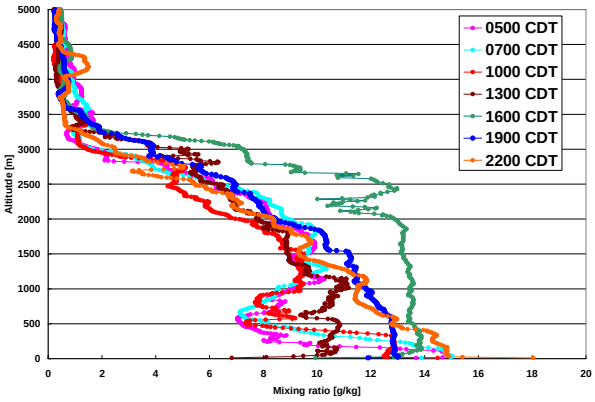

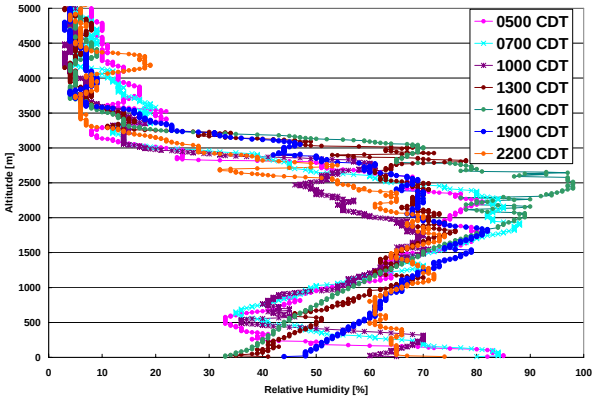

September 08, 2006

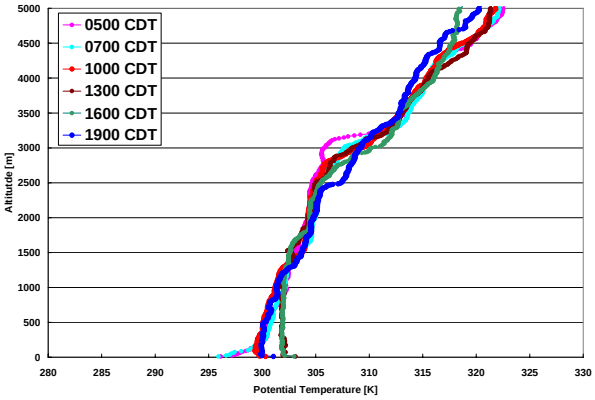

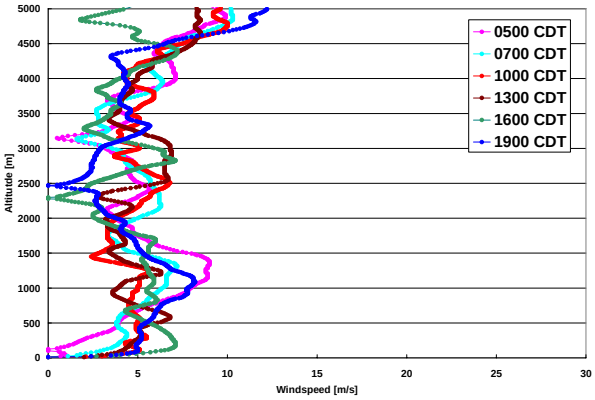

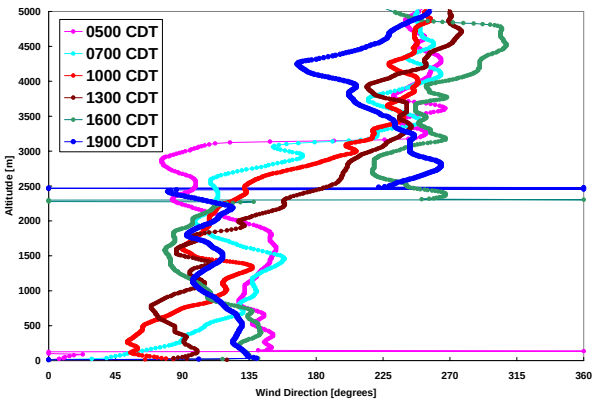

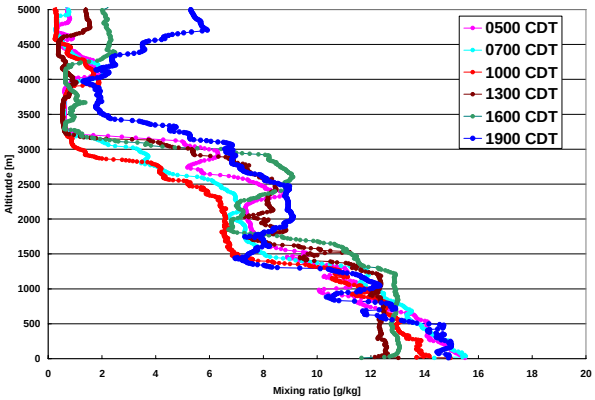

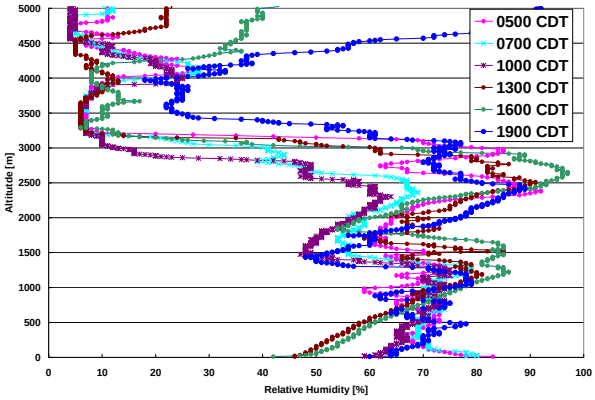

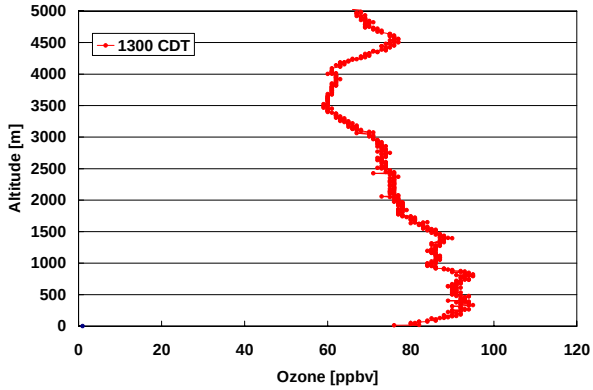

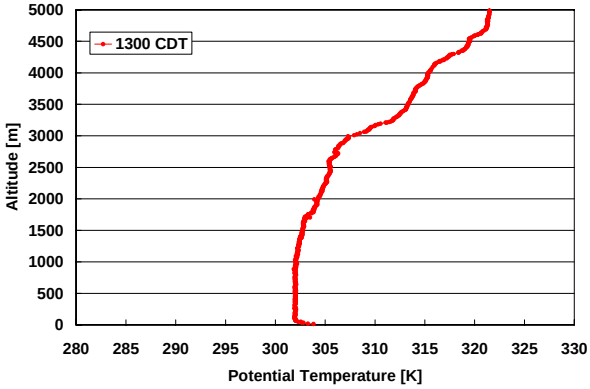

September 14, 2006, "Level Red"

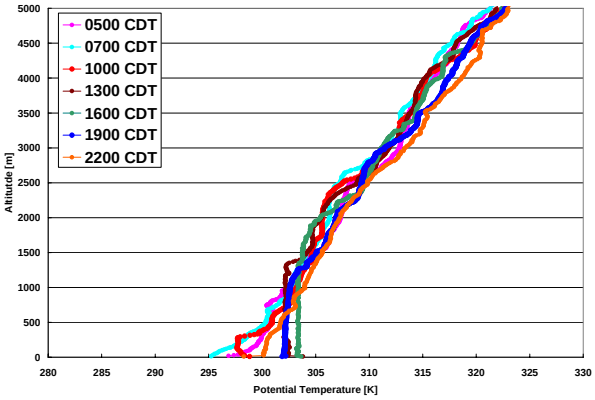

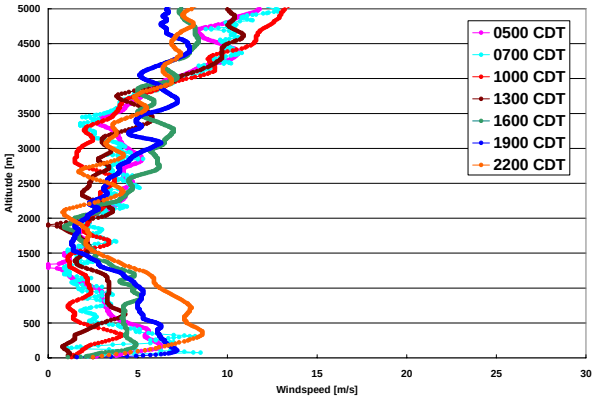

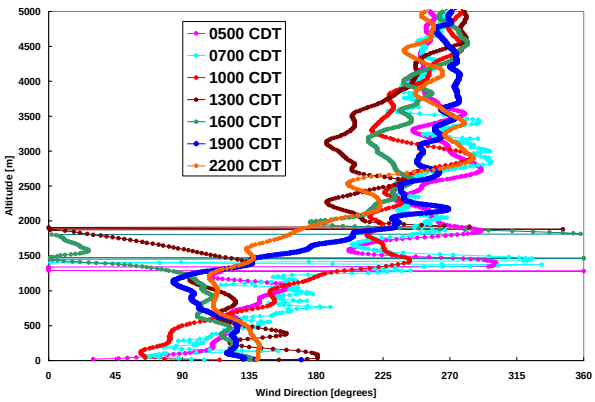

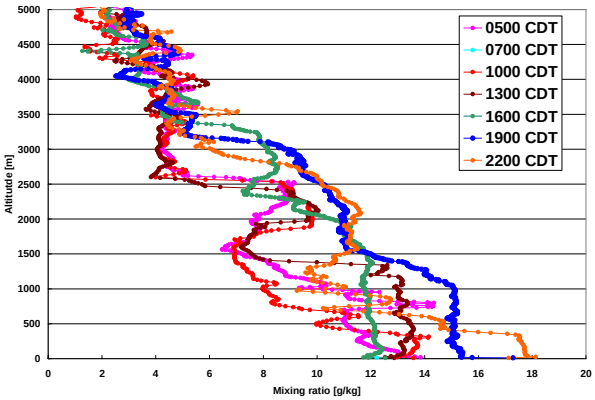

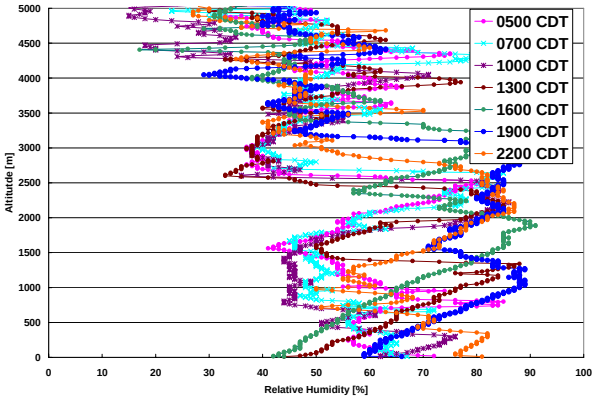

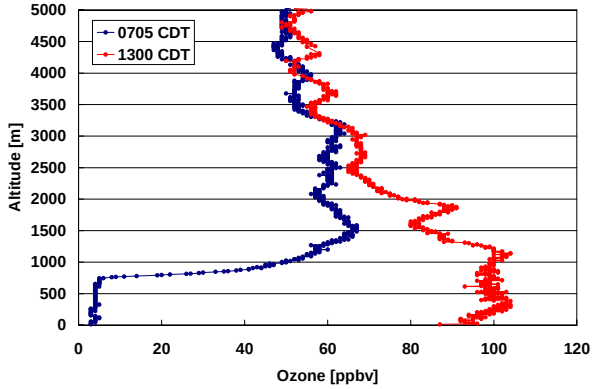

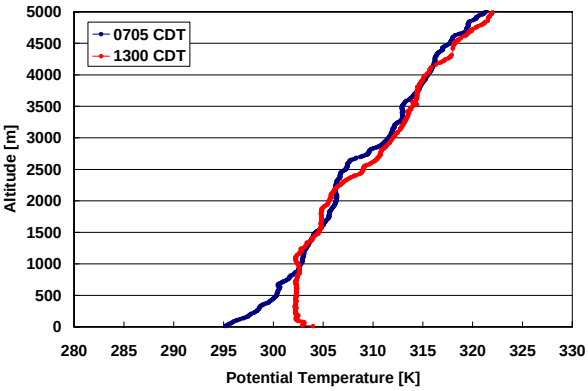

September 15, 2006

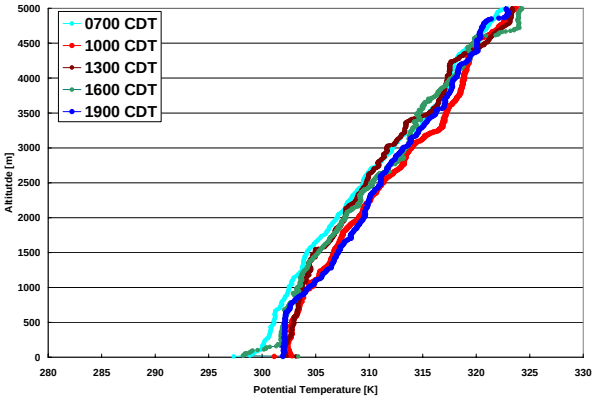

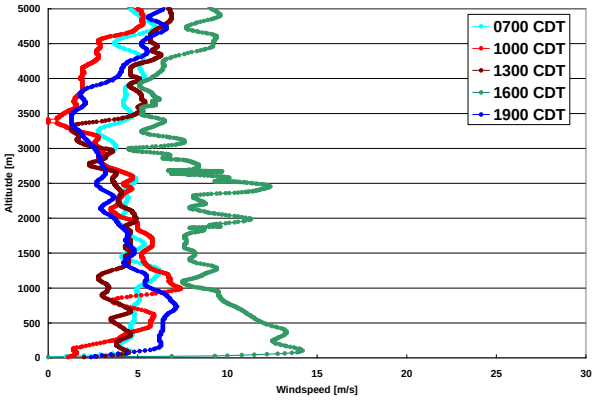

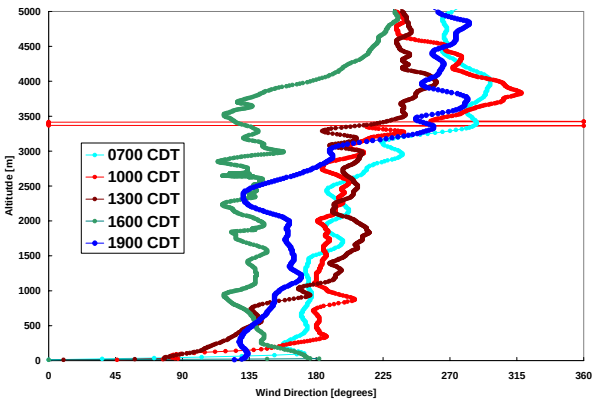

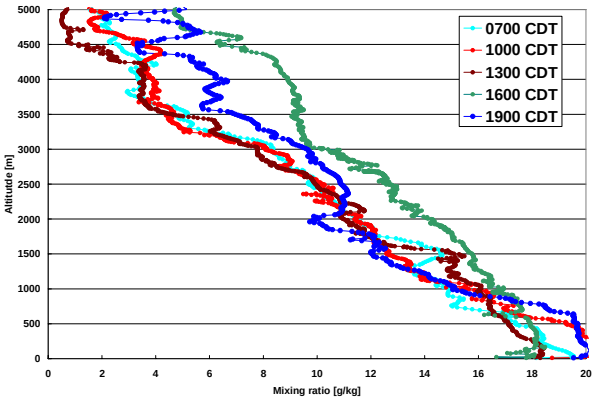

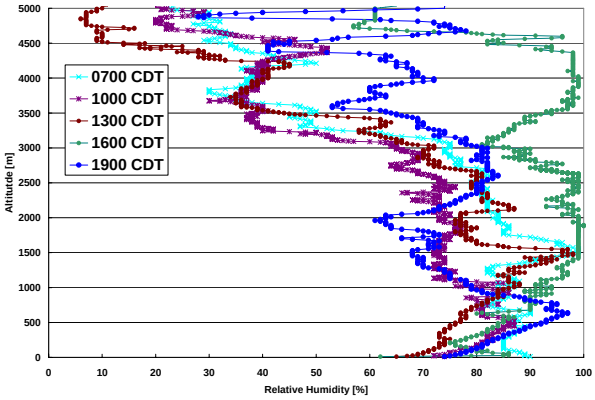

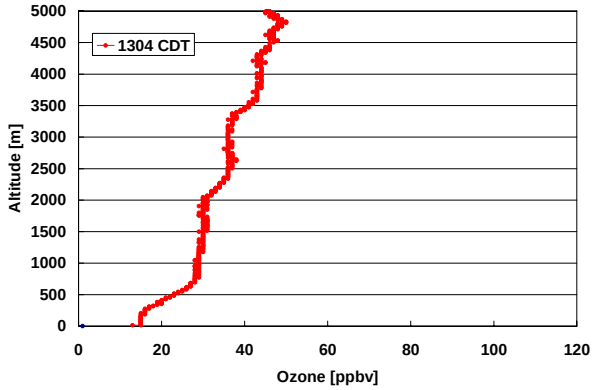

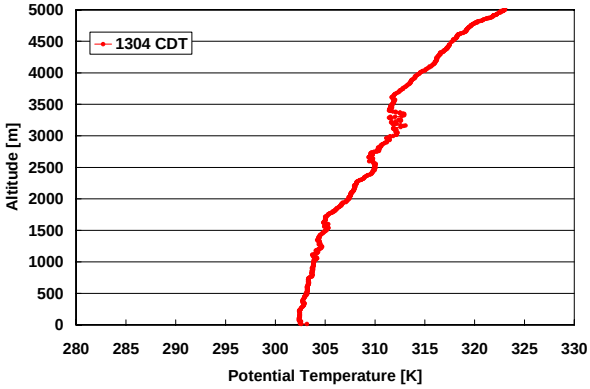

September 20, 2006, "Level Orange"

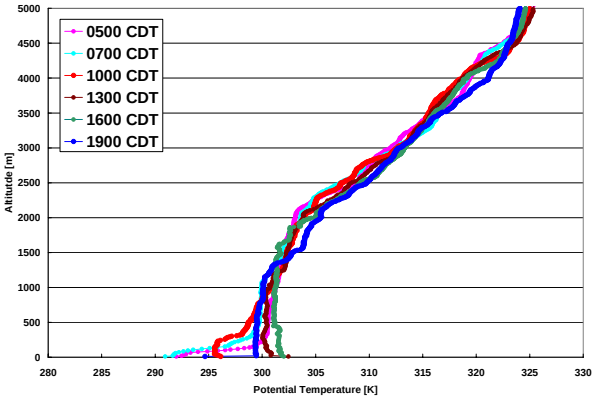

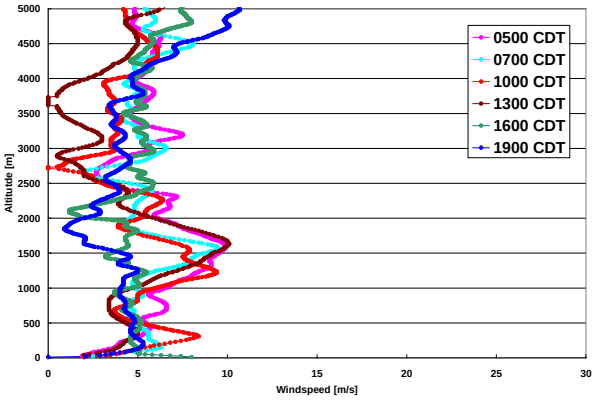

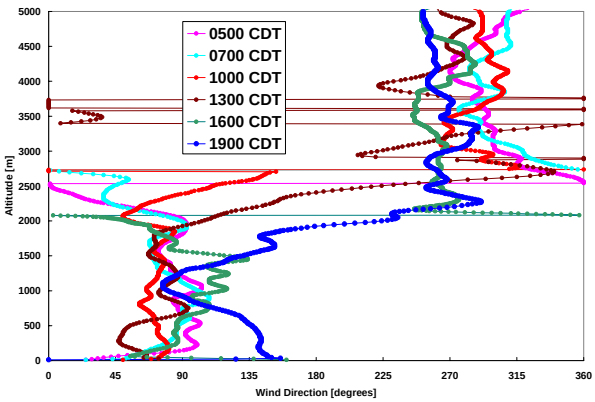

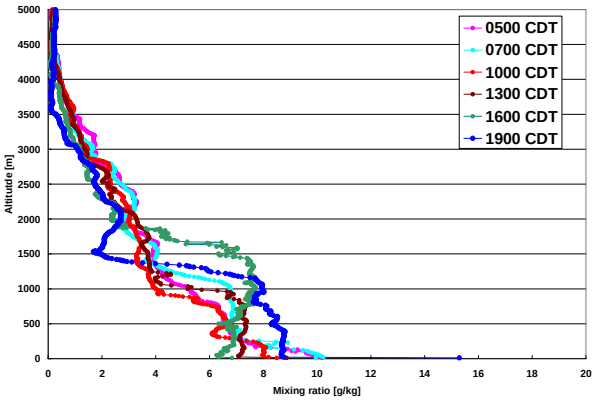

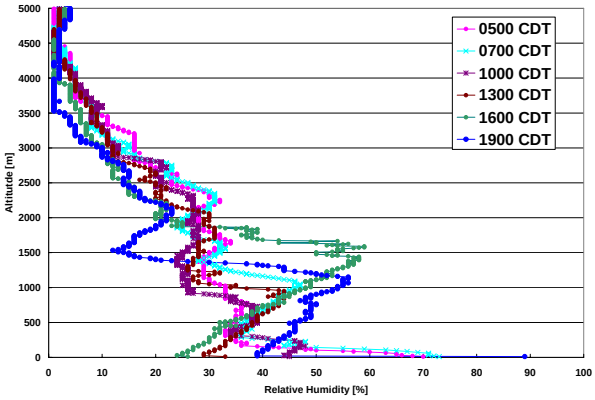

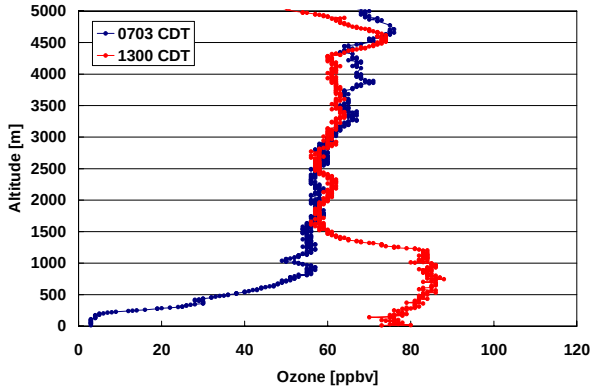

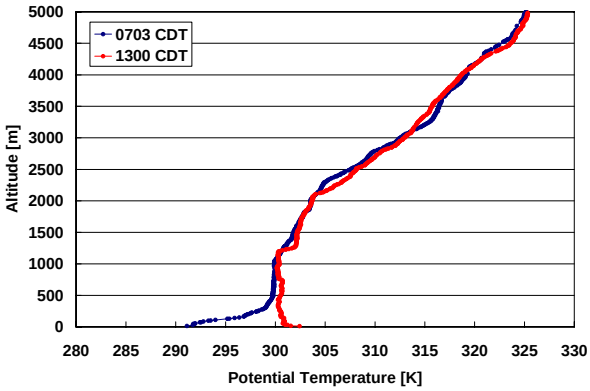

September 25, 2006

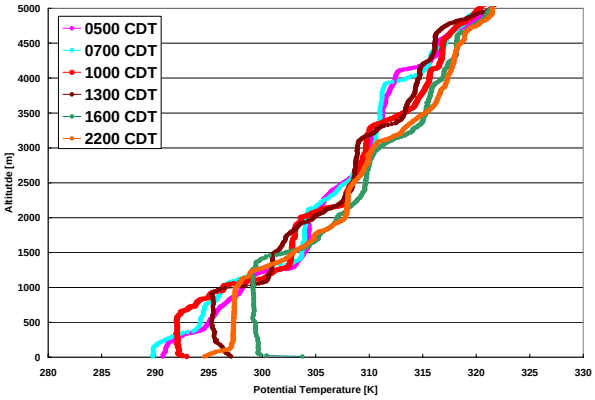

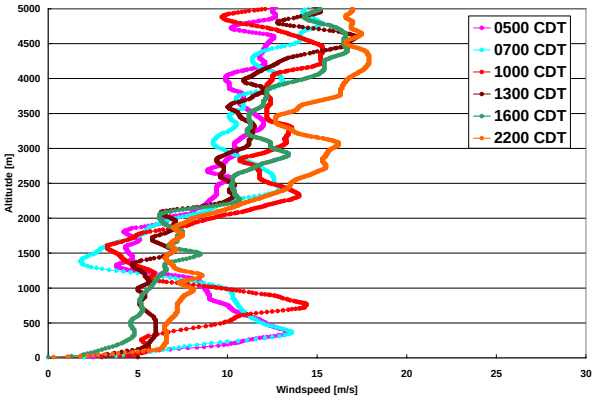

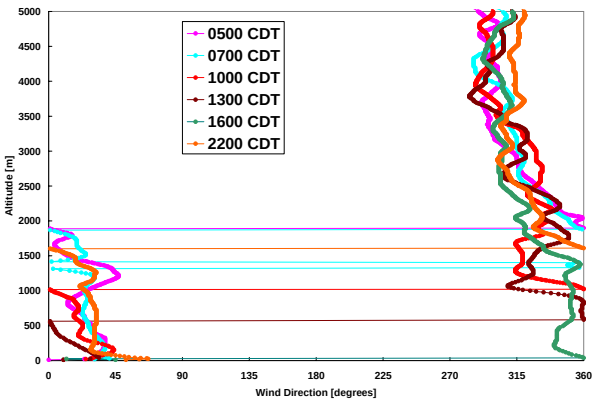

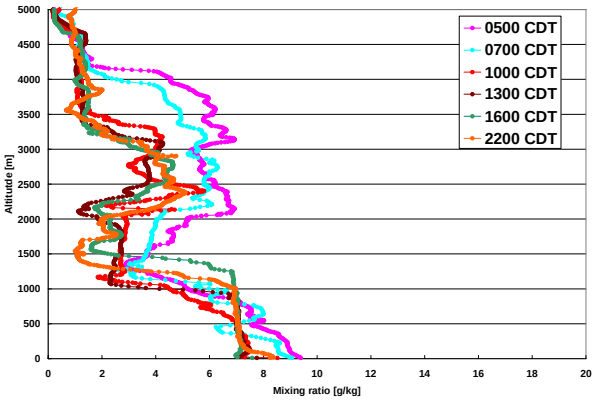

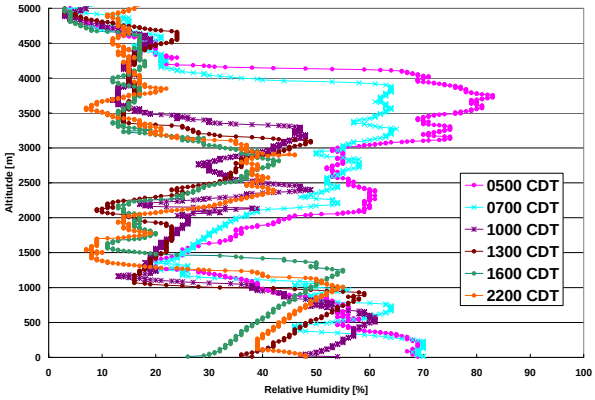

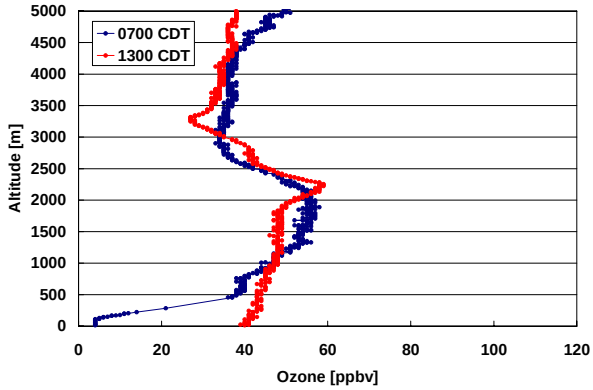

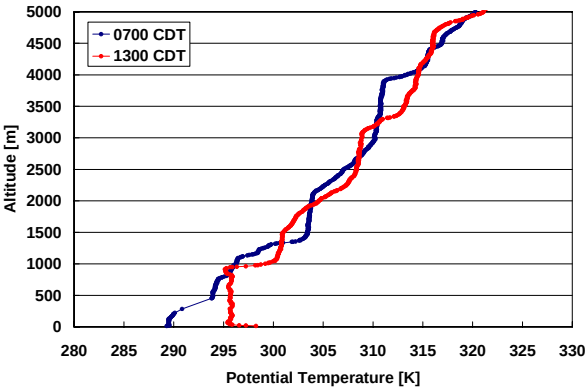

September 26, 2006

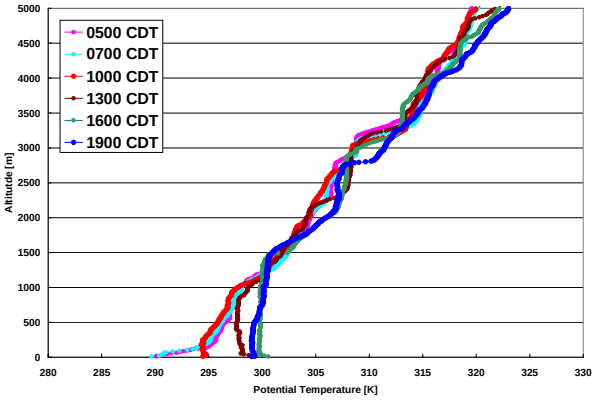

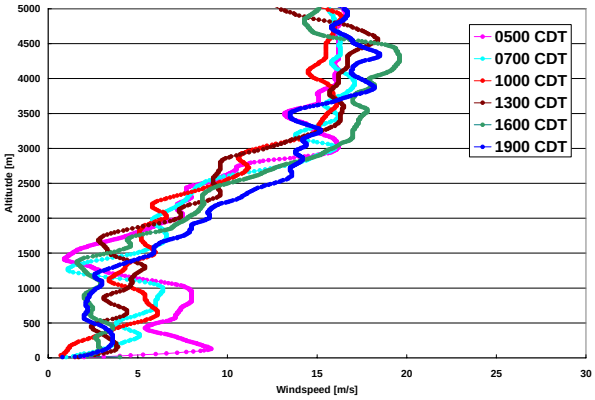

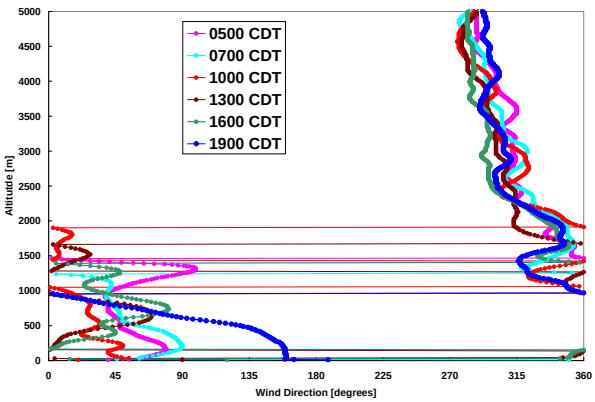

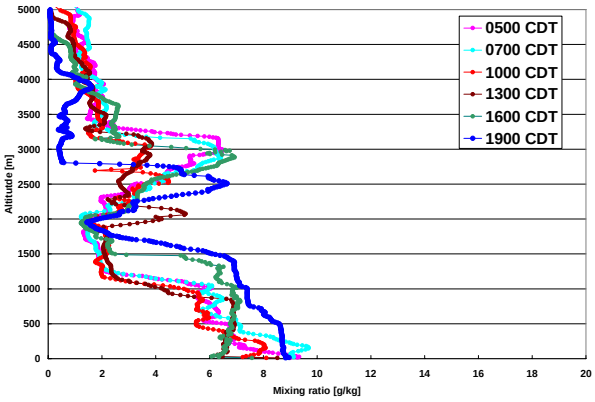

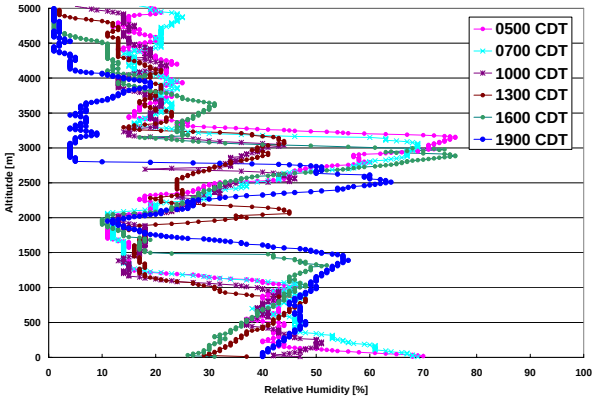

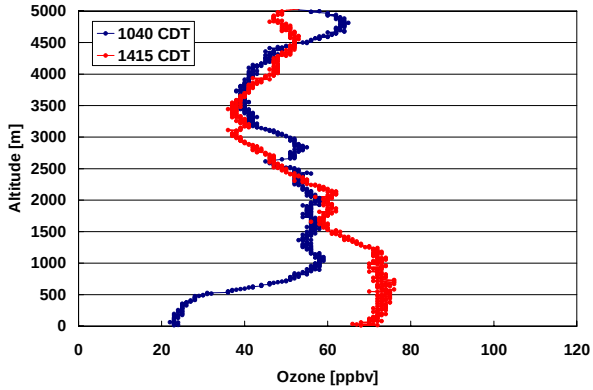

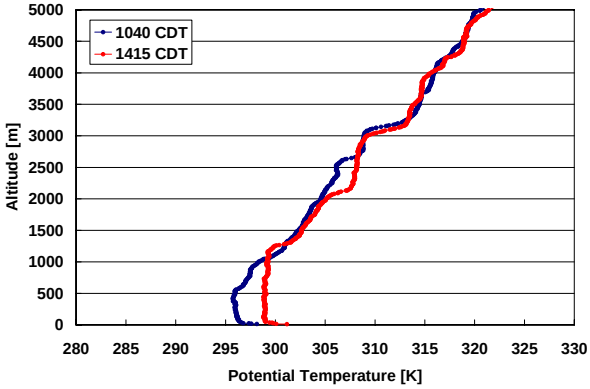

Appendix II – AQI and Ozone Levels – August and September 2006

Date	Peak Ozone Level 1-hr AQI	1-hr ppb	8-hr AQI	8-hr ppb	1-Hour Peak Location	8-Hour Peak Location	Critical Pollutant	Color
8/1/2006	*	39	27	34	Conroe Relocated C78	Conroe Relocated C78	PM-2.5	
8/2/2006	*	59	37	47	Conroe Relocated C78	Conroe Relocated C78	PM-2.5	
8/3/2006	*	70	44	56	Conroe Relocated C78	Conroe Relocated C78	PM-2.5	
8/4/2006	126	145	59	68	Houston Bayland Park C53	Houston Bayland Park C53	Ozone	Orange
8/5/2006	*	93	51	65	Houston Regional Office C81	Meyer Park C561	PM-2.5	
8/6/2006	*	88	44	56	Manvel Croix Park C84	Manvel Croix Park C84	Ozone	
8/7/2006	*	59	34	43	Conroe Relocated C78	Conroe Relocated C78	PM-2.5	
8/8/2006	*	63	38	49	West Houston C554	Katy Park C559	PM-2.5	
8/9/2006	*	109	79	76	Lynchburg Ferry C1015	Mercer Arboretum C557	Ozone	
8/10/2006	*	72	33	42	Wallisville Road C617	Wallisville Road C617	PM-2.5	
8/11/2006	*	66	34	44	Conroe Relocated C78	Conroe Relocated C78 Kingwood Library C555	PM-2.5	
8/12/2006	*	51	33	42	Conroe Relocated C78	Conroe Relocated C78	PM-2.5	
8/13/2006	*	48	34	43	Conroe Relocated C78	Conroe Relocated C78	Ozone	
8/14/2006	*	73	43	55	Crosby Library C553	Conroe Relocated C78	PM-2.5	
8/15/2006	*	98	49	63	Wallisville Road C617	Crosby Library C553	PM-2.5	
8/16/2006	121	141	127	95	Mercer Arboretum C557 Atascocita C560	Mercer Arboretum C557	Ozone	Orange
8/17/2006	142	158	172	113	Tom Bass C558	Tom Bass C558	Ozone	Red
8/18/2006	*	106	111	89	Katy Park C559	Katy Park C559	Ozone	Orange
8/19/2006	*	69	40	51	Bunker Hill Village C562	Houston Bayland Park C53	PM-2.5	
8/20/2006	*	107	77	75	Houston East C1	Houston East C1	Ozone	
8/21/2006	*	102	72	73	West Houston C554	Meyer Park C561 Northwest Harris County C26	Ozone	
8/22/2006	*	93	64	70	Park Place C416	Meyer Park C561	Ozone	
8/23/2006	*	75	38	49	Houston East C1	Smith Point Hawkins Camp C96/C638	PM-2.5	
8/24/2006	*	93	56	67	Lynchburg Ferry C1015	Conroe Relocated C78	Ozone	
8/25/2006	*	92	35	45	Clear Lake High School C572	Clear Lake High School C572	PM-2.5	
8/26/2006	*	60	20	26	Clear Lake High School C572	Conroe Relocated C78	PM-2.5	
8/27/2006	*	36	23	29	Atascocita C560 Bunker Hill Village C562	Conroe Relocated C78	PM-2.5	
8/28/2006	*	47	23	29	Atascocita C560	Conroe Relocated C78	PM-2.5	
8/29/2006	*	103	85	78	Texas City 34th St C620	Smith Point Hawkins Camp C96/C638	Ozone	
8/30/2006	*	95	90	80	Manvel Croix Park C84	Manvel Croix Park C84	Ozone	
8/31/2006	129	147	201	126	Houston Westhollow C410	Houston Westhollow C410	Ozone	Purple
9/1/2006	146	161	192	121	HRM-3 Haden Road C603	Hous. Deer Park 2 C35	Ozone	Red
9/2/2006	*	90	97	83	Manvel Croix Park C84	Smith Point Hawkins Camp C96/C638	Ozone	
9/3/2006	*	107	109	88	Tom Bass C558	Manvel Croix Park C84	Ozone	Orange
9/4/2006	*	101	87	79	Tom Bass C558	Tom Bass C558	Ozone	
9/5/2006	*	82	49	63	Lake Jackson C1016	Lake Jackson C1016	PM-2.5	
9/6/2006	*	101	106	87	Clear Lake High School C572	Clear Lake High School C572	Ozone	Orange
9/7/2006	136	153	164	110	Houston Bayland Park C53	Houston Bayland Park C53	Ozone	Red
9/8/2006	*	102	90	80	Houston Westhollow C410	Katy Park C559	Ozone	
9/9/2006	*	54	36	46	Lynchburg Ferry C1015	Smith Point Hawkins Camp C96/C638 Conroe Relocated C78	PM-2.5	
9/10/2006	*	64	31	40	Houston Bayland Park C53	Northwest Harris County C26	Ozone	
9/11/2006	*	68	35	45	Lynchburg Ferry C1015	Conroe Relocated C78	PM-2.5	
9/12/2006	*	83	61	69	Smith Point Hawkins Camp C96/C638	Smith Point Hawkins Camp C96/C638	Ozone	
9/13/2006	*	109	109	88	Manvel Croix Park C84	Manvel Croix Park C84	Ozone	Orange
9/14/2006	151	165	190	120	West Houston C554	Katy Park C559	Ozone	Red
9/15/2006	*	73	34	44	Northwest Harris County C26	Northwest Harris County C26	PM-2.5	
9/16/2006	*	47	28	36	Kingwood Library C555	Conroe Relocated C78	PM-2.5	
9/17/2006	*	31	19	24	Conroe Relocated C78	Conroe Relocated C78	PM-2.5	
9/18/2006	*	52	33	42	Smith Point Hawkins Camp C96/C638	Smith Point Hawkins Camp C96/C638	Ozone	
9/19/2006	*	81	66	71	Danciger C618	Danciger C618	Ozone	
9/20/2006	*	108	104	86	Houston Bayland Park C53	Houston Bayland Park C53	Ozone	Orange
9/21/2006	*	62	41	53	Smith Point Hawkins Camp C96/C638	Smith Point Hawkins Camp C96/C638	PM-2.5	
9/22/2006	*	37	21	27	Clear Lake High School C572	Conroe Relocated C78	PM-2.5	
9/23/2006	*	33	23	29	Conroe Relocated C78	Conroe Relocated C78	PM-2.5	
9/24/2006	*	56	34	44	Lake Jackson C1016	Danciger C618 Smith Point Hawkins Camp C96/C638	Ozone	
9/25/2006	*	68	45	58	Lake Jackson C1016	Danciger C618	Ozone	
9/26/2006	*	111	106	87	Danciger C618	Danciger C618	Ozone	Orange
9/27/2006	*	112	132	97	Conroe Relocated C78	Conroe Relocated C78	Ozone	Orange
9/28/2006	*	66	47	60	Smith Point Hawkins Camp C96/C638 Manvel Croix Park C84	Smith Point Hawkins Camp C96/C638	PM-2.5	
9/29/2006	*	85	54	66	Conroe Relocated C78	Conroe Relocated C78	Ozone	
9/30/2006	*	59	37	47	Atascocita C560	Atascocita C560 Mercer Arboretum C557	PM-2.5	

* There is no AQI associated with hourly ozone averages less than 125 ppb.
Source: TCEQ website